School of Spatial Sciences

Using a Four-Dimensional Geographical Information System to Visualise the Environmental Impact of Smog

Daniel Calvin Sandison

"This thesis is presented as part of the requirements for
the award of the Degree of Master of Science (Surveying and Mapping)
of the
Curtin University of Technology"

July, 1999

ABSTRACT

This research was developed to investigate the potential environmental impacts of poor air quality in Perth. This involved improving existing vegetation maps (through satellite image analysis techniques) for *biogenic* or forest emissions as a precursor to smog in Perth. Further, to visualise potential environmental impacts associated with poor air quality, a four-dimensional (volumetric over time) animation was created which clearly shows the path and extent of smog in Perth throughout an entire day.

Computer mapping of vegetation using Landsat TM data was performed to create an updated inventory of forest types in Perth as input into a photochemical smog model. By improving the inventory of forest cover, the Department of Environmental Protection (DEP) in Perth can calculate up to date biogenic emission estimates for the photochemical smog model.

Outputs from the DEP's photochemical smog model were integrated into a Geographical Information System (GIS) and subsequently visualised to show plume movement and potential environmental impact. Two datasets (nitrogen oxides and ozone) were provided to investigate the volumetric and dynamic temporal movement of photochemical smog in Perth on one day, March 16, 1994.

Nitrogen oxide sources can range from industry and petroleum refining to motor vehicle exhaust emissions, and are a major precursor to photochemical smog (ozone) formation in Perth. Natural emission sources (forest or biogenic emissions) can also be an important contributing factor to the photochemical smog mix in Perth. Biogenic emissions are comprised of Reactive Organic Chemicals (ROC) or Volatile Organic Compounds (VOC) which act as a catalyst to aid the nitrogen oxide conversion to ozone.

Three-dimensional and four-dimensional GIS techniques were used to highlight both plume movement and environmental impact. These two sets of visualisations have differing chemical levels (higher and lower, respectively) to show movement and interaction effectively. Visualisation of the chemicals allows for a greater

understanding of the mostly invisible chemical movement over the course of a day and its potential impact to humans and vegetation.

The spatial and temporal interaction of the plumes was investigated by creating a series of animations that can be viewed over the Internet. By using multimedia capabilities, these results can be easily distributed to a wide range of decision makers and people generally interested in smog in Perth.

ACKNOWLEDGEMENTS

I would like to thank Dr Robert Hickey, Dr Graciela Metternicht, and Graeme Wright from the School of Spatial Sciences at Curtin University of Technology for their guidance throughout this research. Further, these individuals are thanked for providing advice on gaining leadership, communication and dynamic research skills to complete this work.

Further thanks go to the secretarial staff within the School of Spatial Sciences and the computing support staff for advice on numerous technical issues and all around computing support. This research would have been impossible without the help of kind individuals in the computing support office.

I would also like to thank the Graduate Studies Office, in particular Delia Giggins and Tanya Lerch, for advice on thesis submission and general course information. The Curtin University Postgraduate Student Association (CUPSA) provided an independent body to assist with research matters and provided an excellent source of camaraderie between postgraduate students, and their help was appreciated.

The Department of Environmental Protection (DEP) in Perth must be commended for their assistance, especially Dr Peter Rye and Josie Bailey for data and technical issues of environmental modelling. I wish to thank Dr Richard Smith of the Leeuwin Centre's Remote Sensing Appplications Centre (DOLA) for providing satellite imagery. For provision of Voxel Analyst software, I would like to thank the Spatial Resources Information Group, Department of Agriculture, Western Australia.

Several students provided valuable assistance and provided a research environment that was productive. Of these students, I wish to thank Ross Carew, Troy Forward, Jochen Franke, Samsul Bachri, Jane Lawley, and Melanie Martin for their time and companionship. Final thanks go to those who wish to remain anonymous for thesis editing as well as Tim North of Scribe Consulting for professional editing services. Their help was greatly appreciated and they are generously thanked.

TABLE OF CONTENTS

LIST OF FIGURES

Figure

LIST OF TABLES

Table

LIST OF ABBREVIATIONS AND ACRONYMS

1D	One-Dimensional
2D	Two-Dimensional (plane surface)
2.5D	Two and One Half-Dimensional (terrain surface)
3D	Three-Dimensional (volumetric body)
3DSB	Three-Dimensional Sea Breeze (model)
3.5D	Three and One Half-Dimensional (terrain surface fly-through or time lapse)
4D	Four-Dimensional (3D over time)
5D	Five-Dimensional (4D plus attributes)
AGD66	Australian Geodetic Datum, 1966
AMG	Australian Map Grid
AMG66	Australian Map Grid, 1966
ARVI	Atmospherically Resistant Vegetation Index
AVHRR	Advanced Very High Resolution Radiometer
AVI	Audio Video Interleave
BR	Boundary Representation
BVOC	Biogenic Volatile Organic Compounds
CAD	Computer Aided Design
CALM	Conservation and Land Management
CD	Cell Decomposition or Compact Disc
CIT	CITy Smog Model
CSG	Constructive Solid Geometry
DEM	Digital Elevation Model
DEP	Department of Environmental Protection
DOLA	Department of Land Administration
DTM	Digital Terrain Model
EDG	Edit DesiGn file (Microstation95 Module)
EM	Electromagnetic
EIA	Environmental Impact Assessment
ESRI	Environmental Systems Research Institute
GIS	Geographical Information Systems

GMS	Groundwater Modelling System
GPS	Global Positioning Systems
GVI	Global Vegetation Index
IDL	Interactive Data Language (programming language)
IPVI	Infrared Percentage Vegetation Index
KT	Kauth-Thomas Soil Line
LADM	Langranian Atmospheric Dispersion Model
LAI	Leaf Area Index
MSAVI2	Modified Soil Adjusted Vegetation Index 2
MSS	Multi Spectral Scanner(Landsat)
MX	MatriX (octree)
NASA	National Aeronautical and Space Administration
NDVI	Normalised Differential Vegetation Index
NHMRC	National Health Medical Research Centre
NIR	Near-Ifra-Red (band)
NMHC	Non-Methane HydroCarbon oxidation
NO	Nitric Oxide
NO_2	Nitrogen Dioxide
NOAA	National Oceanic and Atmospheric Administration
NOX	Nitrogen oxides
NSF	National Science Foundation (USA)
PI	Primitive Instancing
PPSS	Perth Photochemical Smog Study
PR	Point and Region (octree)
PVF	Projected Vertical Foliage
R	Red (band)
RAMS	Regional Atmospheric Modelling System
ROC	Reactive Organic Chemicals
RMS	Root Mean Square (error)
RSAC	Remote Sensing Applications Centre
SBI	Soil Brightness Index
SG	Silicon Graphics
SOE	Spatial Occupancy Enumeration

SPOT	Satellite Pour l'Observation de la Terre (Earth Observation Satellite)
STIN	Spatio-Temporal INtersection
TIN	Triangulated Irregular Network
TM	Thematic Mapper (Landsat 5)
TSAVI	Transformed Soil Adjusted Vegetation Index
UAM	Urban Airshed Model
USA	United States of America
USGS	United States Geological Survey
UTM50S	Universal Transverse Mercator Zone 50 South
UV	Ultraviolet Radiation
VOC	Volatile Organic Compounds
VR	Virtual Reality
VRML	Virtual Reality Modelling Language
WA	Western Australia
WHO	World Health Organisation
WWW	World Wide Web (part of the Internet)
km	Kilometre (Kilometres)
m	Metre (Metres)
mm	Millimetre (Millimetres)
nm	Nanno Metres
ppb	Parts Per Billion

Chapter 1

INTRODUCTION

1.1 Aims of This Study

The aims of this research were to investigate the spatial distribution of environmental impacts caused by smog in Perth, Western Australia (Figure 1.1). This was done using Geographical Information Systems (GIS) and remote sensing technologies. Remote sensing was used to map vegetation type and vegetation cover as inputs to smog formation modelling which is carried out by the Deapartment of Environmental Protection (DEP) in Perth. Further, GIS techniques were employed to visualise chemical plume movement in four dimensions throughout the course of a typical smog day in Perth.

The results of this research will permit the DEP in Perth to gain an up-to-date vegetation inventory. Visualisation results will also allow decision makers to see what a typical smog day in Perth looks like in a volumetric and dynamic nature.

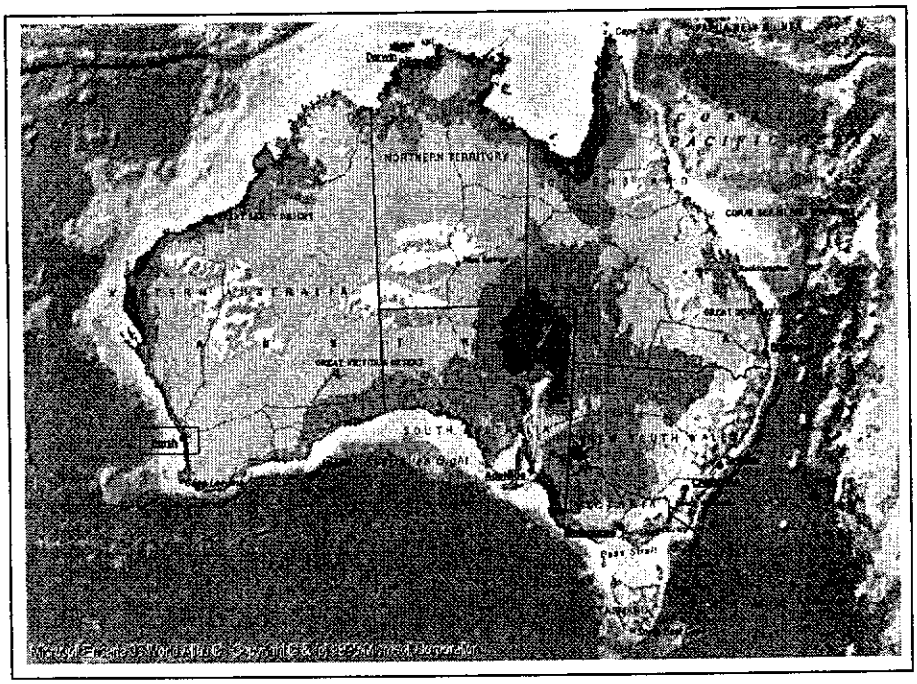

Figure 1.1 The location of Perth, Western Australia

Vegetation mapping was performed on Landsat TM image mosaics acquired in 1996 and 1997 to extract vegetation species and density information. Nine vegetation classes and water have been identified and mapped. Vegetation cover or density was mapped into six classes of percentages. These two vegetation inventories will be used by the DEP to model the total emission impact of biogenic sources. Not only will the current maps be an improvement on previous DEP input maps, but the methods developed here will be useful for future biogenic emissions mapping in Perth.

Visualisation of photochemical smog impact was performed using DEP data to build a series of four-dimensional (4D) plumes for nitrogen oxides and ozone. The aim of this work was to test 4D GIS technologies to produce visualisations on a personal computer platform. By using 4D GIS techniques, a true understanding of smog movement can be fully examined. This 4D method allows the user to appreciate patterns that would not be obvious in standard two-dimensional (2D) maps. A backdrop to the plume visualisation is a digital terrain model, created to show details of relative relief in Perth.

Final plume visualisation was performed through a software package capable of generating digital video movies. The three-dimensional (3D) plumes for each sample period throughout the day were used to generate frames within the animated movie. Even though this work may not prove as efficient as programming and visualisation environments, it aims to prove that 4D GIS techniques are valid for visualisation of environmental phenomena.

Combinations of both nitrogen oxides and ozone are mapped in the same animation. By viewing both plumes, interaction of nitrogen oxides (which are a precursor to ozone and smog) and ozone may reveal processes not yet fully understood.

These visualisations will be useful for investigating chemical interaction as well as terrain interaction with the plumes. Results from this model were generated in output for the Internet (http://www.cage.curtin.edu.au/~sandisd/visuals.html) to disseminate the visualisation in an animated format (requires Internet Explorer 4.0+, Netscape

Navigator 4.0+, Windows95 or later media player). This will aid the overall understanding of photochemical smog formation, movement, and subsequent impacts in Perth, Western Australia.

1.2 Project Goals

There were two major goals for this research (Figure 1.2). The first was to generate two vegetation maps from Landsat TM satellite imagery. This includes nine species groups of natural vegetation and six classes of vegetation density. It should be noted that species groups (assemblage and genera) will be referred to as 'species' throughout the remainder of this thesis. These maps will be included in future DEP airshed modelling of Perth. The second major goal was to develop a computer visualisation of a volumetric plume of nitrogen oxides and to show the interaction of the plume with an ozone plume throughout the course of a specific day (March 16, 1994).

The major link between these two research components is the DEP photochemical smog model. No attempt was made to alter the DEP model, yet research component one (vegetation mapping) aims to improve the inputs into the DEP model; research component two (smog visualisation) aims to improve the outputs of the DEP model on a desktop mapping environment.

The use of multi-dimensional data (2D, 2.5D, 3D, and 4D) will help to visualise the environmental impact of the photochemical smog upon humans and vegetation in Perth. Vegetation maps will provide 2D information and will be used to estimate biogenic or forest chemical emission inputs into smog formation. The terrain in Perth was modelled as a surface in two and a half dimensions (2.5D). Nitrogen oxides and ozone data provided by the DEP are 3D and 4D and were visualised as volumetric plumes over time.

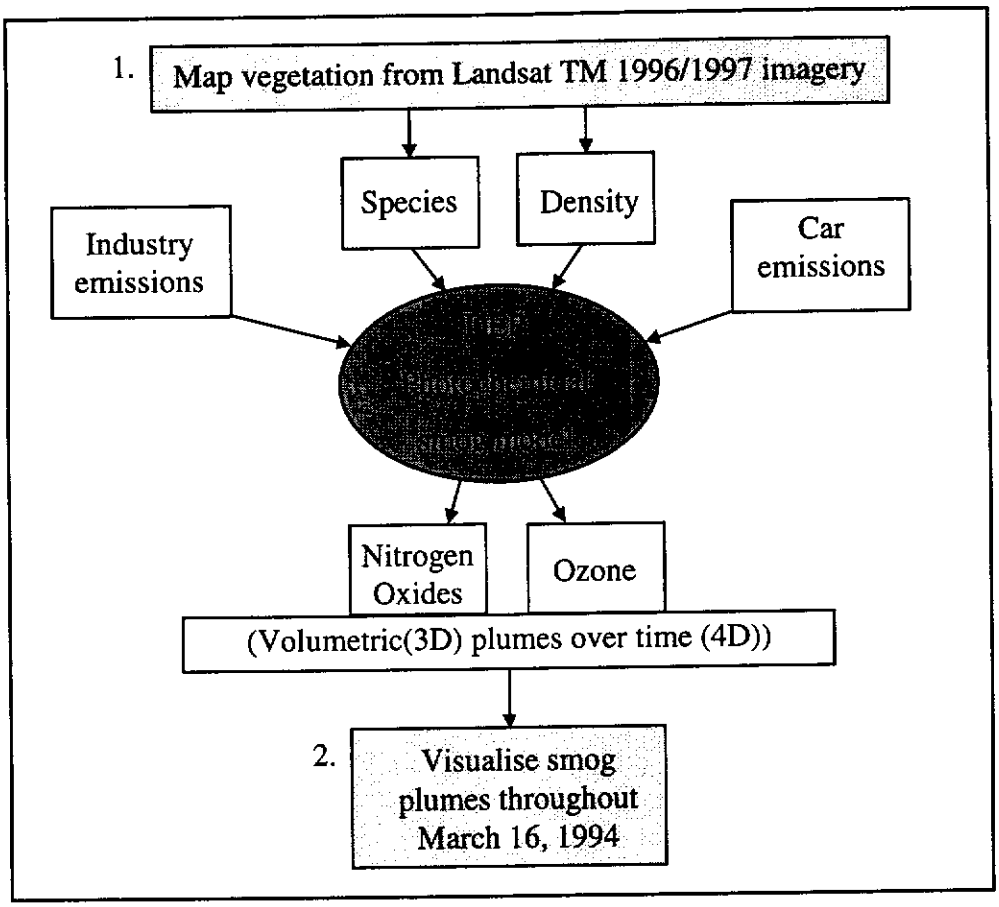

Figure 1.2 Goals of this research: 1. To map vegetation species and density for input into the DEP's photochemical smog model; 2. To visualise output from the DEP model over the course of a day to show environmental impact, with the DEP model as the link between the two research components

The chemistry of smog is also covered, giving insight into some of the many chemical compounds involved in smog formation. It should be noted that chemical compounds (or gasses) are labelled as *chemicals* throughout the remainder of this thesis. This includes emissions of nitrogen oxides, ozone, and hydrocarbons. Natural emissions known as *biogenic* emissions are the main focus of the vegetation mapping. Human sources of emissions (anthropogenic), even though not a major part of this research, will be touched upon.

Weather and climate are also important factors in the photochemical smog mix and previous smog studies in Perth are also investigated. Photochemical smog studies throughout the world have also been reviewed in order to compare test site conditions and the relevance of the methodology applied.

1.2.1 Vegetation Mapping

(a) Species

Using remote sensing and ground truth data, this research extracted nine classes of natural vegetation in the Perth metropolitan area. The classes were defined by the DEP as a standard input variable in the Perth airshed model and cover the majority of significant native vegetation types. These vegetation classes give a good indication of the level of biogenic emissions in Perth.

Classification of imagery involves looking for correlations between training sites (small user-defined areas on the imagery) and the rest of the image bands. Areas of high correlation indicate that those areas can accurately be broken into classes (Jensen, 1986; Jensen, 1996; Lillesand and Kiefer, 1994). Several standard image classification techniques were tested to find the most suitable method of distinguishing species.

Biogenic sources contribute a minority of the emissions where anthropogenic sources contribute the majority, also see Section 1.4.1. Relative contributions for the natural sources in the Perth region are only broken down into landscape groups. The highest emitter of these landscape groups is mixed woodland/crops, followed by coniferous forest, mixed forest, scrub lands, wetland forest, jarrah, deciduous forest, jarrah and marri forest, and scrub woods. The lowest landscape emitters are grasslands and marri (Cope and Ischtwan, 1996).

(b) Percentage of Canopy Cover

The approximate vegetation canopy cover or Projected Vertical Foliage (PVF) for each class is listed in Section 2.3.2. The PVF was an *eyeball estimate* of the vertical foliage contained within ground truth sites. When using PVF for detecting Eucalyptus trees, it is important to note that accurate measurement of perpendicular vertical leaves (i.e. leaves pointing down) remained difficult in the field with the eyeball estimate.

The extraction of vegetation canopy cover was performed using remote sensing and ground truth data. These ground truth data were collected to find a correlation between known vegetation density (PVF) and the multi-spectral reflectance characteristics of vegetation. Once this relationship was established, a regression equation was used to calculate vegetation density throughout the study area.

Both species and density data sets were then generalised from 30 m to 3 km pixel resolutions to match the input parameters of the DEP photochemical smog model. Generalisation is often difficult due to loss of detail, and standard algorithms may not give output classes that truly reflect the spatial nature of data at a higher resolution. Each generalisation method may produce a different result, so care must be taken when choosing the method.

1.2.2 Nitrogen Oxides and Ozone Visualisation

Four-dimensional visualisation was performed on two data sets from the DEP: nitrogen oxides and ozone. These chemicals were not spatially and temporally analysed, but were linked through animations to develop effective visualisation products. This visualisation offers an appreciation of the interactions involved between the two chemicals. These chemicals are important, as nitrogen oxides are known to act as a catalyst to the formation of ozone and are considered a precursor to ozone (Graedel and Crutzen, 1995). An elevation model was added to the visualisation allowing an observer to see the interaction between terrain and smog.

(a) Nitrogen Oxides

Two visualisations were created highlighting both plume movement and environmental impact. The visualisation of nitrogen oxides aimed to produce a 4D animation of a plume of 20 parts per billion (ppb), as this was determined to be significant for environmental impact by the DEP (Rye, 1998). A lower threshold of four ppb was also used to highlight plume movement for final visualisation due to a lack of significant plume extent at 20 ppb. Since nitrogen oxides can be a significant precursor to photochemical smog formation, it is important to see if the visualisation can show the change of oxides into ozone throughout March 16, 1994.

(b) Ozone

The ozone threshold level used for environmental impact during the multi-dimensional visualisation was set at 60 ppb - considered a moderate smog level (Rye, 1997). Moderate levels of ozone were also visualised to show potential human impact. This was accomplished by showing the development of moderate levels of ozone present for long periods over the Perth metropolitan area. Due to low chemical levels, plumes were also thresholded to highlight plume movement in the final visualisation. A lower threshold of 50 ppb was used for the best ozone visualisation.

1.3 Weather and Climate Conditions of Smog Formation in Perth

Perth's climate is Mediterranean and has two distinct seasons: summer and winter. Average daily temperatures range from 14 to 30 degrees C in the summer and from 9 to 21 degrees during winter. Summer rainfall is infrequent with an average of eight to 20 mm, while winter rainfall averages range from 100 to 200 mm per month (McGonigal *et al.*, 1993).

The summer season is dominated by high atmospheric pressure and is generally cloud free. Occasional cyclonic influences can affect Perth, even though Perth lies at about 32 degrees south latitude. Effects range from high rainfall and strong winds to mild weather pattern disturbances.

Winter is dominated by low-pressure fronts bringing temperatures moderately above freezing with frequent rain. Generally, summer conditions are more likely to generate photochemical smog even though winter temperature inversions and Conservation and Land Management (CALM) winter burn-offs can increase particulate matter (Rye, 1996). It should be noted, however, that the photochemical component of smog is enhanced by ultraviolet (UV) radiation and remains strongest in summer. Further winter factors, such as an unstable atmosphere, cause more mixing and, thus, reduced smog formation. Rain events wash nitrogen oxides out of the sky, also removing this catalyst to smog formation.

Morning wind patterns during the summer smog season are generally light to moderate land breezes from the east. In the afternoon, moderate to strong sea breezes from the west often bring relief from high temperatures. The sea breeze can also bring smog back from the ocean over the city. Changes in frontal conditions can make formation of the sea breeze slower, resulting in the morning emissions escaping to sea (Rye *et al.*, 1996). High and low pressure troughs can increase the sea breeze effect by providing a major wind change timed with the arrival of the shore and sea breezes (Rye, 1996; Rye *et al.*, 1996).

Local terrain conditions can have an impact on the speed and direction of winds, so terrain factors must also be considered in photochemical smog modelling. The terrain in Perth is dominated by the Swan Coastal Plain, Darling Scarp, and the Darling Plateau (Figure 1.3).

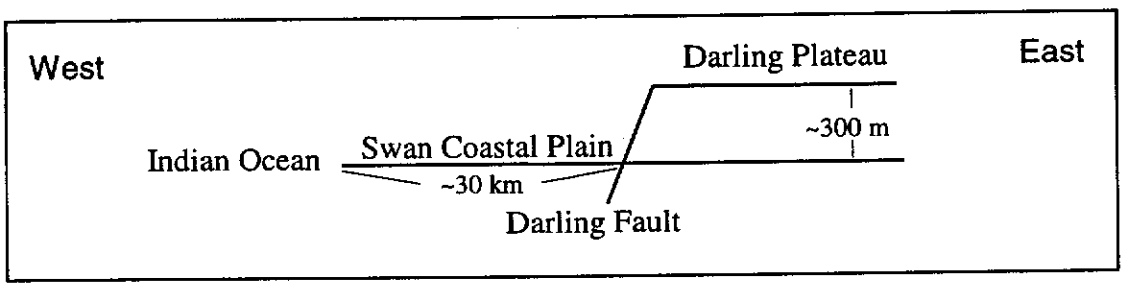

Figure 1.3 Simple cross section of the Swan Coastal Plain, Darling Fault and Darling Plateau

Perth's relatively flat terrain is dominated by only one major fault feature which makes wind calculations and measurements somewhat easier. This fault is approximately 30 km east of the coast and forms a range or ridge of higher elevation (over 300 m) in contrast to the relatively flat coastal plain. Wind mixing increases near the fault and over the ridge. Even with the relatively flat terrain on the coastal plain, mixing levels are smaller still over the ocean. The effect of less mixing causes less dispersion of chemicals. Thus, ideal summer conditions for smog formation are over the ocean. This smog may then be brought back over the city by the afternoon sea breeze to combine with evening rush hour emissions.

1.3.1 Summer

The most important factors contributing to smog formation occur during summer. These include high temperatures, sea breezes, bushfires, and urban emissions. Cloud-free days bring long periods of direct sunlight which provide essential energy for development of photochemical smog. High temperatures (40 degrees C) are common with long stretches without rain. Vegetation emissions also increase during summer, as the leaves *cook* (i.e. release gasses) in high temperatures (Rye, 1997).

The summer sea breeze can be delayed, bringing relief from smog when land breezes allow smog to escape the metropolitan area. If the sea breeze (called the Fremantle Doctor) develops around midday, the photochemical plume can be brought out to sea by the morning land breeze and then brought back over the urban area. This then has the potential to remix with bushfire smoke and further urban emissions (especially during evening rush hour).

Summer bushfires are typically started by carelessness, arson, or lightning. The dry summer conditions make the spread of fire a threat; the strong sea breeze and high temperatures make conditions worse. These fires can further add to emissions of reactive organic chemicals and particulate matter from natural vegetation (Rye, 1997). Fires also affect the density and distribution of vegetation and, thus, the accuracy of existing vegetation maps.

Although the date visualised during this study (March 16, 1994) was late in summer, it is not uncommon to find conditions suitable for smog formation this late in the season. This date was classed as a sea breeze or coastal event with moderate smog levels. Some cyclonic activity generated trough conditions suitable for the dominant winds to switch in time with the sea breeze and also brought high temperatures to the area (Rye, 1996).

1.3.2 Winter

Generally, factors contributing to smog formation in Perth are relatively infrequent during winter (see Section 1.3). Moderately high temperatures do combine with

other factors to decrease air-quality, however. Temperature is not the most important aspect during winter; CALM burn offs, home heating fires (especially open fireplaces), and occasional temperature inversions occur which create significant air quality reductions.

The CALM burn offs are conducted to reduce fuel levels in bush areas. These fires contribute a significant amount of particulate matter, nitrogen oxides, and reactive organic chemicals into the air (Evans *et al.*, 1977; Hurst *et al.*, 1994).

Home heating in winter is commonly provided by wood fires. Open air wood fires burn wood inefficiently, causing gasses to be released from the wood. Ideally, a closed wood stove with a catalytic converter to burn off the gasses should be used. The impact of fires alone, however, would not be a major problem in winter if temperature inversions did not occur. The inversions of warm and cold air masses traps the smoke from the house fires in the lower atmosphere within the metropolitan region (Rye *et al.*, 1996).

1.4 Chemistry of Smog in Perth

Air quality in Western Australia is generally good. Perth, Kwinana, and Kalgoorlie, however, can be linked to urban and industrial emissions and are the three major locations in the state that experience occasional poor air quality (Grant, 1992). This study covers the urban Perth area and the Kwinana industrial zone on the coast approximately 20 km south of the metropolitan area (see Figures 1.4 and 1.5). Interactions of the Kwinana and Perth photochemical plumes are covered in Rye *et al.* (1996).

Generally, poor air quality occurs when numerous chemicals react under light and high temperatures to create ozone, a key indicator of photochemical smog (Rye *et al.*, 1996). Several other chemicals can also play a key role in the creation of ozone and contribute to poor air quality in general, yet nitrogen oxides remain the major catalyst and precursor for ozone formation (Graedel and Crutzen, 1995). Some of the major chemicals are carbon monoxide, sulphur dioxide, nitrogen oxides, hydrocarbons, hydrogen fluoride, and particulate lead. These chemicals have environmental

impacts, yet ozone generally remains a higher threat to human health (Rye *et al.*, 1996).

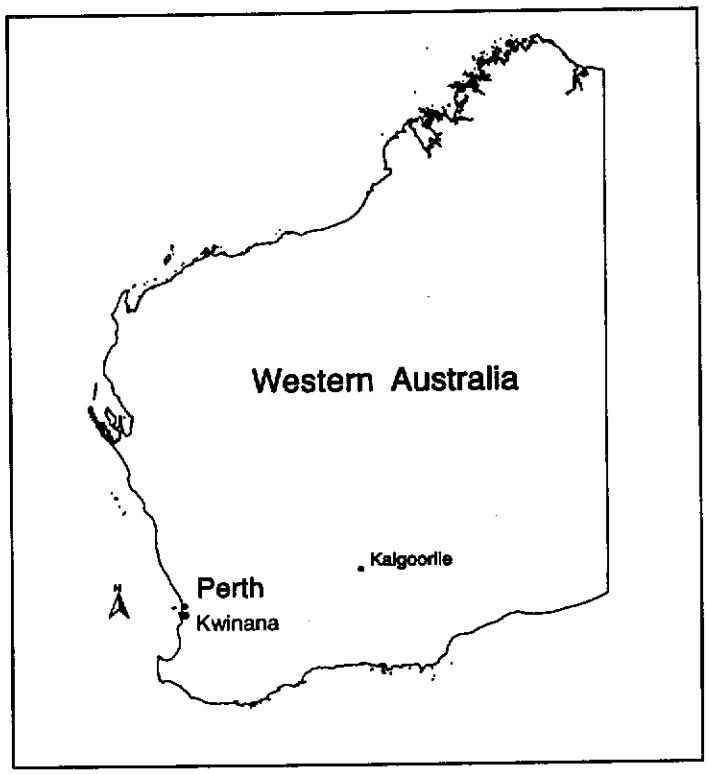

Figure 1.4 Perth, Kwinana, and Kalgoorlie, Western Australia

The formation of ozone and the process of Non-Methane Hydrocarbon (NMHC) oxidation, (oxidation of hydrocarbons excluding methane) results from a series of atmospheric reactions. The combination of molecular oxygen (O_2) and atomic oxygen (O) with a molecule (M) of nitrogen oxides (NOX) produces ozone (O_3). The rate of conversion to ozone is dependant upon the amount of NOX and solar radiation present.

$$O + O_2 + NOX + \text{light (UV)} \Rightarrow O_3 \qquad (1.1)$$

Thus, emissions of reactive chemicals and pollution can combine with solar radiation to produce nitrogen oxides which then form ozone (Rye *et. al.*, 1996; Graedel and Crutzen, 1995).

Figure 1.5 Perth Metropolitan Area and Kwinana Industrial Zone (Landsat TM mosaic 1996/1997, bands 1,4,5 in red, green, blue channels respectively)

Fine particles or aerosols such as dust and organic chemicals can be harmful as well (Grant, 1992). Particulate matter is greatly increased during bush fire events in Western Australia (see Figures 1.6 and 1.7). Smoke from these fires is a visible sign of air pollution, whereas ozone is clear to whitish and difficult to see (see Figures 1.8 and 1.9).

Figure 1.6 shows smoke dominating the urban area from a winter fuel-reduction burn off conducted by CALM. Figure 1.7 shows a summer bush fire in Kings Park, where smoke again dominates the urban area. Figures 1.8 and 1.9 show two non-bushfire days of relatively poor air quality with the whitish ozone blocking the view of the city.

Initiatives to remove lead from petrol and sulphur dioxide from industrial emissions have significantly improved environmental air quality. Further international air quality standards to control the depletion of upper level ozone and the creation of greenhouse gases will also help the lower atmosphere where direct human impacts occur (Grant, 1992). Less emissions from urbanised areas bring some relief from poor air quality. More control measures for air-quality should result from well known international summits, such as in Kyoto, Japan in 1997, where emissions were clearly an issue to the global community. This is despite the fact that Australia is widely known to have gained an increase in allowable emission levels, partially due to *carbon sink credits* from forest reserves.

Perth is affected by photochemical smog mainly during the summer, but conditions can cause localised impact in winter. Perth experiences significant photochemical smog on approximately ten days per year when ozone levels are above 80 ppb for an hour or more (Rye *et al.*, 1996). Frequency of smog events in Perth (up to ten days of 80 ppb or higher ozone for one hour exposure) is relatively low compared to other cities in the world.

Figure 1.6 Smoke from Conservation and Land Managment (CALM) burn off (1997)

Figure 1.7 Bushfire smoke dominating the city from King's Park fire (1996)

Figure 1.8 Perth skyline with poor air quality (ozone) (1997)

Figure 1.9 Perth skyline with very poor air quality (1997)

1.4.1 Chemicals

The sheer number of chemicals involved in the formation of smog is not fully understood at this time. Rye *et al.* (1996) give an indication of previous chemical measurements relevant to Perth conditions. Suitable chemical mixes for photochemical smog formation include nitrogen oxides, reactive organic chemicals, and ozone. Particulate matter from bushfires, diesel fuel burning, and other sources also combine with airborne chemicals to create smog.

Two forms of emissions are necessary for ozone formation: nitrogen oxides (NOX - a combination of NO_2 (nitrogen dioxide) and NO (nitric oxide)) and reactive organic chemicals (ROC) (Rye *et al.*, 1996). These chemicals can adversely impact upon humans and vegetation if sufficiently high levels are present. However, ozone still remains the dominant indicator of smog and is a stronger irritant.

Nitrogen oxide sources can range from industry and petroleum refining, to motor vehicle exhaust emissions and these anthropogenic sources can form up to 80 percent of the total nitrogen oxide production with the remainder from natural and other sources. Nitrogen oxides are major precursor components of photochemical smog and ozone in Perth and must be mapped effectively.

Only a portion (37 percent) of the reactive organic chemicals (ROC) or volatile organic compounds (VOC) comes from vegetation, but as Rye *et al.* (1996, p.6) state, "...natural ROC emissions (commonly categorised as "forest" or "biogenic" emissions) must be included, and can constitute a significant proportion of the total ROC inventory." The remaining sources include fuel evaporation and un-burned combustibles. When ROC or VOC is combined with nitrogen oxides, ozone production is increased. It is, therefore, critical that mapping of natural sources be also performed accurately.

Ozone in the upper atmosphere (stratosphere) is needed to protect the Earth and humans from harmful ultraviolet rays (Grant, 1992). Ozone in the lower atmosphere, however, can be harmful to health. Health effects include respiratory problems and eye irritations. Several studies (Woodward *et al.*, 1995; Crapo *et al.*, 1992; White *et*

al., 1995; Edwards, 1995; Drechsler-Parks, 1987; Monk, 1994; O'Conner *et al.*, 1975) show the health effects of ozone on humans and Australian vegetation. The impact on vegetation may be seen at lower concentrations, yet human health remains the greater concern.

Ozone levels are usually averaged over either a one-hour or eight-hour period. Health recommendations have been made for high ozone exposure over time. Eight-hour averages are preferred to assess potential impact where possible (Rye *et al.*, 1996). Eight hour averages have lower chemical levels; however, the risk associated over the longer time is deemed greater.

In 1987, the World Health Organisation (WHO) set a maximum one-hour level of 76 to 100 ppb of ozone for protection of public health. The 1987 decision also recommended that the level for eight hours should be no higher than 50 to 60 ppb. The WHO also recognised ozone impact upon vegetation by recommending an eight-hour level of no higher than 30 ppb, and a 24 hour level of 32.5 ppb (WHO, 1992).

Australian limits, set by the National Health and Medial Research Council (NHMRC) in 1995, are a slightly higher limit of 100 ppb for a one-hour average that is not to be exceeded more than once per year. The NHMRC eight-hour limit of 80 ppb, not to be exceeded more than once per year, is also slightly higher than the WHO recommendations. Only the state of Victoria has set (eight-hour) limits for protection of vegetation, with ozone at 50 ppb not to be exceeded more than three times per year. Maximum levels should also not exceed 80 ppb to protect vegetation (Rye, *et al.*, 1996).

1.4.2 Emissions

Biogenic emissions from forests include isoprene, monoterpenes, and x-pinene. These chemicals are emitted from vegetation under high daytime temperatures. Emissions during the night are minimal. Other biogenic emissions include limonene, cymene and cineoline (Rye *et al.*, 1996; Carnovale *et al.*, 1991; Guenther *et al.*, 1991). A study by Finlayson-Pitts and Pitts (1986) shows that over 350 other

chemicals are emitted from vegetation, but their impact on photochemical smog formation is unknown at this time.

(a) Biogenic Emissions (Natural Sources)

There is a great deal of uncertainty involved in estimating the role of biogenic emissions in Australia (Carnovale *et al.*, 1991; Rye *et al.*, 1996), even though it is widely known that vegetation can uptake chemicals and large tracts of vegetation are referred to as *carbon sinks*. A few key points are known, however, in natural hydrocarbon emission systems. Some vegetation species emit more gasses with strong sunlight than others, and the spatial location of emissions can be important for tracing potential sources. Certain chemical mixes can be broken down into component parts through *tracers* to pick out major influences in smog creation (Rye *et al.*, 1996).

A biogenic hydrocarbon emissions inventory performed in the USA by Lamb *et al.* (1987) examined several chemicals and measured coniferous and deciduous forest types. Agricultural sources were also studied; however, little agricultural area is present in the Perth metropolitan area other than small plots and some medium sized vineyards. This study found that isoprene emissions can be responsible for up to 80 percent of total deciduous emissions. Further, x-pinene emissions can be as high as 25 percent of the total coniferous output.

Chameides *et al.* (1988) argues that the USA has understated biogenic emissions and their contribution to smog, thereby incorrectly estimating the impact that vegetation has on smog formation. Further, in Atlanta, it is indicated that biogenic emissions are as large as, or larger than, emissions from anthropogenic sources. Overall, it appears that not enough emphasis was placed on biogenic sources in early air quality studies.

Emissions not only react to daily fluctuations in light and temperature but also to seasonal variations. Muller (1992) investigates these variations to create an average

annual estimate of emissions, as well as investigating spatial distribution of the emissions present on a global scale.

Volatile organic compound or biogenic emission rates vary under conditions such as directness of light, the temperature of the vegetation foliage (leaves), evaporated water density (humidity), and the age of the foliage (Guenther *et al.*, 1993). As well as climactic variables, Geron *et al.* (1994) recommend that elevation be considered in the estimation of Biogenic Volatile Organic Compounds (BVOC) for factors such as temperature and atmospheric width.

Guenther *et al.* (1994) found that 58 percent of US woodland biogenic emissions are isoprene and that 18 percent are monoterpenes. The remaining 24 percent are made up by other organic compounds. It should be noted that these figures may not apply to Australian conditions, even though some of the species sampled were also found in Australia. Further work shows that isoprene emissions are higher than monoterpenes during the day, but drop significantly at night when monoterpenes drop only slightly.

Sampling of vegetation emissions under true field conditions is often difficult due to the equipment needed to take chemical air samples. Further, the sampling procedure itself often affects the results, so care is needed when sampling is performed. Lamb *et al.* (1993, p. 1674) cite a study by (Guenther *et al.*, 1993) where sampling was performed by placing a bag around the branch to be measured. Most of the air was squeezed out and emission measurements taken after a few minutes.

Tanner and Zielinska (1994), used a frame built around a tree branch with enough air space for temperature and wind conditions to be natural. Their model only tested three tree species in the USA, and results showed that the effect of previous rough handling of vegetation when sampling occurred was minimal.

Nutrient distribution within a forest stand is another factor to be considered. Hingston *et al.* (1980 and 1981) measured the biomass of several small eucalyptus trees in an area just south of Perth. Even though the focus was predominantly on the

biomass of small trees and forest litter, the role of biomass decomposition was noted in the atmospheric exchange of gases.

A recent account of measuring biogenic emissions from satellite imagery is given by Luman and Ji (1995). With Landsat TM imagery, basic emission categories were established for high isoprene, low isoprene, deciduous, no isoprene, coniferous, and agriculture. After defining the species to be mapped, they were subsequently placed in an emission category. This work demonstrated the efficient use of remote sensing to define species and subsequent emission categories.

(b) Anthropogenic Emissions

Anthropogenic emissions are defined as emissions created by human activity (Rye *et al.*, 1996; Carnovale *et al.*, 1991; Grant, 1992). There are several sources, but the major contributors are two-stroke engines such as lawn mowers, manufacturing, all motorised fuel combustion, and refining. Motorised vehicles globally contribute between 30 and 50 percent of nitrogen oxide emissions. Anthropogenic emissions of ROC such as paints, solvents, fuel evaporation, and printing add to the photochemical smog mix and are covered by Rye *et al.* (1996). It is important to note that natural sources of nitrogen oxides such as bushfires also may have human causes (e.g. arson).

Extreme examples of poor air quality clearly demonstrate the impact upon the human environment. In Donora, Pennsylvania, coal burning, industry, and factory emissions combined with a temperature inversion in 1948 to create very high pollution levels in the valley that the town occupied. This event led to the health of thousands of people being affected and twenty deaths (Strahler and Strahler, 1997, p110). Even more severe was the London pollution episode of 1952 which took approximately 4000 lives, again a partial result of coal burning (De Blis and Muller, 1996, p. 234).

A reduction in emissions that contribute to photochemical smog is necessary to reduce the frequency of smog events. Research referenced earlier shows that a greater understanding of the role of biogenic emissions in photochemical smog is necessary in order to more completely understand the overall smog formation

process. Reduction in biogenic emissions may be possible. Ideally, and more realistically, the reduced output of emissions from human sources would be beneficial both to local conditions and in reducing the greenhouse effect. Such measures would include increasing vegetation cover to absorb pollutants and create *carbon sinks*.

1.5 Smog Studies in Perth

1.5.1 Perth Photochemical Smog Study

The most notable study undertaken in Western Australia is the Perth Photochemical Smog Study (PPSS) (Rye *et al.*, 1996). This is a comprehensive study of all factors currently known to be involved in smog formation in the Perth metropolitan region. As well as smog components, measurement schemes and modelling components are covered.

The models used in the Perth Photochemical Smog Study include meteorological models such as the 3D Sea Breeze (3DSB) (a local model developed by Rye (1989)), Langranian Atmospheric Dispersion Model (LADM) (CSIRO) and Regional Atmospheric Modelling System (RAMS) (Murdoch University model adapted from USA model) (Rye *et al.*, 1996).

The 3DSB (three-dimensional sea breeze) model does not take into account terrain, but allows for fast interpolation of the typically large data sets in 3D. The LADM includes terrain effects and allows for 4D data. The RAMS also includes terrain effects; however, the speed of processing was slow and showed little advantage over the other two models (Rye *et al.*, 1996).

Photochemical models used in the PPSS include the CIT (CITy) and the Urban Airshed Model (UAM). At this time no data was available from the CIT model, so focus remains on the UAM, even though the CIT model showed a better result upon comparison (Rye *et al.*, 1996).

The UAM was the model used by the DEP to interpolate the nitrogen oxides and ozone files used in this study. This 3D grid model attempts to model both active and inactive chemical processes that can lead to photochemical smog production. Key meteorological inputs into the model are temperature, wind, and inversion or shear zones. Emission inputs are entered as 2D grids with optional point sources. Terrain and boundary conditions are also used along with chemical reaction rates to create the output 3D files for each time period (Scheffe and Morris, 1993). The data obtained for photochemical smog visualisation (this research) was produced by the UAM.

1.5.2 Perth Photochemical Smog Study - Airshed Modelling Component

The airshed modelling component of the PPSS covers contributions of emissions towards photochemical smog. Each emission type (motor vehicles, industry, area based sources, and biogenic emissions) is broken down for several test dates including March 16, 1994, the day that visualisation was performed upon for this research (Cope and Ischtwan, 1996).

1.5.3 Perth Data Visualisation

These models provide an accurate measurement and analysis of smog in Perth. A major limitation remains, however, when visualising the data on three plus-dimensional platforms. Most of the output is 2D with some cross sections for wind and temperature measurements in the vertical direction. Output from this project brings to light conditions present in the data from the DEP that would have been hard to see with 2D cross sections.

1.6 Other Smog Studies

1.6.1 Latrobe Valley

The Latrobe Valley stretches between 50 and 100 km east south-east of Melbourne, Victoria. High levels of ozone (over 100 ppb) have been observed in this valley. The model used to study photochemical smog was Langranian-based and was primarily one-dimensional (1D) and 2D (Cope *et al.*, 1988). Results of modelling

showed no impact of downwind emissions or precursors from the city of Melbourne. An airshed trajectory model, however, showed that significant measured events outside this model may have been influenced by Melbourne. It is noted that full 3D modelling is yet to be implemented.

1.6.2 Port Phillip Control Region

Port Phillip Bay and metropolitan Melbourne form the central areas of this study area (Carnovale *et al.*, 1991). The study focused mainly on the emissions of chemicals within the Melbourne metropolitan region using AUSPLUME, a plume dispersion model developed in 1986 by the Victorian Environmental Protection Authority. Mapping was generally done in two-dimensions, as emissions can be effectively sourced using a 2D plane. It was again noted that biogenic emissions remain uncertain, and that they may play a stronger role than previously thought.

1.6.3 Tokyo

In Tokyo, Japan, complicated terrain and high relief makes wind difficult to measure and model (Wakamatsu *et al.*, 1988). Very high ozone (up to 160 ppb) and nitrogen oxide levels occur in Tokyo during summer. This study concludes that 25 percent of Japan's total nitrogen oxides are generated within the Tokyo study area.

A variant of the 3D UAM was used in the photochemical smog modelling (Wakamatsu *et al.*, 1988). Multiple-day smog events previously observed were supported by this model. Multiple-day smog events are where smog forms in one day and is still present the next morning when car, industry, and biogenic emissions recommence. In Perth, multiple-day smog events are rare, except when bushfires are present. Rye *et al.* (1996) stress, however, that the potential for future events over multiple days should be watched carefully.

1.6.4 Los Angeles

The first measurements were made for photochemical smog in Los Angeles, California. It was found that anthropogenic emissions in the 1950s led to ozone concentrations ranging from 400 to 600 ppb (Elsom, 1992). Despite recent air

quality legislation and relatively reduced emissions, levels still reach unacceptably high levels (200 to 300 ppb).

1.7 Thesis Outline

1.7.1 Chapter 1

This chapter discusses some of the background to the research components of this thesis. The focus remains on Perth, with a project description and aims of this research covered. The study site is covered with conditions suitable for photochemical smog formation in Perth and elsewhere in the world.

1.7.2 Chapter 2

Chapter 2 covers the background factors involved in vegetation mapping in Perth. This includes vegetation indices and satellite imagery for extraction of vegetation information. Species and density classes to be mapped for the DEP are covered. This chapter is distinct from Chapter 5, which outlines the vegetation mapping methodology.

1.7.3 Chapter 3

Chapter 3 discusses the background to 2D Geographical Information Systems (GIS) for environmental studies. Terrain models (2.5D) for environmental applications are covered as well as are 3D and 4D GIS for environmental studies. Several applications are noted for a three plus-dimensional GIS, and the requirements for visualisation of smog plumes in Perth are covered.

1.7.4 Chapter 4

Chapter 4 outlines the test site of metropolitan Perth, Western Australia and covers computing issues such as data, hardware, and software. Test site conditions are covered. Data integrity, size and other factors to be considered, such as scale and currency, are also covered. Hardware issues discussed include platforms and configurations. Software issues covered include the operating systems, stability, performance, and capability to perform required functions.

1.7.5 Chapter 5

Chapter 5 details the methodology used in the 2D vegetation mapping. Image processing techniques and choice of methodology are covered. Image classification methods are investigated and generalisation of data from 30 m pixels to 3 km pixels is covered.

1.7.6 Chapter 6

Visualisation of photochemical smog is discussed in Chapter 6. Integration issues of the digital terrain model into the 3D and 4D visualisation are covered. The 3D plume creation within Voxel Analyst (Intergraph Corporation, Huntsville, Alabama, USA) is covered with the 4D animation throughout March 16, 1994.

1.7.7 Chapter 7

Chapter 7 documents the results and conclusions obtained throughout the research as well as future recommendations. The vegetation mapping results are shown through ground truth sites and confusion matrix (accuracy) statistics. The multi-dimensional visualisation is examined for areas of error propagation and visualisation effectiveness.

Chapter 2

VEGETATION MAPPING IN PERTH

2.1 Introduction

The process of mapping vegetation can be greatly aided by interpretation of air and satellite-based images. These images (often captured in multiple spectral bands) can be used to delineate a variety of vegetation types based upon species and/or structure. Further, the use of multi-spectral data with supervised and unsupervised classification can be applied to highlight certain features of interest (such as pine forests), thus aiding the mapping process.

By breaking the vegetation down into component species, mapping of biogenic emissions can be greatly improved. This can be performed through the use of supervised classifications and will allow for vegetation inventories to be produced quickly and efficiently.

Density of vegetation can be derived through a combination of field data and common indices such as the Normalised Difference Vegetation Index (NDVI) and the Leaf Area Index (LAI, a measure of vertically projected foliage). These satellite derived densities are useful for many vegetation studies and will be the base for vegetation density mapping in Perth.

Vegetation mapping of species in Perth includes examining several types of mixed and non-mixed vegetation to produce nine classes. Vegetation density mapping in Perth includes six differing density classes to be mapped. These two sets of class data will cover the biogenic emission classes used by the DEP photochemical smog model.

2.2 Satellite Imagery for Vegetation Mapping

Methods of processing remotely sensed imagery that have found particular application to vegetation mapping include classification (the cross correlation of various bands) and the application of band ratios. Several ratios have been tested; however, Tucker (1979) using Landsat Multi Spectral Scanner (MSS) data, found the red and near-infra-red ratio was seven to 14 percent better at detection of vegetation than the green/red band combination methods previously used for vegetation detection. The main vegetation component that the band combinations detect is the green leaf biomass or green leaf area. These ratios are primarily used for vegetation density measurement.

Platforms such as the Advanced Very High Resolution Radiometer (AVHRR) have proved efficient at mapping vegetation at global and continental scales (Tucker *et al.*, 1985; Goward *et al.*, 1985; Justice *et al.*, 1985; Kogan, 1991; Nogi *et al.*, 1993; Kaufman *et al.*, 1992). The AVHRR is a National Oceanic and Atmospheric Administration (NOAA) satellite and provides pixel resolutions of one and four kms. For continental mapping of vegetation, NOAA data has been used to calculate the Global (or Green) Vegetation Index (GVI). The GVI, with its 4 km pixels, can be applied to forest ecosystem modelling and atmospheric emissions of vegetation at a global scale (Gaston *et al.*, 1997).

The scale of mapping with the systems such as AVHRR and indices such as GVI may prove efficient for the Perth metropolitan region. Yet, due to urban influence, the pixels would not have been suitable for detecting changes over smaller areas of vegetation mixed with roads and buildings. It should also be noted that Beard's vegetation inventory for Perth may have been just as accurate as Landsat TM data as the satellite data accuracy may be reduced by generalisation. Research focused on the TM dataset instead of Beard's vegetation maps by request from the DEP, so that when they improve smog modelling resolution, the methodology and data can be used without generalisation.

Higher resolution multi-spectral imagery available from platforms such as Landsat MSS (80 m pixels), Landsat Thematic Mapper (TM) (30 m pixels), and Satellite Pour

l' Observation de la Terre (SPOT) (20 m pixels) have been investigated for larger scale data sets (Gjertsen, 1993; Luman and Ji, 1995; Coppin and Bauer, 1992; Matthews, 1983; Peterson *et al.*, 1987). Vegetation mapping with SPOT data is generally improved over mapping performed using TM data, particularly where heterogenous areas of vegetation are found, or where outlying pockets of vegetation exist (Gjertsen, 1993). All of these platforms exhibit improved results when compared to AVHRR data.

Building a knowledge base into a classification system for remotely sensed imagery can improve mapping accuracy. Kimes (1991, p. 2299) focused primarily on "spectral and directional reflectance relationships" to improve vegetation class mapping. Results were promising for the reflectance relationships established; however, when developing a knowledge base, considerable time was spent achieving semi-significant results. This limitation may be overcome with future knowledge-based mapping using a GIS which incorporates a *knowledge layer* into processing algorithms.

The scale of remotely sensed data for vegetation mapping is important because using a large pixel size may not be suitable for urban or mixed species and cover. Factors such as the optical properties of vegetation have been investigated, and the effect of scale on NDVI and LAI have been shown to change accuracy of final maps (Friedl *et al.*, 1995; Moody *et al.*, 1995; Goel and Qin, 1996).

2.2.1 Biogenic Emissions and Biomass

Several studies have measured the total biomass of vegetation and attempted to measure and predict evaporation of water to investigate atmospheric interactions (Gholz *et al.*, 1997; Montieth, 1976; Gholz, 1982; Running *et al.*, 1989). Leaf biochemistry was correlated to the spectral properties of vegetation for remote sensing (Jacquemond *et al.*, 1994).

Internal leaf pigments and cell structure, as well as reflection or scattering of light, have been addressed in the literature (Buschmann and Nagel, 1991; Maracci *et al.*,

1991). Ultraviolet light effects on vegetation are also important for remote sensing of vegetation due to absorption and reflection characteristics (Mazzinghi *et al.*, 1994).

Three notable remote sensing studies concentrated on the contribution of chlorophyll to vegetation detection (Gitelson *et al.*, 1996; Kharuk *et al.*, 1994; Kim *et al.*, 1993). These studies focused on the range of red and near infra-red band wavelengths and found that chlorophyll reflectance can range from 550 nm to 700 nm in deciduous and tobacco plants. The absorption range of chlorophyll was not covered, but needs to be distinguished from the reflectance range for vegetation detection. This is an important aspect of vegetation detection from remote sensing.

2.2.2 Vegetation Indices

One form of a vegetation index is a band ratio of the red band with the near infra-red band. An abundance of indices are available for detection of vegetation from remote sensing (Elvidge and Chen, 1995; Jackson, 1983). In its simplest form, the division of the near infra-red band by the red band correlates to vegetation density and health (greenness). Other more advanced forms of indices include corrections for the influence of soil and atmosphere.

Generally, most vegetation indices are ratios that eliminate shadowing effects through highlighting the difference in reflectance between two image bands. Removal of shadow and albedo effects from vegetation indices can offer improvements in classification (Huemmrich, 1996; Qi *et al.*, 1995).

The Leaf Area Index (LAI) is one property being measured in remote sensing using vegetation indices. The principal of LAI is to measure the ratio of the total leaf area to the ground surface area within an image scene. This variable is an important property of vegetation reflectance and depends upon the radiometric and geometric lighting effects of the scene, as well as the internal leaf optics and the layers (PVF) of vegetation that the light must penetrate (Baret and Guyot, 1991).

The ability of vegetation to store carbon can also be measured with the LAI, although it is widely known that carbon measurements can be difficult to obtain with LAI

(Badhwar *et al.*, 1986). Investigation of ground-based measurements, low-flying helicopter data, and satellite data was performed during this study. This research shows that data can be scaled from ground measurements to satellite platforms if due consideration for carbon storage effects and seasonal variation is given.

Using a known test site for vegetation mapping of coniferous forests shows that the LAI is not completely responsible for changes in spectral responses of pixels (Peterson, *et al.*, 1987). Cleavers (1988) demonstrate a LAI measurement system for agricultural crops that takes into account soil moisture, sun, and satellite sensor angles. The soil adjustment derived was found to be effective across a range of moisture categories.

Leaf area can also be investigated in the field by sampling ground cover or *litter fall* (leaves, twigs, branches fallen from trees). Further, calculations of tree basal area against leaf area, based upon measurements by portable radiometers, can be used to calculate a LAI for any site (Pierce and Running, 1988). The use of radiometrics (and light metres) have also been important for quantifying field measurements of remote sensing studies.

The estimation of leaf area is affected by the density of vegetation cover. This means that multiple layers of leaves, branches, and trunks (i.e. density) are a factor in light absorption and reflectance by a canopy. A thick vegetation canopy can mean a very high leaf area index, thus, the density of a canopy must be considered when LAI studies are performed (Price and Bausch, 1995).

The Soil Adjusted Vegetation Index (SAVI) and Transformed Soil Adjusted Vegetation Index (TSAVI) incorporate a fixed soil line factor or a variable soil line factor, respectively, in the calculation of vegetation (Huete, 1988; Qi *et al.*, 1994). Both studies show that by using the known soil influence, improved detection of vegetation can be obtained in varying soil moisture and vegetation conditions (Cleavers, 1988).

Most studies of the soil background factor in remote sensing have been for investigations related to agricultural cropping (Richardson and Weigand, 1977; Pinter *et al.*, 1994). Regional forest mapping should also investigate the influence of soils on image data (Huete *et al.*, 1985).

A range of vegetation indices is covered in Table 2.1, from which four have been chosen for use during this research. These four indices are the Normalised Difference Vegetation Index (NDVI), the Infra-red Percentage Vegetation Index (IPVI), the Atmospherically Reduced Vegetation Index (ARVI), and the Modified Soil Adjusted Vegetation Index 2 (MSAVI2).

The main problem in using vegetation indices for detection of density is that most were developed for use in cereal crop studies. These indices, when applied to other vegetation types, do show high correlation but are not finely tuned to the response of the vegetation type being detected (Wallace, 1999). A more suitable solution for this study would have been to develop an Australian native forests and scrublands index, but this was well outside the scope of this research. By using several indices and choosing the one with the highest correlation against ground truth, the application of standard vegetation indices remained sufficient.

Some problems also emerge when using vegetation indices for large areas. That is, areas that cover several climatic zones. Matheson and Ringrose (1994) point out that indices apply the same association across climatic zones, and that variation in green vegetation cover may not be detected due to lack of flexibility in the indices. This study was entirely within one climactic zone, so this limitation to vegetation indices was not an issue.

The four vegetation indices used in this study (NDVI, IPVI, ARVI, and MSAVI2) were chosen to represent general indices and indices with correction for soils and atmosphere. The four indices will be tested to determine the best method for evaluating vegetation density in Perth and are described below.

Index and Source	Name	Formula
SR (Huemmrich and Goward, 1992)	Simple Ratio	NIR / RED
NDVI Rouse *et al.* (1973)	Normalised Difference Vegetation Index	NDVI = (NIR-R) / (NIR+R) See (a) below
RVI Jordan (1969)	Ratio Vegetation Index	$RVI = \frac{NIR}{RED}$
WDVI (Clevers, 1988)	Weighted Difference Vegetation Index	$WDVI = \rho NIR - \gamma \rho RED'$
SAVI Huete (1988)	Soil Adjusted Vegetation Index *	$SAVI = \frac{NIR - RED}{NIR + RED + L}(1 + L)$
TSAVI Baret *et al.* (1989)	Transformed Soil Adjusted Vegetation Index **	$TSAVI = \frac{a(NIR - aREd - b)}{RED + aNIR - ab}$
SAVI2 Major *et al.* (1990)	Soil Adjusted Ratio Vegetation Index **	$SAVI_2 = \frac{NIR}{(RED + b/a)}$
IPVI (Crippen, 1990)	Infra-red Percentage Vegetation Index	IPVI = NIR / (NIR + R) See (b) below
PVI Richardson and Weigard (1977)	Perpendicular Vegetation Index **	$PVI = \frac{NIR - aRED - b}{\sqrt{1 + a^2}}$
DVI Tucker (1979)	Difference Vegetation Index	DVI = NIR - RED
ARVI Qi *et al.* (1994)	Atmospherically Resistant Vegetation Index	ARVI = NIR - RB / NIR + RB See (c) below
1DL_DGVI Elvidge and Chen (1995)	First Order Derivative Green Vegetation Index using local baseline ***	$= \sum_{\lambda 1}^{\lambda n} \lvert \rho'(\lambda_i) - \rho'(\lambda_i) \rvert \Delta_i$
1DZ_DGVI Elvidge and Chen (1995)	First Order Derivative Green Vegetation Index using zero baseline ***	$= \sum_{\lambda 1}^{\lambda n} \lvert \rho'(\lambda_i) \rvert \Delta_i$
2DZ_DGVI Elvidge and Chen (1995)	Second Order Derivative Green Vegetation Index using zero baseline ***	$= \sum_{\lambda 1}^{\lambda n} \lvert \rho''(\lambda_i) \rvert \Delta_i$
MSAVI2 Qi *et al.* (1994)	Modified Soil Adjusted Vegetation Index Two	$MSAVI2 = (1/2)(2(NIR + 1) - \sqrt{(2(NIR) + 1)^2 - 8(NIR - R)})$ See (d) below
GVI Gaston *et al.* (1997)	Global Vegetation Index	NOAA product derived from NDVI

* L is a soil adjustment factor (in SAVI, it ranges from 0 to 1 and is normally used at .5)

** a and b are rock soil baseline from NIR vs. RED

*** i = band number, λ_i = center wavelength at ith band, λ_1 = 626nm, λ_n =795nm, ρ' = first derivative reflectance, ρ'' = second derivative reflectance

Table 2.1 Commonly used vegetation indices (partially adapted from Elvidge and Chen, 1995)

(a) Normalised Difference Vegetation Index (NDVI)

The most common form of vegetation index is the Normalised Difference Vegetation Index or NDVI (Tucker *et al.*, 1985; Nogi *et al.*, 1993). The NDVI is basically the difference of the red (R) and near-infra-red (NIR) band combination divided by the sum of the red and near-infra-red band combination or:

$$NDVI = (NIR-R) / (NIR+R) \quad (2.1)$$

This index has a range of -1 to +1.

(b) Infra-red Percentage Vegetation Index (IPVI)

This index is computationally faster than the NDVI and scales data in percentages. It eliminates negative numbers, and output data ranges from zero to one (Crippen, 1990). This index is effectively the same as NDVI and may be preferred with large data sets or slow computers. The IPVI is calculated as:

$$IPVI = NIR / (NIR + R) \quad (2.2)$$

This index has a range from 0 to +1.

(c) Atmospherically Resistant Vegetation Index (ARVI)

Atmospheric disturbance in acquisition of satellite imagery is obvious when clouds mask part of the image; however, other invisible atmospheric processes are at work and need to be modelled (Nogi *et al.*, 1993). It was shown that by adding parameters to the NDVI, an enhanced remote sensing product can be used (Kaufman *et al.*, 1992).

$$ARVI = NIR - RB / NIR + RB \quad (2.3)$$

where RB = RED - gamma (R - B) and gamma is usually equal to 1.0 (equivalent to NDVI)

This index has a range of -1 to +1.

(d) Modified Soil Adjusted Vegetation Index 2 (MSAVI2)

This index is used without a standard Kauth-Thomas (KT) soil line (Qi, *et al.*, 1994). Problems in software functionality were encountered with KT soil lines in this research, so the method without KT soil lines was preferred.

$$MSAVI2 = (1/2)(2(NIR+1) - \sqrt{(2(NIR)+1)^2 - 8(NIR-R)}) \qquad (2.4)$$

This index has a range from -1 to +1.

2.2.3 Studies in Western Australia

In semi-arid regions such as Western Australia, areas of sparse vegetation can be misclassified if too much background-soil spectral response is present (Huete *et al.*, 1994). Strategies to remove the soil background effects can be undertaken by using a tasselled cap transformation (Kauth and Thomas, 1976). This method, which creates a Soil Brightness Index (SBI), can be plotted to obtain an improved discrimination between the background soil spectra and vegetation.

The most extensive forest cover type in Western Australia is the jarrah, or *Eucalyptus Marginata*, that covers much of the south west corner of the state and extends through the western portion of the study area. The distribution of nutrients within a typical jarrah stand near Dwellingup (just south of study area) was measured. This included leaves, trunks, bark, branches, ground litter, and soil nutrient levels (Hingston *et al.*, 1980/1981). This information was used to aid in vegetation classification. Most of the vegetation in the Perth region is jarrah. No nutrients were measured during this research.

The Department of Conservation and Land Management has defined objectives for mapping over one million hectares of the jarrah forest in Western Australia. The conceptual data capture system used large scale aerial photography and Global Positioning Systems to capture data for integration into a GIS (Spencer *et al.*, 1997;

Sun *et al.*, 1996). If the DEP model for photochemical smog required high resolution mapping, this would have been a good method, yet model requirements remain at a level suitable for satellite-based methodologies.

2.3 Vegetation Mapping in Perth

2.3.1 Species Investigated

The vegetation classes here are defined by the DEP for showing the dominant species emission rates (Rye *et al.*, 1996). Combinations of species within certain classes makes mapping more difficult, as spectral response can be found within classes that are not wholly distinct.

It should be noted that many urban features such as roads, buildings, airports and even clearing for agriculture and recreation are found within the Perth Metropolitan region. There are no DEP defined classes for these urban features in the species categories, but future mapping may include classes for urban/other (non-vegetation).

The nine classes of species covered a wide range of vegetation types and conditions within Perth. The water class is easily detected, and little will be said here about this class. Vegetation classes and their percentage of study area coverage are:

- Banksia low woodland (Figure 2.1) ~ 6 percent of the study area,
- Pine plantation (Figure 2.2) ~ 2 percent of the study area,
- Coastal heath (Figure 2.3) ~ 3 percent of the study area,
- Tuart woodland (Figure 2.4) ~ 4 percent of the study area,
- Open marri woodland (Figure 2.4) ~ 7 percent of the study area,
- Jarrah/marri forest (Figure 2.4) ~ 30 percent of the study area,
- Banksia and sheoak woodland (Figures 2.1 and 2.5) ~ 7 percent of the study area,
- Swampy, sheoak and melaleuca (Figures 2.5 and 2.6) ~ 3 percent of the study area,
- Jarrah and tuart with sheoak and banksia (Figures 2.4 and 2.5) ~ 5 percent of the study area and
- Water - ~ 33 percent of the study area.

Figure 2.1 Banksia (low woodland)

Figure 2.2 Pine (plantation)

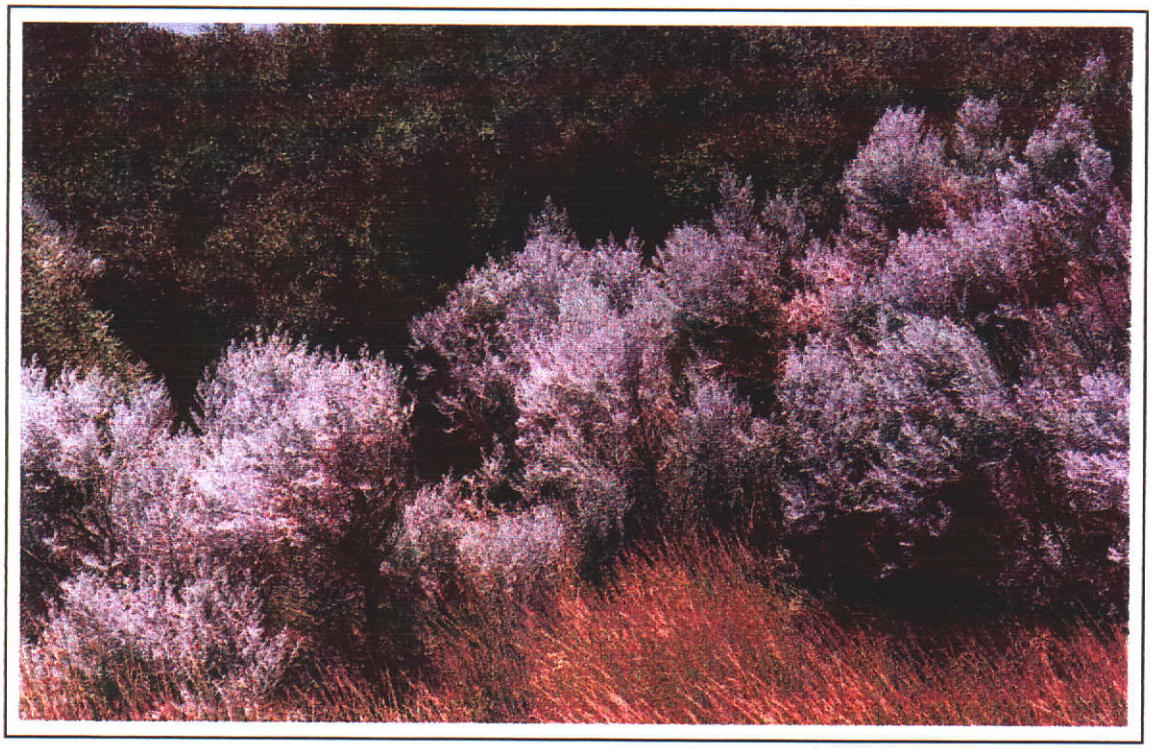

Figure 2.3 Coastal heath

Figure 2.4 Eucalyptus - tuart (woodland), jarrah and marri are similar in appearance

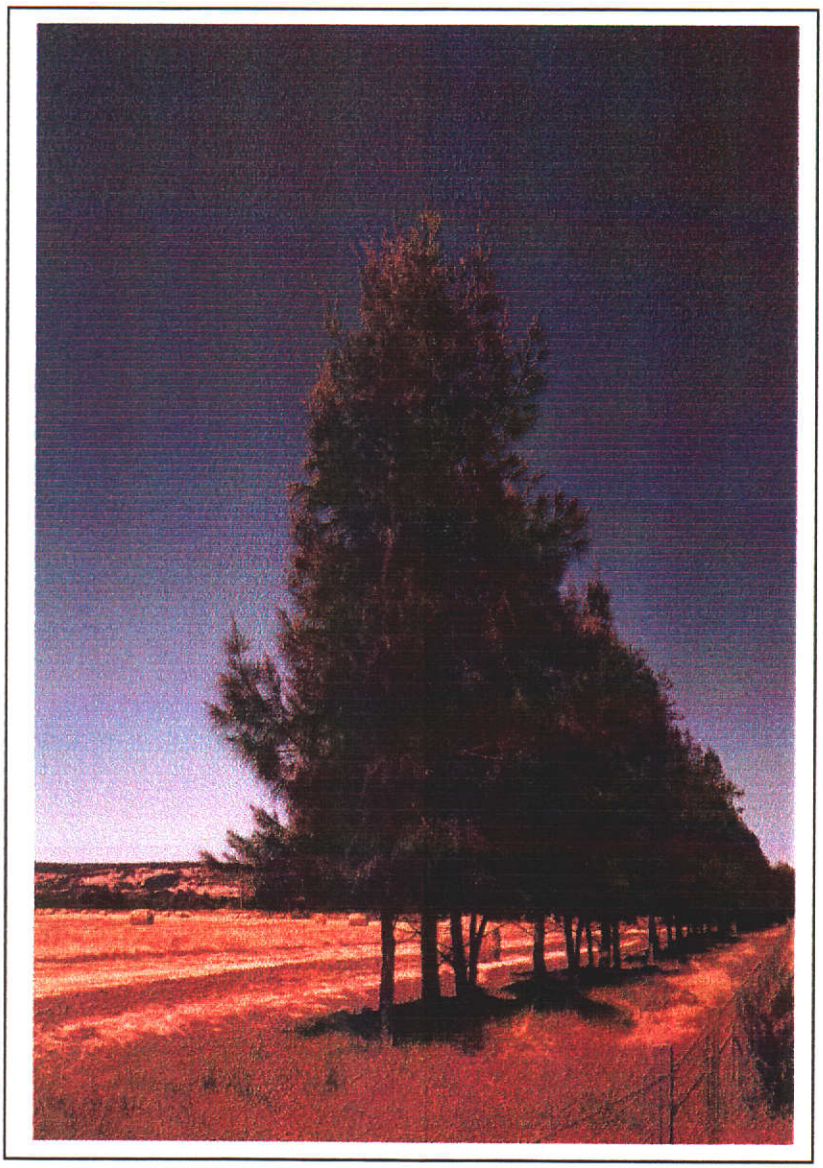

Figure 2.5 Sheoak (swampy, sheoak and melaleuca)

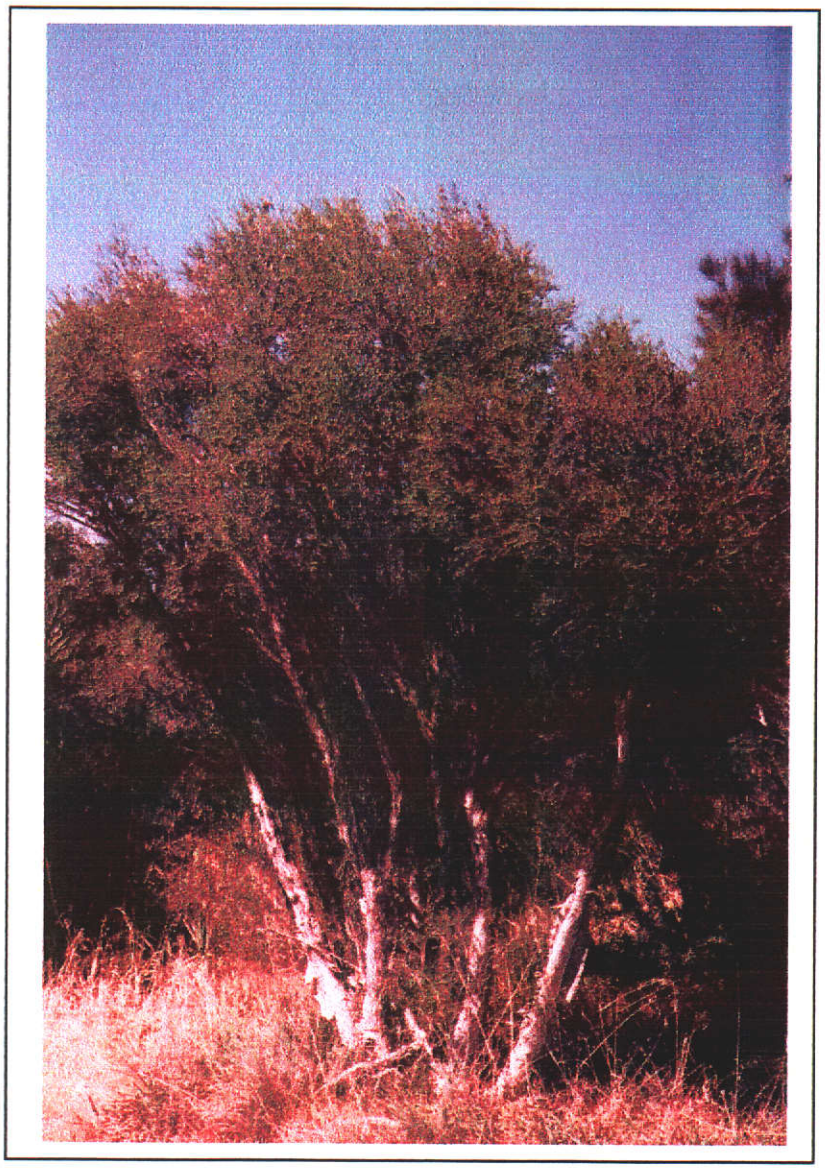

Figure 2.6 Melaleuca (swampy, sheoak and melaleuca)

As defined by Cope and Ischtwan (1995), jarrah and tuart with sheoak and banksia are equal to a jarrah and marri scrub woodland for Perth photochemical smog inputs. Also, tuart woodland is deemed equal to an open marri woodland for biogenic emission modelling in Perth. The mapping performed here did not combine these classes, as the DEP model will incorporate this information by later reassigning classes based on equivalent species emissions.

There are three Eucalyptus species in the class list: tuart, jarrah, and marri (Figure 2.4). These species are similar in appearance from a distance; however closer inspection reveals differences. To distinguish between the three species, bark, leaf size, leaf shape, and fruits or seeds must be compared (Cronin, 1988).

Species identification was aided through three key guides to Australian plants, shrubs, and trees (Cronin 1988; Holliday and Watton 1989; Newbey 1968). These guides were useful for the field work undertaken in this research. The vegetation classes defined above contained a variety of other vegetation species mixed with the dominant species. The resulting classes reflect dominant species within the region, and field work notes show a mix of vegetation even within the most homogeneous areas.

2.3.2 Percentage Canopy Cover (Density)

Identification of percentage of canopy cover or density is important for quantifying the total biogenic emissions from each species. Defining this attribute of Perth's vegetation is dynamic and complex due to plant growth, clearing, and fires. Throughout the year, bushfire smoke is visible, and there have been 150 fires in the Mundaring shire alone since the imagery was taken (Bushfires Report, 1997).

The cover classes (projected vertical foliage) mapped are as follows:

- 100 percent to 81 percent ~ 8 percent of the study area,
- 80 percent to 61 percent ~ 10 percent of the study area,
- 60 percent to 41 percent ~ 23 percent of the study area,

- 40 percent to 21 percent ~ 17 percent of the study area,
- 20 percent to 1 percent ~ 11 percent of the study area, and
- Zero cover ~ 31 percent of the study area (mostly water).

The definition of the classes and calculated emission rates assigned to each class were developed by the DEP (Cope and Ischtwan, 1995). Field estimates were used to correlate data with vegetation detection algorithms or vegetation indices.

2.4 Summary

Various vegetation discrimination methods can be used on remotely sensed data, but most are built upon the red near-infra-red band correlations. The use of classification, indices, and generalisation are important features of data extraction from satellite platforms.

Final biogenic emissions can be accurately mapped with due consideration of variables unique to this study area. Data then can be obtained for vegetation discrimination with satellite extraction methods. By mapping vegetation from satellites, the DEP can quickly and efficiently update their biogenic inputs into photochemical smog formation in Perth.

Species mapping in Perth involves nine classes of various mixtures of vegetation plus one class for water. These nine species classes cover the majority of biogenic emissions in the Perth region. Density maps give the relative amount of emissions of the species types and will be used to show high emission areas by the DEP.

By using remote sensing methodologies to create inputs into the DEP photochemical smog model, an improved biogenic emission inventory is gained. Previous hand-drawn maps of vegetation in Perth should now be replaced by satellite-based extraction methods in the future.

Chapter 3

TWO, THREE, AND FOUR-DIMENSIONAL GIS FOR ENVIRONMENTAL STUDIES

3.1 Introduction

Two-dimensional mapping and analysis is performed on a Cartesian (x, y) coordinate system. Two and one half-dimensional mapping and analysis uses these Cartesian coordinates but adds an attribute such as height to achieve the extra half of a dimension. This is sometimes incorrectly referred to as 3D mapping and analysis. Three-dimensional GIS uses the concept of volumetric objects, and 4D GIS adds time to volumetric analysis and mapping.

Two-dimensional mapping of environmental phenomena has been used with significant results. There are some advantages and disadvantages of 2D GIS for representing data which are inherently 3D and 4D. Map components include vector objects (points, lines, polygons) or raster grids which are used to display phenomena.

Mapping of environmental phenomena in 2.5D deals primarily with surfaces. In particular, relief surfaces. These resulting surface interpretations can represent the natural terrain of the earth's surface, which is useful in environmental studies. Raster grids with elevation values, vector point elevations, and contour terrain models can be used for surface generation. These surfaces can be animated (surface fly-throughs or time lapse) and are called three and one half-dimensional (3.5D).

Visualisation of geographical data can be performed with an emphasis on 3D and 4D methods and output through animation and dissemination through the World Wide Web. Resulting visualisations will allow a wider audience to see environmental phenomena and their impact on humans, flora, and fauna. Five-dimensional (5D) GIS can be used, (defined as 4D plus attributes), but the focus here remains on purely spatial dimensions.

3.2 Two-Dimensional GIS

Two-dimensional mapping is based on a Cartesian coordinate system and is usually tied to a mapping datum. Davis and Williams (1989, p. 51) back this by stating "These [coordinates] have been part of mapping since its inception and they form the fundamental base on which to present geographical data." Two-dimensional mapping is limited to representation of data on planar surfaces. Elevation is represented through the use of attribute values.

Further dimensions such as z (height or volume) and t (time) can be implemented using cross sections within a 2D system to simulate pseudo-3D maps and representations. These cross sections can also be used along with fence diagrams to improve representation. Fence diagrams allow interpolation and calculation of phenomena within a specified area or *fence* by using the known components of the fence sections or cross sections. Mapping of x, y, t over several time slices can be an efficient way to represent dynamic phenomena as well. Other combinations can include x, z, t and y, z, t.

This multi-dimensional structure allows for mapping and modelling of a large number of geographical phenomena. Common applications include land database systems, utilities mapping, asset collection, social and census mapping, and transportation network flow. Other applications, such as mining, hydrology, and environmental modelling, have crossed over the 2D boundary into 3D modelling.

A wide range of new remote sensing products can easily be incorporated into 2D GIS (Turner, 1997a). Remotely sensed imagery is generally used to produce maps in two-dimensions (3D if time lapse is used); however, surfaces can be extracted from stereo pair imagery to represent terrain (2.5D).

3.2.1 Vector Systems

Vector data structures represent features as a series of discrete linearly connected points within a database. Building upon the points, connections between points are made to represent lines (vectors). A series of lines can then connect to form

polygons. Point, line and polygon features also contain associated data such as attributes which are used to describe the characteristics of features they represent. These basic features are used to build topology between objects and, therefore, define their spatial relationship. This spatial foundation for storing objects allows for query of information and attributes attached to those objects (Worboys, 1995).

3.2.2 Raster Systems

Raster data structures are generally quite simple and are comprised of arrays of pixels. These pixels or cells hold values about the attribute being mapped or modelled. Positional information is stored in rows (x) and columns (y), and topology is inherent in the data structure (Worboys, 1995). Cells of varying shape can be accommodated within the data structure; this allows the user to reflect the sampling density of the data obtained in the database.

3.2.3 Collections of Studies

Previous 2D GIS studies fill many volumes. Most books like Introductory Readings in Geographical Information Systems, (Peuquet and Marble, 1990), Spatial Analytical Perspectives on GIS (Fischer *et al.*, 1996) and Principles of Geographical Information Systems (Burrough, 1986) give an insight into various GIS topics using 2D systems. Journals such as the International Journal of Geographical Information Systems, Cartography, and Transactions in GIS cite many studies using predominantly 2D techniques. Trade journals, such as GIS World (USA) and GIS User (Australia), are laden with articles pertaining to 2D studies.

Two-dimensional studies are frequently found in conference proceedings, including the Urban and Regional Information Systems Association (URISA) (USA), the Australasian Urban and Regional Information Systems Association (AURISA), and the Western Australian Land Information Systems (WALIS) Forum. Finally, even though most studies available on the World Wide Web are written with little editorial checking, there are a very large number of papers on the web. No web addresses are listed here due to the dynamic nature of web sites and addresses, but good search engines can find many GIS sites and links to other GIS sources.

3.2.4 Advantages

A 2D GIS has the advantage over three-plus-dimensional GIS that the data structure is relatively simple and data volumes relatively small. Data output can be plotted without undue difficulty representing objects. This is unlike volumetric objects (3D) which can be difficult to plot efficiently.

Two-dimensional attribute query is a key component of systems that has been established for quite some time. The information in GIS means that data about geographical phenomena can be queried, selected, analysed, and plotted. Spatial query of attributes allows the user to select phenomena based upon their locational characteristics then display them in colours or sizes based on those characteristics.

Cross sections of data, or *stacked layers*, are a viable method for interpolating 2D slices through a 3D body. Some volumetric capability is present; however, a simple and relatively efficient representation can be made. Even with complex 3D geology, cross sections have been used in a 2D GIS and CAD study to link with cross section data to provide some insight into regional 3D geology (Shetselaar, 1995).

Two-dimensional GIS has proven beneficial for data preparation for a volumetric GIS. By using slices of a 3D body and some macro programming, 2D data structures can be reworked for input into 3D water quality models (Calkins and Fuxiang, 1994).

A further application of 2D systems shows the 2D cross section of geology in different windows with top, bottom, left, right, front, and back views. This project uses several 2D coordinate pairs to map features in x, y at a certain z level (e.g. x, z plane at y level) (Mason, 1997). The output of this cross section data was used for visualising mine shafts in a proposed underground toxic waste dump.

Two-dimensional mapping on x, y with a t (time) instead of a z was applied to mapping climatic data with effective results (Lin and Choi, 1994). This spatio-temporal or STIN (Spatio-Temporal Intersection) data structure plotted temperature on x and y coordinates with time on the z dimension. Multiple variables were also visualised over time and plotted on a 3D perspective view.

3.2.5 Disadvantages

The lack of proper spatial statistics in 2D (as well as 3D and 4D) software, such as regression analysis and confidence levels, is one limitation noted by Bailey and Gatrell (1995). Another disadvantage includes the lack of calculus for advanced modelling capabilities. Statistics are starting to emerge in 2D software such as IDRISI (IDRISI Project, Clarke University, Boston, Massachusetts, USA), Arc/Info (Environmental Systems Research Institute, Redlands, California, USA), MapInfo (Troy, New York, USA) and the Modular GIS Environment (MGE - Intergraph, Huntsville, Alabama, USA), so this disadvantage should soon be reduced with advanced modelling a short step behind.

Environmental modelling requires more than a 2D system to capture truly volumetric 3D and temporal 4D phenomena. Volumetric phenomena that often occur in nature (e.g. smog) cannot be fully represented with a 2D system. Two-dimensional systems also lack the ability to calculate volumes and show interaction of objects in true 3D and 4D space.

Further disadvantages include plotting of volumetric slices as compared to a visual volumetric scene. The temporal nature of phenomena is difficult to express on hardcopy maps, while softcopy visualisation offers full 4D animation.

3.3 Two and One Half-Dimensional GIS

Two and one half-dimensional GIS generally refers to the modelling of surfaces or terrain through x, y, and attribute values. Fritsch (1990) proposes that 2.5D terrain models are no longer sufficient for mapping some volumetric phenomena with the appearance of newer full volumetric capabilities. This study focuses primarily on 2.5D surfaces. It refers to Digital Elevation Models (DEMs) as raster and Triangulated Irregular Networks (TINs) as vector means of handling elevation data.

These terrain representations have been used extensively for *line of sight* or visibility studies. Calculations can be performed to generate a viewshed from any particular point on the model. In addition to view sheds, urban areas with 3D building objects

can be used for planning and engineering works. Landscape changes, though usually slow to occur, can also be modelled (Hoinkes and Lange, 1995). A full range of 2.5D issues and methods for building terrain models is covered in Burrough (1986) and Clarke (1990).

Other applications for terrain models include slope and aspect studies for showing high erosion risk areas. Erosion and slope length calculation are also important tools for terrain modelling (Hickey *et al.*, 1994; Hickey and Jankowski, 1997). Soil properties and geology can be modelled as well as potential slope failure. Aspect or flow direction of a particular point can be important for sun exposure to vegetation. Hydrological modelling is dependent upon a catchment to predict rainfall run off and loss through evaporation and infiltration. Potential fire spread is also dependent upon terrain surfaces, and valleys that might increase wind flow can be mapped. Full 3D mapping remains better, however, at representing any phenomena above the terrain surface (e.g. air-quality) or below the terrain surface (e.g. salinity).

Digital Elevation Models (DEMs) can be generated from analogue stereo photography or digital imagery (Gugan and Dowman, 1988; Petrie and Kennie, 1990). The digital remotely sensed data type is already gridded, so the format can be easily converted to an elevation value, rather than the normal pixel brightness value. Analogue photographs must be scanned and rectified for digital processing. Software is available that can automatically generate a stereo perspective from one image allowing the user to extract potentially detailed DEMs (depending on the scale of imagery and ground control) (Jensen, 1996).

The use of 2.5D representation of surfaces has some disadvantages for environmental modelling. The most obvious being the lack of volumetric capabilities other than cut and fill type volumetrics. Many surface representations are derived from interpolation between points or contours, which may also lead to questionable results depending on the data sample size. The interpolation process may also be inefficient in modelling terrain. Essentially being only a 2D representation with a height attribute, true volumetric capabilities are not available; nonetheless, simple and

efficient surface generation can be valuable for investigations that do not require 3D capabilities.

The capability to model surfaces offers tremendous potential for planners, engineers and landscape architects. For example, hydrologic applications use surface modelling to calculate potential run off. The results may be used as an input into 3D models in association with 2.5D data layers to represent geology, geochemistry or other features. This data may form the basic input from which a 3D model can be generated.

3.3.1 Vector Systems

Triangular Irregular Networks and contour lines are vector representations of a surface and are classed as 2.5D representations. Regular data grids can also be used for surfaces. More commonly, however, irregular x, y point files with a z height can be turned into surfaces. Contours are also valid for creating TINs. Break lines may be used as hard breaks in the interpolation surface. They are commonly places where there is a radical change in slope. This is primarily due to peaks, pits, ridges, and valleys (Kummler, 1994).

3.3.2 Raster Systems

Raster terrain environments are handled by DEMs, which are a 2D grid-based data structure where each grid cell value represents a terrain height. DEMs are often referred to as 3D; however, the assigning of an attribute for height represents surfaces that are only 2.5D (i.e. not volumetric).

An important study of some 50 test sites compared TINs and DEMs to determine which was more efficient for representing terrain at a set scale (Kummler, 1994). Kummler indicated that TIN and DEM interpolation methods depend on several variables (sampling density, area size, and changes in terrain). It was shown that DEMs are generally more efficient for representing terrain, yet TINs look better. So often, a choice of methods may be guided by such factors as software limitations, data availability in a suitable format, scale, and sampling density.

3.4 Three-Dimensional GIS

The 2D point, line, and polygon vector representation of objects now extends to include a volume element in 3D space (Kraak, 1989). However, 3D raster grids can also be used in analysis and display. The 3D grid cell or cube is referred to as the *voxel* (volumetric elements) (Jones, 1989). This voxel data structure is relatively simple, nonetheless, storage and data reduction remain key issues.

Vector structures build upon 2D methods but describe volumes via a volumetric polyhedra. These volumetric vector and raster systems evolved from early solid modelling (Mantyla, 1988). Systems required to undertake such volumetric work, must have a sound data structure and a modelling capacity that can handle the processing requirements of multi-dimensional data. Vector systems can represent edges of phenomena to be modelled much better than raster systems (Sides and Hack, 1995).

Data volume, obtainability, handling, and processing with an extra dimension of data are often difficult in a 3D environment (Van Driel, 1989). Historical uses of 3D GIS often lacked necessary computing technology to deal with the large data sets and volumetric analysis. However, current systems are appearing with enhanced tools. Combined with faster processing environments, many investigations can be readily accomplished. Future systems, with the availability of ever-increasing computing performance, will enable the development of virtual GIS worlds where objects can be picked up and examined.

The topological relationship of 3D objects is used to manipulate elements within a data base. When relationships between objects are stored with elements, a user can search for objects that have a certain spatial or adjacency relationships. This fundamental topologic search can be implemented within raster and vector data structures to highlight volumetric features along with attribute values. Objects can be represented by iso-surfaces (3D contours) of similar attribute values. This basic technique can be applied to volume calculation and object intersection operations (Smith and Paradis, 1989).

Voxel environments were originally developed for medical imaging; however, a natural adaptation to modelling other multi-dimensional objects has occurred. The conversion from medical imaging has also included the addition of attribute queries in order to analyse environmental phenomena (Knapp, 1991). Further, the attribute query system inherent in GIS is applicable to the medical imaging field. This allows spatial relationships of objects to be mapped and utilised in subsequent analysis.

Three-dimensional GIS is important for environmental phenomena as 2D studies of the earth "... have become increasingly inefficient and, in many cases, inappropriate." (Bak and Mill 1989, p. 155). Further, 3D studies must be able to handle *holes* or *voids* within volumetric bodies (e.g. caves). Finally, mathematical analysis such as buffering, overlay analysis, volume and surface area calculation, tunnelling, and modelling should be an important component of multi-dimensional systems.

Due to difficulty in obtaining sub-surface 3D data, sampling density and grid layout becomes important in underground and marine environments. This is because sampling can be expensive if a large regular grid is used for an object that covers only part of the area. Further, some field work and prior knowledge should be gained before sampling occurs to narrow down places that are not of interest (Raper, 1989b). This will eliminate those areas where the volumetric object has little impact.

The need for correct data interpolation remains a critical factor in achieving an accurate representation of objects from sampled points. Gold (1989) shows the use of point interpolation algorithms on surfaces. Even though this triangulated method was not volumetric, layers or surfaces within volumetric systems can be constructed using triangulation methods.

Building on this, kriging, and for less densely sampled areas, co-kriging can be performed on 3D data sets to achieve improved results (Leenaers *et al.*, 1989). These methods of interpolation show good estimation of interpolation weights, and error feedback given can be useful for improving interpolation (Burrough, 1986).

Computers are becoming faster at the same time that costs are falling. This gives full multi-dimensional GIS the ability to be implemented more efficiently on lower priced machines. Accuracy can be improved with denser sampling regimes and faster volumetric modelling. This is supported by several authors (Raper, 1989b; Jones, 1989; Kluijtmans and Collin, 1991; Knapp, 1991; Turner, 1994, cited in Sides and Hack, 1994, p. 151).

Davis and Williams (1989), show that this improvement in technology can be effectively negated due to increasing complexity of source code and the addition of Graphical User Interfaces (GUIs) to software. Further, inefficient code and lack of system stability (bugs) in major software releases remains a problem. Fully multi-dimensional systems are appearing even with the need for more computing resources, however, and bugs are being overcome with more research into volumetric GIS.

Some promising indications are also present for the future, in that computing tasks for most scientists are now available in personal computer environments as the computers gain more power and functionality. This lessens the need for the more expensive UNIX workstations to perform common multi-dimensional analysis (Marschallinger, 1991). This research also aims to show that by using the steadily improving and affordable PC environment, volumetric tasks can be performed effectively.

3.4.1 Raster Data Structures

The 3D raster data structure is a series of rows and columns of cubes. The relative simplicity of 3D raster grids comprised of voxels is important; however, raster volumetric environments do have some limitations (Samet, 1990a). For example, the boundary of an object can be somewhat jagged if voxel resolution is low.

Grid spacing (resolution) is an important feature of raster systems. A grid with large spacing (low resolution) may not represent elements effectively, and a grid with small spacing (high resolution) may store too much data about an object to permit efficient processing. A balance must be struck so that the grid spacing is similar to the sampling density (Eddy and Looney, 1993).

Voxel (raster) grid models can offer a flexible grid size to suit the purpose. One application is to represent horizontally layered sediments in a grid spacing that reflects the layering (Eddy and Looney, 1993). Combined representations of layers that are not uniform in size can reduce processing multiple cells that are similar. Voxel platforms also offer quick processing of data arrays (rows and columns of cells) which are easily computed.

Processing and storage requirements are large for voxel platforms. Attributes are easily handled, but not easily searched. Voxel representations can lose resolution on the edges (map boundaries) of objects with all but the highest resolutions.

The topology of voxel data is inherent in the data structure, with cell values in the grid accessible by row, column, and level (z). Searching for attribute data within a 3D grid can be enhanced with octrees (Bak and Mill, 1989). By subdividing the volumetric phenomena into octants, an octree can be used to partition the object space.

Octree subdivision is a method of data compression applied to eliminate storage of similar data for identical valued adjacent cells. If all the cells within one octant are similar, the whole octant is stored as one element. If features do not fill an entire octant, that area is subdivided by eight again until the highest resolution of storage is reached. By compressing the similar voxels, data can be reduced efficiently, yet when objects are complex, little or no data reduction may occur. Octree data structures are similar to their 2D counterpart, the quadtree (Jones, 1989).

3.4.2 Vector Data Structures

Boundary models are used to construct the outer boundary of a 3D object. These vector representations generate polyhedra which are geometric cells (either full or empty) composed of faces or facets, edges, and vertices (Hoop *et al.*, 1993; Molenaar, 1992; Molenaar, 1990; Jones, 1989; Pigot, 1992). Coordinates for the z dimension are stored within the nodes that define the vertices of the volume faces.

Attributes are handled well with vector data structures. Vector systems can better integrate the diverse nature of multi-dimensional data compared with raster systems (Youngmann, 1989). This is because raster systems must convert all data types to volumetric elements, whereas vector structures can directly use non-volumetric elements such as points and lines.

Data structures in vector format can be relatively simple for elementary objects. When complex structures are mapped in 3D, however, the inherent complexity of the data makes computation and organisation of data difficult (Youngmann, 1989).

Interpolation of 3D contours into volumetric elements can lead to complex structures and, as stated by Dobkin and Laszlo (1987, p. 90), "... can create the most exquisite garbage." This garbage is produced by lack of efficient and effective interpolation algorithms. These complex data structures can be a problem when Boolean logic is applied to volumetric objects, such as when a union or overlay is applied.

Topology of vector 3D objects is performed through facets, nodes and vertices. Binary relationships are performed between objects, such as point-to-point and solid-to-solid to find areas that either meet criteria or do not. Molenaar (1990) defined 12 conditions of topological relationships between points, lines, and faces. Molenaar (1992) furthered this work by creating the *edge* to compensate for a volume intersection with a line. The 2D concept of left-right topology of the line is extended into left-right volume of the face bordered by edges.

Many-to-one relationships exist with the edges of each facet (Hoop *et al.*, 1993). This working topology system built upon the work by Molenaar (1990; 1992), allowing points and arcs to lie within solid objects and also includes holes or islands within objects. Implementation of the Standard Query Language (SQL) for spatial query of attributes in 3D is added by Rikkers *et al.* (1994). Thematic query was not possible on a simple data set of a few geometrical shapes, lines, and points. It was shown, however, that simple spatial relationships could be correctly queried through SQL.

Samet (1990a; 1990b) explains the use of vector octrees such as the MatriX (MX), Point (P), K-D Tree, Point and Region (PR), Constructive Solid Geometry (CSG), and Polygon (PM) octrees to query spatial relationships between objects. Thus, there are emerging methodologies to allow full volumetric data sets to be queried.

3.4.3 Historical Three-Dimensional GIS

Early 3D modelling was often limited by the lack of available software for handling and displaying data. To model 3D geology, surfaces were built into crude block models (Unger *et al.*, 1989), even though they were lacking suitable voxel based data structures.

Complex data sets hampered early processing performance, and loss of data sometimes led to inaccurate results. The need for a balance in accuracy versus reduction in complexity was important for early studies (Lukatela, 1989). Today, this balance must still be maintained, even with higher resolution data sets and faster computers.

Early models were often limited in the number of points or cells that could be handled (Broome, 1992). However, custom-designed software proved valuable for mapping in 3D. Further, work was often performed on databases with no means of visualising 3D data other than simply examining arrays of numbers in a database.

Early work was performed to represent 3D objects. Primitive Instancing (PI) defines volumetric objects by building a series of simple shapes such as cubes, rectangles, balls and cones. Spatial Occupancy Enumeration (SOE) uses fixed sized cells, while Cell Decomposition (CD) uses cells with differing sizes and shapes. Boundary Representation (BR) is more commonly used and defines an object by its boundary. Constructive Solid Geometry (CSG) is similar to PI except that it adds geometric calculations (Fritsch, 1990). Another method of *sweeping* was used. This method is similar to breaking a box down into a flat plane by laying the panels flush with the plane (Samet, 1990b) (see Figure 3.1).

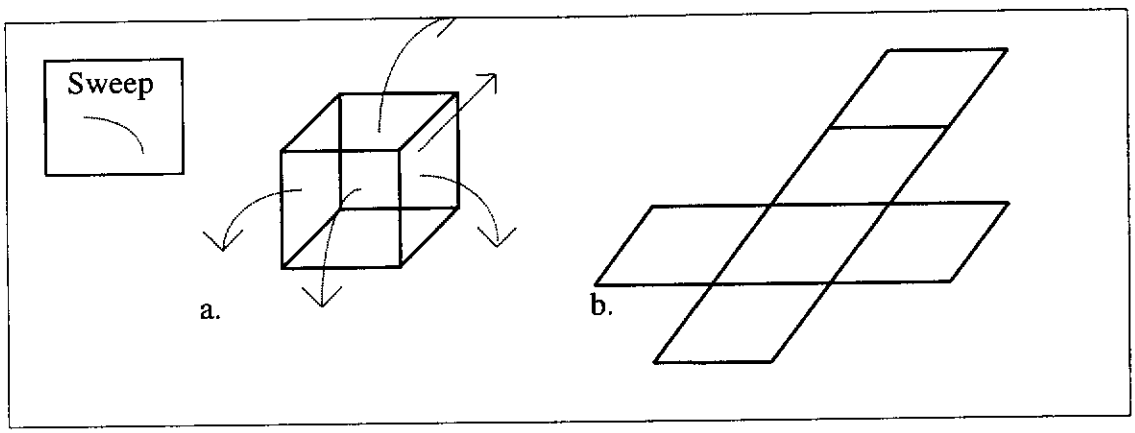

Figure 3.1 Sweeping method to decompose a box into a single plane (a. before sweeping, b. after sweeping)

Much work has been performed on edges, facets, and vertices for representation of 3D objects (Molenaar, 1990; Molenaar, 1992; Dobkin and Laszlo, 1991; Hoop *et al.*, 1993; Rikkers *et al.*, 1994). A further model uses tetrahedrons to simulate 3D buildings (Kraak and Verbree, 1992). This model uses aerial photography to construct the x, y, and z coordinates of buildings, yet no topology exists.

Computer Aided Design (CAD) was often used for early 3D investigations. However, shortfalls are noted by Cambray (1993, p. 221): "Unfortunately [no CAD models] exist [that are] perfectly adapted to 3D modelling in GIS." Three-dimensional CAD programs are generally used for creating objects, whereas geoscience modelling analyses and explains objects that already exist in nature (Renard and Courrioux, 1994).

Three-dimensional CAD programs (e.g. AutoCad, Microstation) also build objects from simple primitive shapes but lack the crucial topology of GIS. The CAD models can be useful for showing buildings and structures upon a 2.5D landscape (Bishop *et al.*, 1995). Some early multi-dimensional GIS used these primitives as input; however, full 3D and 4D modelling requires more than a CAD structure for input and subsequent analysis.

3.4.4 Current and Future GIS

Until complexities of vector systems (topologic query) can be overcome, raster environments will dominate (Hack and Sides, 1994). Being relatively new, 3D GIS has few exchange formats and work needs to be done to allow data transferability between systems.

Current geographical information systems also involve linked models where the full multi-dimensional capabilities are provided by external processes, and the results are brought back into the GIS. This has the advantage of using a specialised product, but, as full multi-dimensional functions are added to GIS, these linked models may not be needed. Linked models may always be an efficient method of obtaining specialised results, however.

Visualisation is a key component within some systems, and other software systems are now adding visualisation capabilities that will show data on the web. Methods to enhance visualisation include the ability to rotate, set lighting, zoom, use cross sections and various transparency values for plumes. Output, in formats for the Internet, can be animated to show a 3D object rotating in space or changing attribute values. This affords easy dissemination of results, yet current technology only allows for efficient viewing of relatively small animation windows and files.

It is important to note that all future GIS need not be three-plus-dimensional. Many studies of natural or environmental phenomena, however, should take advantage of three-plus dimensions for analysing the dynamic nature of those phenomena (Sides and Hack, 1995).

The focus on object-oriented modelling for 3D GIS has been around for a number of years (Fritsch, 1990). Little emphasis is found in the literature, however, as most programmers tend to write code, not papers, and working software systems are not yet widely available for 3D and 4D studies.

Virtual reality or simulated worlds will be used for GIS modelling in three-dimensions in the future (Hack and Sides, 1994). This may stem directly from movie

and computer game animations (Raper, 1994) (cited in Hack and Sides, 1994, p. 72). The ability to enter a scene will prove useful by allowing the user to walk through a volumetric object or rotate and scale the object inter-actively.

Most 3D software packages were designed for geologic and mining applications, yet new systems offer more cross-application functionality. Many environmental areas are open to modelling, yet complex environmental phenomena need to be processed with differential equations that are not present in most systems to date. Again, the opportunity for linked models becomes important.

(a) Three-Dimensional GIS Systems

(i) Voxel Analyst (Intergraph, Huntsville, Alabama, USA)

This software can use variable sized and shaped grids to perform 3D mapping. This software was provided for research and proved to be fairly good at representing data. Problems existed with system stability, however. No animation (4D) is offered in Voxel Analyst, so alternative methods of dynamic display are needed.

Relatively easy volume generation and default viewing parameters (lighting and angle) give a good visual picture of the attribute to be modelled. Vertical exaggeration is handled well, but limitations arise when multiple data sets are needed. Multiple data set import is offered, yet frequently does not work, and each volumetric object must be generated individually for the same threshold. Problems remain with system and data stability, data import and export, and non default lighting parameters.

Application of Voxel Analyst to contaminated waste mapping and clean-up are covered by Williams and Jones, (1994); Fowles, (1995); Ferguson *et at.*, (1996). It was shown that these volumetric maps of the contaminants offered tremendous visual impact to those involved. Further, contaminant clean up strategies could be more cost efficient by knowing where and how to focus clean up efforts.

(ii) Arc/Info and Arc/View (ESRI, Redlands, California, USA)

Using Arc/Info and Arc/View an underground bunker for nuclear waste disposal was constructed using 2D tables of data linked to a 3D database (Manson, 1997). Arc/Info does not yet have volumetric analysis capabilities, but Arc/View version three allows for 3D objects to be placed upon 2.5D surfaces for visualisation. Arc/Info also has a simple node height to represent overpasses in its network module.

(iii) Other Systems

Surpac (Surpac Corporation, Belmont, Western Australia) is a vector-based software product developed for the large mineral industry in Western Australia and abroad. The software is predominantly used for mining, yet further work is being done to convert the software for use in environmental arenas (Bebb, 1997).

Other systems include EarthVision, gOcad, Stratamodel (Hack and Sides, 1994), and Maptek's Vulcan (Hood and Summerson, 1997). The Lynx system described by Rychkun (1997) and Houlding (1994) adds visualisation capabilities that are missing in Voxel Analyst. Modflow (United States Geological Survey (USGS), Reston, Virginia, USA) incorporates 3D modelling of sub-surface hydrology and groundwater movement and offers limited visualisation.

3.4.5 Advantages of Three-Dimensional GIS

Obviously, with 3D GIS capabilities comes more realistic environmental modelling. Coupled with increased research and advances in computer technology, systems offer great potential. The increase in understanding gained through volumetric visualisation is important for environmental science.

Cross sections of volumes may be viewed on top of volumetric plumes. Other options to cut away a portion of the scene will allow viewing inside an object. Realistic 3D graphics also allow for efficient lighting (e.g. front, back, universal, and internal), and dynamic rotation can yield a complete picture of a volumetric object.

Volume calculation and 3D intersections or overlays are important advantages of 3D GIS for environmental science. Being able to probe a data set and calculate statistics becomes useful for finding trends such as what attribute thresholds to use for attribute value colours and importance.

3.4.6 Disadvantages of Three-Dimensional GIS

Most environmental phenomena are truly 4D and need to be modelled with the dynamic element of time (Floris and Ritsema, 1994); (cited in Hack and Sides, 1994). Further, with the addition of more than two dimensions to GIS, data processing and management becomes more difficult. Problems in obtaining 3D data are tremendous, as sampling can be sparse and data may not be released or provided from agencies. Data for environmental phenomena can be difficult to capture, and thus many environmental objects remain difficult to fully understand. As mentioned earlier, most systems lack the necessary computational functionality to truly model dynamic environmental phenomena.

Cost of systems remains a stumbling block at the moment, especially for developing countries (Sides and Hack, 1995). This is in part due to the extra complexity involved with 3D functionality which is not needed in 2D systems. With the increased use of personal computer platforms instead of UNIX platforms, however, significant cost savings can occur. Further, full volumetric software for the personal computer can also be obtained for just over $300 (Voxel Analyst, academic cost).

Generalisation of data in a 3D environment is difficult, and further work needs to be done in this area (Sides and Hack, 1995). Based on 2D methods and new volumetric methods, both raster and vector environments should be tested.

3.5 Four-Dimensional GIS

Four-dimensional GIS is defined here as volumetric elements (3D plumes) combined with temporal (4D) data. Calculating topology for 4D environments remains limited, yet advantages include animation and the tremendous visual impact and understanding gained through volumetric movement. Other limitations include the

amount of data to process and manage as well as temporal sampling and the resulting interpolation between *time slices*.

By studying 3D and 4D phenomena, a greater understanding can be achieved through visual means (animation or interactive videos). This dynamic ability is needed to study natural environmental objects as they occur in both time and space. With the addition of the temporal element, Davis and Williams (1989) investigate the need to show data in between time periods and consider this *flow data* to be an interpolated volume at *n*-time for continuously sampled data. Interpolation methods for irregular temporally sampled data are needed.

Langran (1992a) has broken time into two methods for modelling. The first method is a before and after picture of a landslide or cliff collapse; the second is to show the collapse occurring (Langran, 1992a). A full discussion of time in GIS is covered by Langran (1992b). Even though the work and research by Price (1989) focuses primarily on time as the third dimension, the handling of 4D time is much the same.

Handling time in a series of 3D snapshots is similar to the 2D cross section concept used to simulate volume (Pigot and Hazleton, 1992). A proposed system by Mulder (1994) (cited in Hack and Sides, 1994, p. 65), shows the use of *chrono-voxels* to represent features in 4D states. These chrono (temporal) voxels are used to represent adjacency in space and time. The concept of objects (their state and functionality) at a certain time can also be applied to represent dynamic environmental phenomena (Worboys, 1995).

True spatio-temporal systems are needed to overcome the barrier faced in this research, which is having to generate 3D volumes in one package and export them to another for visualisation. With increasing research being done in four-dimensions, systems are likely to eventually catch up with environmental needs (Mason *et al.*, 1994). A discussion of the concept of a spatio-temporal overlay is covered by Lin (1997).

3.5.1 Previous, Current and Future Four-Dimensional GIS

Previous 4D GIS systems, similar to the early 3D systems, faced computing, data, and processing shortages. Current systems are making environmental modelling more affordable and efficient. Future applications have tremendous potential for viewing accurate data over periods of movement and change. These systems will provide the user with a level of understanding that was only theoretical in the recent past.

3.5.2 Advantages of Four-Dimensional GIS

Dynamic features in the natural environmental can be modelled more efficiently with a 4D system. This is due to the perception of the dynamics of the event being modelled. Data can be portrayed as a series of snapshots linked together to form animations. However, if data in the temporal-dimension is sparse, interpolation between times must be used with caution. Phenomena between time slices cannot be truly known, yet estimation methods can represent objects well for visualisation purposes.

Having more than one object visibly interacting with one another may yield an understanding that would be difficult to gain with a 2D or 3D system. The visual knowledge gained can be used for future research into those interactions.

3.5.3 Disadvantages of Four-Dimensional GIS

With the addition of more than three dimensions, data storage, processing, and management becomes more difficult. Computing technology and software functionality are likely to offer tools to handle the volume of 4D data in the near future. Until then, hardware limits and software stability remain disadvantages to the efficient models proposed in research and industry environments.

Improvements in cartographic techniques to produce hardcopy plots of 4D objects in space-time have occurred, yet user understanding may become more difficult as dimensions increase. Full animation in a digital format is needed to comprehend the

large amount of dynamic information that is not revealed on a series of time snap shots on paper.

3.6 Applications of Three and Four-Dimensional GIS

At present, most of the work in three and especially 4D systems is in the fields of mining and geology. However, a wide range of other applications of multi-dimensional analysis are available to users in general.

3.6.1 Sub-Surface Applications

(a) Mining Applications

Some mining applications are covered Raper (1989), Raper (1989b), Hack and Sides (1994), and Manson (1997). Raper (1989b), Jones (1989), and Hack and Sides (1994) show potential uses for oil exploration and extraction. These studies indicate the importance of three-plus-dimensional GIS for scientists and industry. A great amount of emphasis is placed upon accuracy of mining operations, and three-plus-dimensional technologies can increase profit margins significantly.

(b) Geologic Applications

The three-dimensional geologic applications are significant, as almost all underground studies must include geologic conditions. Even though geologic time is slow, computer modelling allows the geologist to speed up the time dimension, and events such as floods and landslides can be modelled (Turner, 1997a).

Further geological applications are covered by Raper (1989b), Renard and Courrioux (1994), Jones (1989), Belcher and Hoffman (1992), Belcher and Hoffman (1992), Marschallinger (1991), Turner (1997b), Bell *et al.* (1990), Albertin *et al.*, (1995). A complete review of 3D geological issues is covered in Houlding (1994).

(c) Groundwater Applications

Geology is often studied concurrently with groundwater in underground applications. Turner (1989) gives an indication of the application of 3D GIS to hydrogeology. This work highlights the *parameter crisis* in modelling, which is the lack of

parameters or variables to measure all the factors involved in real-life 4D phenomena.

The United States Geological Survey (USGS) has produced software and animation add-ons to assess groundwater issues through the Scientific Software Group (http://www.scisoftware.com). The software has several groundwater and geologic visualisation applications. These include the Groundwater Modelling System (GMS), EQuIS Geology, Watershed Modelling System (WMS), Visual Groundwater, Visual MODFLOW, Aquifer Test, AquaChem, and Visual HELP.

(d) Electromagnetic and Gravity Applications

Three-dimensional electromagnetic (EM) applications are covered by Ellis (1995), and gravity measurements have been made with a simple 3D model (Broome, 1992). The SALTMAP program in Western Australia attempts to measure the 3D EM response of salt. To reduce salinisation of agricultural areas, SALTMAP attempts to map these phenomena and may benefit from 4D investigation of the problem (Street, 1995).

3.6.2 Environmental Applications

(a) Atmospheric Applications

Atmospheric science and global meteorology needs a very dynamic platform to measure and model air movements (Knapp, 1991; O'conaill *et al.*, 1992; Bell *et al.*, 1990). Visualisation is a key component to air quality studies due to the dynamic nature of atmospheric interactions such as wind patterns (Koussoulakou, 1994). Climate modelling in three-plus-dimensions is covered in Henderson-Sellers and McGuffie (1987). Acid rain is another application, and previous mentions of smog studies were covered in Chapter 1.

Atmospheric applications have often relied on programming and hardware tools to create visualisations. Software applications built upon C code and OpenGL libraries are often used to visualise data. These applications can be developed on UNIX (in particular Silicon Graphics platforms) or PC platforms with slightly differing

interfaces, yet the graphics core remains the same, a benefit of OpenGL (Rye, 1999). The Interactive Data Language (IDL) is a PC/UNIX visualisation and programming platform that is often used to replace the FORTRAN or C programming languages for scientific visualisation in 3D or 4D. More information on IDL can be found at http://www.rsinc.com. Another powerful tool funded and used by NASA in atmospheric sciences is PolyPaint+. This volumetric visualisation software runs on Sun SparcStation, Silicon Graphics Indigo or Indy platforms. See http://lasp.colorado.edu/polypaint/ppaint_body.html#gen_desc for a full description.

There are a wide range of other organisations conducting visualisation on UNIX-based platforms such as the National Science Foundation (NSF) and the Bureau of Meteorology in Perth. These visualisations include meteorological phenomena such as tropical cyclones and global atmospheric changes, and localised weather/frontal patterns.

Again this work aims to conduct visualisation within a GIS platform (Voxel Analyst), so discussion of UNIX platforms and specialised programming for visualisation remains brief.

(b) Hazardous and Toxic Waste and Pollution Applications (Interaction with Groundwater)

Heavy metal pollutants downstream from a mine were mapped and interpolated using a volumetric system to show environmental damage had occurred (Leenaers *et al.*, 1989). Methods for 3D environmental monitoring and management were employed on sites previously used to manufacture nuclear products (Eddy and Looney, 1993; Williams and Jones, 1994; Rychkun, 1995). Other applications of underground contaminant investigation were done by Fowles (1995), Ferguson *et al.* (1996), Rychkun (1997), and Bell *et al.* (1990).

(c) Environmental Impact Assessment (EIA) Applications

Complex environmental conditions may need to be modelled to show potential environmental impacts of a proposed development. Kluijtmans and Collin (1991)

focus primarily on the visual impact upon sites (terrain, 2.5D) and view-shed impacts. Volumetric analysis for EIA requires enormous amounts of data; however, improved systems can explore new and quicker possibilities of assessment.

3.6.3 Oceanographic Applications

The temperature of water bodies and salinity measurements can be handled in 4D systems, but ocean measurement in 4D can be a tremendous task. This is due to the expanses that ships must cover during oceanic data sampling. Further, a regular grid in 4D would be difficult to obtain unless several sampling vessels were used. With satellite imagery, however, some ocean-surface attributes can be readily extracted (O'Conaill *et al.*, 1992).

That study combined volumetric and temporal data with AVHRR data to study sea temperatures in a GIS. Large data sets were implemented with a hierarchical data structure for query purposes. Query implementation was performed by breaking the hierarchical structure into streams for processing with an eight processor parallel array. Other oceanography applications have been shown by Hack and Sides (1994) and Bell *et al.* (1990).

In Antarctica, the feeding habits of emperor penguins were tracked with Global Positioning Systems (GPS) satellite implants and radio signals. The resulting data in a 4D system allowed researchers to identify ice formations that played a role in feeding as well as visualising the track that penguins had taken throughout the feeding (Hood and Summerson, 1997).

3.6.4 Municipal Applications

Municipalities can benefit from multi-dimensional GIS in several ways. Surveying (GPS height), road infrastructure, grade and clearance data (overpasses and power lines), road design (asphalt thickness and line of sight), and sewer and water planning (pipes, manhole depth, and interference checking) can all be performed. Further applications include parks and planning design (landscaping, drainage and tree heights) and street scaping (tree and power line visualisation). Even the police use

bullet trajectories and traffic accident re-enactments to give evidence in courts of law (McConomy, 1993; Hoinkes and Lange, 1995; Bishop *et al.*, 1995).

(a) View-Shed Applications

A 2.5D surface can be used to add 3D building objects and towers. This application of a cityscape does not allow for volumetric object query, yet viewsheds can be generated with the inclusion of the 3D object topology (Batten, 1989). Three-dimensional objects such as highway overpasses, water towers, and even forest canopies upon 2.5D surfaces, can be also be visualised (Cambrey, 1993; Hoinkes and Lange 1995).

(b) Planning Applications

Land use and farm planning can also be aided with 4D systems. Four-dimensional systems prove useful for shallow soil studies to plan for crop placement and visualisation of future sites (Coleman 1991). Further work would be useful to help planners deal with development applications and the associated impact on the environment.

(c) Civil Engineering and Construction

Engineering works can be enhanced with a greater understanding of underground conditions such as geology and hydrology (Raper, 1989b). For construction purposes, a walk through tour of building and construction sites can be generated (Kluijtmans and Collin, 1991). This leans more towards CAD and Virtual Reality (VR) systems, but multi-dimensionality remains a key component of those systems as well.

3.7 Visualisation of Geographical Data

Rendering 3D and 4D data on 2D maps can be a problem. Hard-copy visualisation aims to make 2D maps that can represent 3D objects efficiently. The next challenge is to represent objects efficiently on computer screens (McLaren and Kennie, 1989).

The perception of objects on a flat map or computer screen is a key component to the full realisation of their form. For maps, cartographic symbols (for 2D map legends) have been proposed to show volumetric features on a map (Hsu, 1979; Dent, 1985; cited in Kraak, 1989, p. 109). Further, colour and shading has been used, but some care is needed when generating colour and shading pattern that colour-blind people may find hard to recognise (Kraak, 1989).

Illumination or shading of objects can be "... a powerful cue to the three-dimensional structure of an object" (McLaren and Kennie, 1989, p. 89). Another technique to aid visual interpretation of multi-dimensional objects is total illumination of a scene with ambient light. Used at various levels and angles, this false light can simulate sunlight upon a scene.

To visualise data, a static display is not enough. Being able to rotate an object depends upon the *view plane normal* or viewing plane. This plane should be rotatable in x, y, and z directions, and rotation should be dynamic (Bak and Mill, 1989). Further, users of multi-dimensional data have to be able to peel back layers, slice edges, and zoom in and out of the scene (Smith and Paradis, 1989).

Another common function required in multi-dimensional systems is the ability to scale data along the axis. Typically, this is performed on the z axis (Kraak, 1994). By doing this the user can exaggerate elevation. Two and one half-dimensional surfaces with relatively low relief can be scaled to aid visual understanding. Further, 3D bodies can be exaggerated to see nuances that were not noticed at the proper scale. Other functions include being able to clip cutting planes and peel back layers to see within objects.

Animation of GIS objects allows for movies to be created to visualise spatio-temporal objects in the environment (Davis and Williams, 1989). Video players allow for motion or 4D scenes to be downloaded and viewed as well. The web may one day be used as the ultimate visualisation tool. Including any computer linked to the Internet, images can be downloaded and viewed in 3D and 4D with Virtual

Reality Modelling Language (VRML) browser capabilities (Hood and Summerson, 1997).

3.7.1 Audio Video Interleave (AVI) Format

The AVI file format is an audio and video format that can be used by systems that support multimedia capabilities. For visualisation of objects with little or no sound, the audio channel can be eliminated. Visualisations are started and can be stopped with a mouse click on the scene. To restart the video a further mouse click is required. This format can be used to view video files from the Internet and files resident on the local machine or from a CD ROM.

Obtaining large 4D animations on the web can often require long download times. At the moment, the entire file must be downloaded before visualisation can occur. Once downloaded, the visualisation can be stopped and restarted.

3.7.2 Virtual Reality Modelling Language (VRML) Format

The virtual reality modelling language provides a structure where a 3D picture can be generated at the web-browser level (Hood and Summerson, 1997). By using VRML, objects can be investigated by rotation and scaling.

3.8 Summary

There are a tremendous number of applications of 2D GIS for environmental purposes. This includes previous and current methods and models investigated for mapping on plane surfaces with no elevation. These applications have great potential for environmental mapping but are limited to non-volumetric applications.

Two-and-one-half-dimensional GIS, or terrain modelling, can be performed in both raster and vector models for mapping elevation surfaces. The use of attributes to assign an elevation value is sometimes referred to as 3D mapping and analysis, yet no true volumetric capabilities are available.

Three-dimensional GIS involves volumetric objects and the ability to query attributes about those objects. Raster and vector data structures have differing needs and processing speeds. Volumetric GIS is beneficial for environmental modelling, but its limitations include data processing and hardcopy output. Current and future 3D GIS use will grow with the ongoing improvements in computing hardware and software.

Four-dimensional GIS (volumes over time) is important for improved perception of processes that occur in nature. Current and future systems will continue to be used by more and more GIS and non-GIS professionals; however, there are some limitations at present such as data handling and system stability. Applications are diverse for 4D GIS, and future expansion of spatial research is likely to occur in a diverse range of business, industry, and government uses.

Data visualisation is important to the user or decision maker. Methods of visualisation for effective presentation of 4D phenomena can be difficult to present on 2D media. Methods of softcopy output such as animation and videos can display 4D data. Output can be sent via the Internet for viewing by remote computers.

Chapter 4

TEST SITE, COMPUTING REQUIREMENTS AND DATA

4.1 Introduction

The test site used during this research was the Perth metropolitan region in Western Australia (Figure 4.1). The metropolitan study area covers a square of 120 km from north to south and 120 km east to west centred on Perth. The vertical dimension of the test site is limited to 1000 m, as sampling in the vertical dimension becomes more difficult as height increases.

Computer packages used included ER Mapper (West Perth, Western Australia), for image processing and vegetation mapping, and Voxel Analyst for 3D visualisation. Four-dimensional visualisation and output to a web readable format (AVI) that allows animation through digital movie frames was performed using Macromedia Director (San Francisco, California, USA).

Various computer platforms were used throughout the research with the majority of processing carried out on a Pentium 133 computer. Other computers were also used, as some software was located on different machines throughout the research laboratory. Some minor work was performed on a UNIX machine, but when the UNIX licences (ERMapper, Arc/Info) were converted to PC based platforms, the remaining tasks were performed on the PC.

Satellite image data for vegetation mapping was obtained from the DOLA Remote Sensing Applications Centre (Leeuwin Centre) in Floreat, WA. Nitrogen oxides and ozone data from the DEP were obtained for visualisation of a typical smog day in Perth. Various other data sets on vegetation were also provided by the DEP.

4.2 Study Area

4.2.1 Perth Metropolitan Area

The study area was centred over the Perth CBD, and extends 60 kms in each cardinal direction from the city centre with a height of one kilometre. Figure 4.1, a 1996 Landsat TM scene, is a combination of bands four, three and two in the red, green and blue channels, respectively. This image, which highlights vegetation in red, is shown together with the study area boundary.

The northern boundary is near Two Rocks; the southern boundary extends to just north of the inlet at Mandurah. The western boundary extends approximately 60 km into the ocean and includes both Rottnest and Garden Islands. The eastern boundary extends just past Mundaring. Some data are missing from the northern coastal area near Two Rocks because it was outside the scanning path of the satellite images available for the mosaic.

The majority of the land area is on the Swan Coastal Plain, an area of low relief with elevations ranging from zero to 80 m. Further east, a major north-south fault called the Darling Fault has created a scarp with a sharp change of elevation from approximately 60 m to an elevation of approximately 200 m. The elevation of the area to the East of the fault is between 100 and 300 m above sea level. Larger changes in elevation are present to the east of the Darling Fault on the Darling Plateau.

There is a marked change of vegetation near the Darling Fault that is quite visible in Figure 4.1. The change of geology and soils on either side of the fault suit different vegetation species and densities and are important features for the current mapping. Species to the east of the fault are predominantly jarrah and marri forest with some open marri woodlands. Species to the west of the Darling Fault on the coastal plain include sheoak, melaleuca, pine, coastal heath, and tuart which are mixed with some urban exotic species.

Figure 4.1 Study area (note: the north/south running Darling Fault can be seen where there is a sharp change in vegetation)

4.2.2 Study Area Scale

The DEP in Perth models biogenic inputs to photochemical smog formation on a 3 by 3 km grid (Figure 4.2). The background image is the Landsat TM mosaic with 30 m pixels. In Figure 4.2, it is possible to see how generalising data to the 3 km grid can be a difficult step in the vegetation mapping process. Smog modelling is performed by the DEP on a regular x, y grid; however, the vertical resolution varies.

The spacing of z was based on layer thickness with a tighter z spacing closer to the ground (Figures 4.3. and 4.4). The size of these grids was deemed appropriate by the DEP for modelling photochemical smog in Perth. The outputs of this research were interpolated voxels on a regular grid (9 x 9 x 9 in Voxel Analyst format of i, j, and k parametric space) for visualisation. The vertical point heights interpolated by the DEP are listed in Table 4.1

Point height	Thickness of air body
4.14m	Sea level - 8.3m (8.3 m)
16.65m	8.3m - 25m (16.7 m)
45.85m	25m - 66.7m (41.7 m)
91.7m	66.7m - 116.7m (50 m)
141.7m	116.7m - 166.7m (50 m)
200.05m	166.7m - 233.4m (66.7 m)
350.05	233.4m - 500.1m (266.7 m)
618.4m	500.1m - 1000.1m (500 m)

Table 4.1 Department of Environmental Protection (DEP)
sample point heights and widths for visualisation (DEP outputs for visualisation)

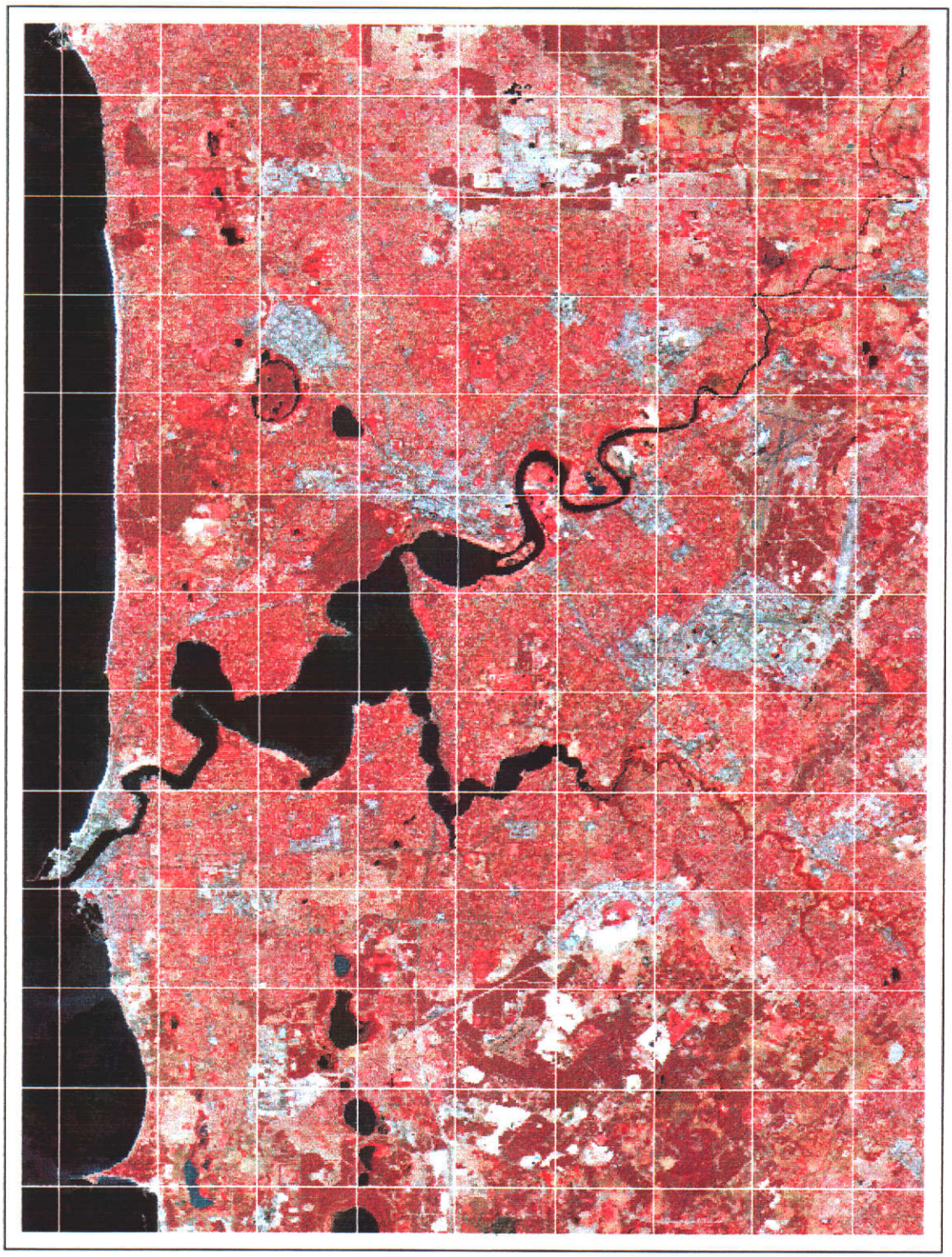

Figure 4.2 Grid spacing (3 x 3 km) used in vegetation mapping

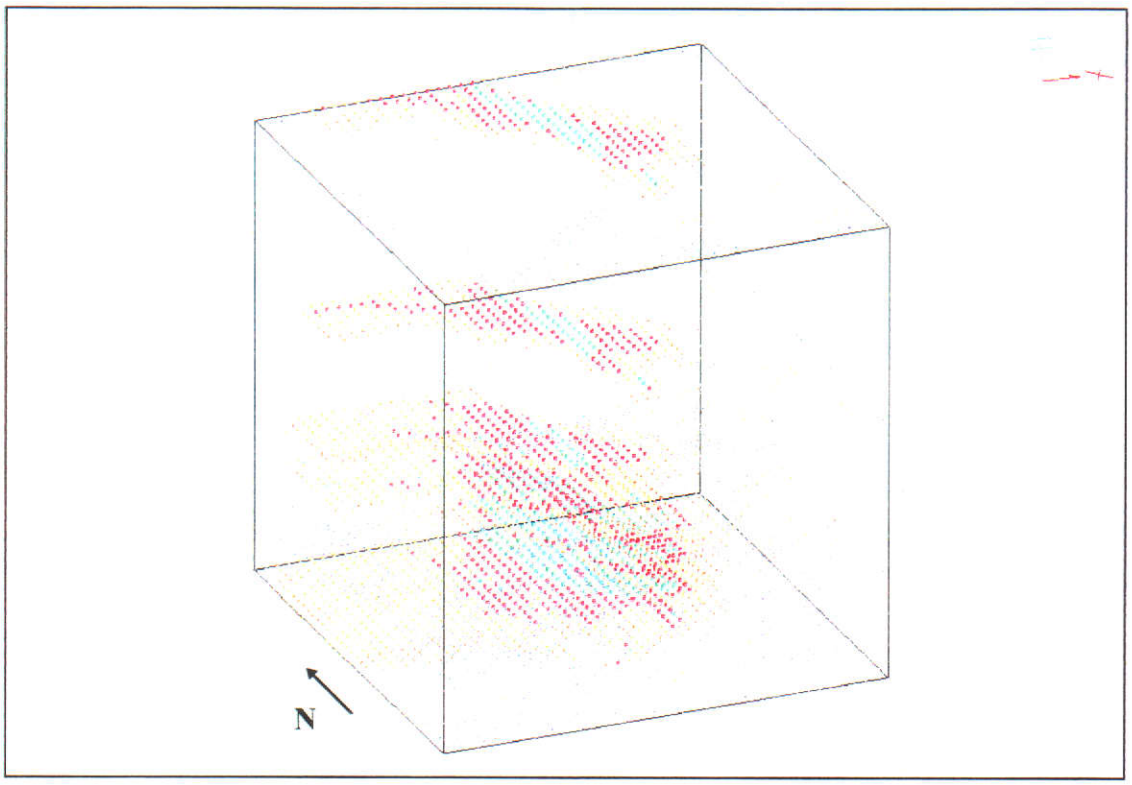

Figure 4.3 Sample point data from the Department of Environmental Protection (DEP) (vertical exaggeration x 200) (colours are arbitrary to enhance display)

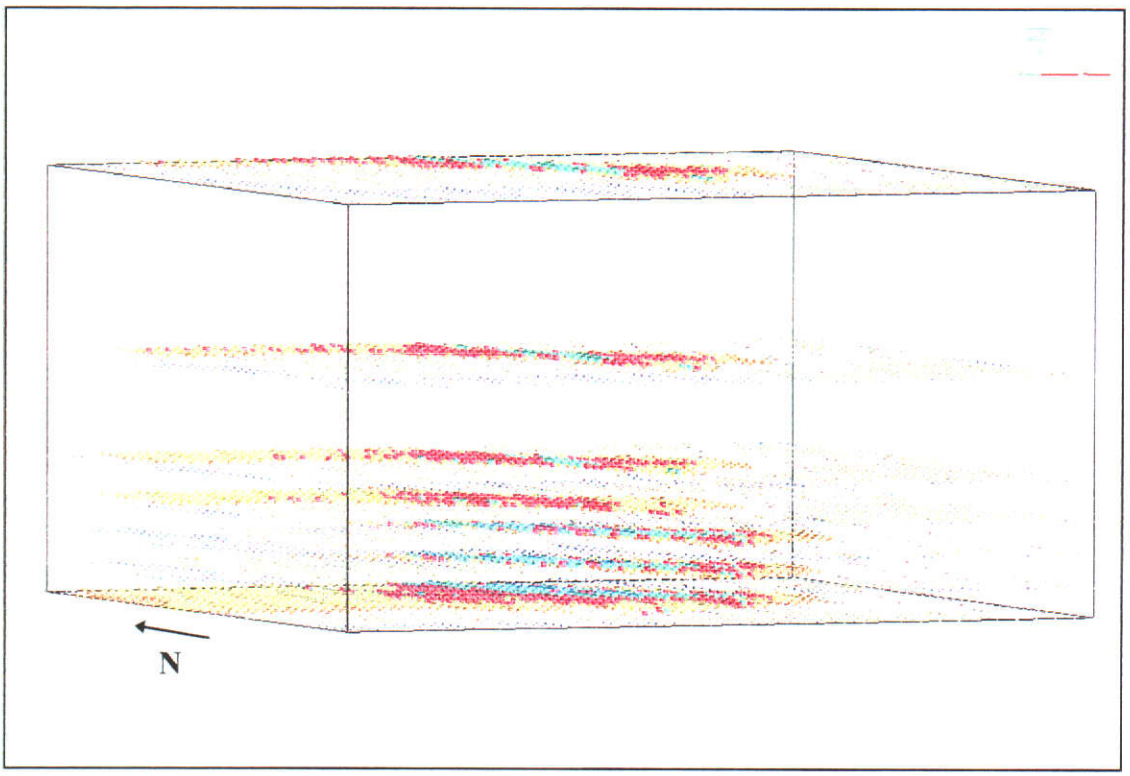

Figure 4.4 Department of Environmental Protection (DEP) sample points (vertical exaggeration x 100) (colours are arbitrary to enhance display)

The vertical exaggeration in these figures was set at 200 and 100 to highlight the sparse nature of the data as height increases. The point colours represent ozone sample point concentrations; however, colours were chosen to highlight sample point differences only.

Increasing computing power and data handling capabilities could be used to model smog with a higher resolution; however, it is important to note that the current modelling resolution may be appropriate without further improvements. Visualisation may prove that the study area requires expansion more than an improved resolution.

The satellite imagery was obtained with a 30 m pixel resolution. Previous biogenic studies in Australia have used the Landsat MSS data with 80 m pixels (Carnovale *et al.*, 1991). In Perth, however, previous biogenic mapping was performed without the use of satellite imaging techniques (Rye, 1998).

Improved mapping should be achieved over previous non-image based methods. However, during data generalisation to the 3 km square grid, data loss may eliminate the improved use of moderate resolution (30 m) data.

Pertinent scales of remote sensing data are needed for mapping vegetation (Marceau *et al.*, 1994a). Due to the data provided, this study used remote sensing data with a higher resolution than was needed. This allowed improved initial mapping due the to lesser influence of mixed vegetation pixels (over lower resolution methods). The data set used here was the one that was most practical for the model requirements and the processing abilities of the software and hardware.

Early vegetation mapping was commonly performed using pixel resolutions such as the Landsat MSS (80 m) and more recently the NOAA Advanced Very High Resolution Radiometer (1.1 km). Townshend and Justice (1990, pp. 149) state that "[Little] is known about spatial variability and hence resolution requirements at coarser spatial resolutions [than 100 m]."

Studies such as Marceau *et al.* (1994b), have shown high resolution images (.5 m) generalised to just under 30 m pixels for coniferous vegetation can yield an optimal resolution from 2.5 m to 21.5 m. With the 30 m pixel resolution used in this study, coniferous vegetation was outside these optimal limits. Single age pine stands, good training sites, and high contrast between coniferous and native Australian plants have, nonetheless, shown high accuracy with the resolution used.

Woodcock and Strahler (1987) further support the need to select an appropriate scale for remote sensing studies. They indicate that scale factors are becoming more important with higher resolution satellites, even though other factors such as spatial, temporal, and radiometric variables should be considered as well.

With the introduction of higher resolution satellites in the very near future (Solberg *et al.*, 1996), improved vegetation mapping will be possible. At this point, the DEP model resolution does not require smaller pixel sizes for vegetation mapping, even though they could prove useful for other purposes.

If model resolution is increased in the future, imagery resolution should remain acceptable until model resolution drops below 30 m cells. There remains a threshold of resolution above which environmental phenomena need not be modelled. Ultimate resolution for smog and many environmental pollutant levels are yet to be determined within the GIS arena, due to a lack of proper research into this area.

4.3 Maps

Several maps were used in various stages of the research (Table 4.2). Vegetation maps from Beard (1979a, 1979b, and 1981) were used to help find areas of remnant vegetation for training sites and ground truthing the species map. Topographic maps provided some assistance with field work and were used to generate the DTM as a backdrop to the 4D visualisation. The Perth street directory was used extensively during field work to find potential ground truth sites.

Map	Use	Source
Beard's vegetation maps 1:250,000	To focus field work efforts	Beard (1979a, 1979b)
Beard's vegetation map 1:1,000,000	To focus field work efforts	Beard (1981)
Topographic maps 1:100,000	To digitise contours for terrain model	Department of Land Administration
Perth street directory 1995	Field work street guide	UBD, a division of Universal Press
Existing vegetation and density maps	To focus field work efforts	DEP
Digital Maps from DEP	To show previous biogenic classes	DEP
Landsat TM 457 RGB poster	To focus field work efforts	(DOLA) Remote Sensing Applications Centre
Screen print outs	To delineate vegetation characteristics; note taking	This research

Table 4.2 Maps used during research

The original model vegetation species and density maps from the DEP were received as text files. These *text maps* were in column and row form to show the 3 km x and y cell widths. Numbers were used instead of colours to represent classes. After printing the text files, some manual class delineation proved useful for gaining an understanding of the existing classes.

Three digital vegetation maps were provided by the DEP with various vegetation data sets. These maps included remnant (remaining natural) vegetation, vegetation complexes and geomorphology, and a Conservation and Land Management (CALM) vegetation map. These three maps were used as visual aids throughout the research. No class delineation was performed with these digital maps.

A composite Landsat TM poster from DOLA that highlighted vegetation in red was helpful in the field and when perusing the study area. This four, five, seven band combination in blue, green and red was taken on February 25, 1990. Several screen captures of vegetation indices and red, green blue band combinations were printed at various scales for field work. These maps proved extremely useful when defining training sites and ground truth sites.

4.4 Hardware and Software

4.4.1 Hardware

Several computers were used during the research including Hewlett Packard workstations and personal computers with various configurations and speeds. The majority of the research was carried out using a personal computer with a network name of Sublime (see Table 4.3). Two digitisers, a Calcomp 9000 and a Calcomp Drawing Board III, were used for digital terrain model data capture.

Computing Hardware Components
Pentium 133
64 MB RAM
2 MB 3D Video Card
9 GB Hard Drive
Network Card

Table 4.3 Computer hardware used during research

4.4.2 Software

Several software packages were used throughout the research, with frequently used packages listed in Table 4.4. The major software packages were ER Mapper for 2D vegetation mapping, Voxel Analyst for 3D smog plume creation, Microstation95 with Site Works MDL for terrain modelling, and Macromedia Director for visualisation. Idrisi (Clarke University, Mass, USA) was used for regression calculation.

Software	Purpose
ER Mapper ver. 5.2	Remote sensing of vegetation
ER Mapper ver. 5.5 (version obtained after the majority of research was conducted.)	Statistics not present in version 5.2, and exporting not present in version 5.2. Improved system stability
Voxel Analyst ver. 2.00.01.10	Smog plume creation, three-dimensional
Microstation95 ver. 5.05.02.23 With Site Works MDL	Terrain model creation
Macromedia Director ver. 5.0	4D Visualisation (Video)
Arc/Info (UNIX) ver. 7.0.3 and ver. 7.1.2 (NT) (ver. 7.1.2 obtained after the majority of research was conducted.)	Statistics, importing, exporting, editing, and some vegetation mapping
IDRISI ver. 2 (for windows)	Regression calculation
Microsoft Excel ver. 97 and 95	Data reformatting
Qbasic program ver. 4 (Appendix A)	Data reformatting

Table 4.4 Computer software used in this research

Arc/Info on a UNIX platform was used for data conversion throughout the research. Further, the UNIX system was useful for storing backup data during the research. Digital vegetation maps from the DEP were obtained in Arc/Info export format and then printed on the UNIX system for use as visual aids throughout the research. Final Arc/Info data conversion was performed on PCs when the licence was changed to a Windows NT environment.

Data reformatting programs for 3D smog plume data were needed. The majority of data reformatting was accomplished with a QBasic program (Appendix A). This reformatting program read the DEP Nitrogen Oxide and Ozone plume data and wrote the data into Voxel Analyst format. Microsoft Excel was used prior to running the data through the QBasic program for minor data reformatting.

Various software such as Microsoft Word, Netscape, Eudora Light, and FTP were used for researching background information, file transfers between computers, and

(a) Nitrogen Oxides

This file was obtained to examine the various oxide emissions (and their role as an ozone catalyst) from cars to industry as well as bushfires. Ideally, a biogenic emissions file would have been obtained for final visualisation. Since a reduction in human sources is more beneficial, however, visualisation will remain focused on human sources. The nitrogen oxides involved in ozone formation can be significant (Rye *et al.*, 1996).

(b) Ozone

This file contained data to visualise the potential change from nitrogen oxides into ozone throughout the day. Further, with ozone being a major contributor to respiratory problems, this file was important for visualising a typical *coastal smog event* in Perth. Potential vegetation damage due to ozone exposure can also be visualised with the data contained within this file; however, quite high levels (100+ ppb) are needed to damage vegetation. Such conditions are infrequent in Perth (Rye *et al.*, 1996).

These two chemicals are a small part of the extremely large number of chemicals involved in smog formation (Rye *et al.*, 1996); however, they do represent the major factors involved in smog formation, and provide a good indication of potential human and environmental impact.

4.6 Summary

The Perth metropolitan study area covers the major population and chemical emission air-sheds. The study grid spacing for 2D vegetation mapping maintains the DEP grid of 3 km^2. The sampling grid of 3 x 3 by n km cells was deemed appropriate by the DEP for volumetric work. Points were interpolated and voxels were generated on a regular grid for final visualisation.

Several maps were obtained to conduct this research. Topographic maps were used to digitise contours for a terrain model. Print outs and screen captures were used throughout this research for visual aids and field work. Text maps from the DEP

gave an indication of previous biogenic emission classes and were used to fill the small portion missing from the images for species and density.

Image processing was performed using ER Mapper and visualisation was performed using Voxel Analyst and Macromedia Director. Personal computers and software provided the majority of research tools. A UNIX workstation was also used for data backup storage and minor statistical analysis. Other software for data reformatting and analysis gave the ability to generate statistics and transfer data.

Remotely sensed imagery from the DOLA Remote Sensing Applications Centre gives the necessary foundation for vegetation mapping and data extraction. Nitrogen oxides and ozone data from the DEP will be used to generate volumetric bodies to be studied over time. Interpolated *plume* data and terrain interaction are unknown and will be investigated.

Chapter 5

VEGETATION MAPPING RESEARCH METHODOLOGY

5.1 Introduction

Remote sensing is a tool that can facilitate the efficient and effective mapping of vegetation. By mapping several species classes and the percentage of canopy cover from remotely sensed data, biogenic emissions can be assessed for input into photochemical smog formation.

Vegetation mapping involved two maps. One map detailed species; the other vegetation density. Nine species were chosen for mapping on the first map, along with six classes of density (percentage canopy cover) on the second map. Supervised classification delineated the species types and density mapping was performed through a vegetation index.

The satellite images needed to be prepared for classification and vegetation delineation. The 1996 image was pre-rectified, with the 1997 image fit to the 1996 image through an image-to-image method. Once the 1997 image was rectified, missing data was mosaiced from the 1996 image. The final mosaic contained 1997 values with an appended strip of data from the 1996 image with band values matching the 1997 image. Initial data reduction was performed by clipping the image to an area slightly larger than the study area.

Finally, generalisation of species and density maps from 30 m to 3 km was performed and data was clipped to the study area extents. The final data are written to a file for use by the DEP to update the existing biogenic emissions inventory for the Perth metropolitan area.

5.2 Preparation of Images

Images were provided by the DOLA Leeuwin Remote Sensing Applications Centre, on CD ROM in ER Mapper format. Both images were mosaic scenes from various cloud-free images. Most of the original images making up the two mosaics were comprised of summer data. The 1996 mosaic was rectified by the Leeuwin Centre to the Australian Geodetic Datum 1966 (AGD66). The mapping grid used was the Australian Map Grid 1966 (AMG66) with the Universal Transverse Mercator Zone 50 South (UTM50S) projection (Cacetta, 1996). The 1997 mosaic was not rectified.

5.2.1 Rectification

Due to a strip of image data missing from the 1997 image, the 1997 image was combined with the 1996 image which contained this missing data. The unrectified 1997 image had to be fit to a ground-based mapping coordinate system. The image datum and map grid used by the Leeuwin Centre for the already rectified 1996 image remained in use during this research (AGD66 and AMG66).

(a) Checking 1996 Image Accuracy

To verify the accuracy of the 1996 image, ten points were obtained from the image and cross referenced with DOLA topographic quadrangle sheets. An average RMS error of 15 m was present, about what would be expected with 30 m pixel resolution. The accuracy of the RMS errors are adequate for this study, especially when generalisation will reduce data accuracy more significantly than minor changes in rectification accuracy. It was an aim, however, to achieve high accuracy throughout to minimise final errors.

(b) Ground Control points and RMS

The unrectified 1997 image, referenced by column and row, required suitable control points to be read in the column-row (c-r) format to fit to the 1996 image. The control points on the rectified 1996 image could be extracted in AMG66 coordinates to match the raw 1997 control points. Technically, the 1997 image was fit using ground control points extracted from the 1996 image due to software functionality. This method is similar to image matching techniques used to fit one image to another.

By using rectification, or image matching, the c, r coordinates of the 1997 image can be fit to the AMG66 coordinate system built into the 1996 image using various methods. When using control points for rectifying images, care must be taken to ensure an adequate number of points which should be spread throughout the image (Jensen, 1986; Jensen, 1996; Lillesand and Kiefer, 1994, Sabins, 1997).

Thirty ground control points were chosen on the 1997 image, primarily on clearly visible road intersections (Figure 5.1). Other features, such as coastal points and sharp changes in vegetation, were also used as ground control. The points were spread quite evenly throughout the image, allowing for good control. Note the angle of the coastline and the approximate study area, which shows the needed rotation and rectification of the raw image to mapping coordinates. Further, note the bushfire scar in the Mundaring area which shows vegetation damage from one of the frequent fires in Western Australia.

Image software allowed for easy zooming and on-the-fly contrast enhancement to assist in point selection. The points were registered in the header file of the image for later rectification. Once all ground control points were compiled, some error checking was used to gauge the efficiency of points used. The RMS error for three methods of rectification were examined with varying accuracies, all approximately 10 m in displacement error.

(c) Accuracy

Measures of accuracy are needed for showing how errors can impact processing of remote sensing data. Image rectification, mosaicing, classification, and generalisation all need to be statistically tested. The need for statistics in GIS and spatial sciences is noted by Bailey and Gatrell (1995) and Soares (1993).

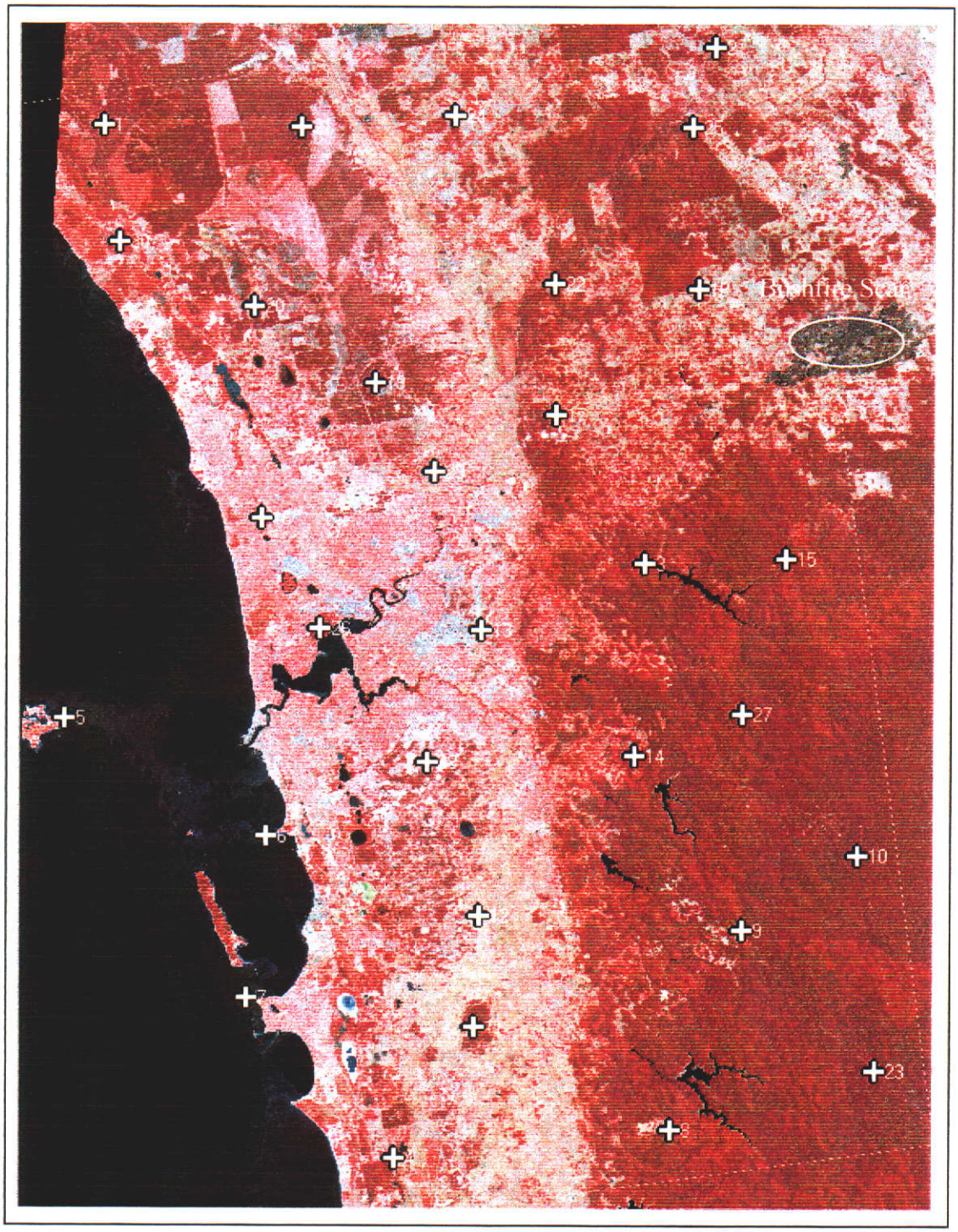

Figure 5.1 Ground control points (dashed line is approximate study area)

(i) Image Rectification and Mosaic

Nearest neighbour ground control point rectification methods gave varying results with the options for linear, quadratic and cubic convolution resampling (see Table 5.1).

Ground control points near the edge of the image had slightly higher errors; however, the 30 well-spaced points gave quite high overall accuracy. The rectification method chosen (linear), with just over ten m displacement, is quite good considering the final scale of data needed by the DEP.

Method	Linear	Quadratic	Cubic convolution
RMS error	10.23 m	10.14 m	9.06 m
High error	20.319 m	18.423 m	21.16 m
Low error	1.9 m	.35 m	.9 m

Table 5.1 Nearest-neighbour ground control point rectification accuracies

To test final accuracy against topographic map coordinates, ground truth data were sampled at ten locations on the 1996 image and the 1997 image. Since the 1997 image was being fit to points taken from the 1996 image, minor error propagation occurred (Table 5.2). Further errors may have arisen from the use of 1:100,000 scale topographic sheets, but final generalised images should overcome this error propagation.

An average error of about 20 m was present in the 1997 image. This is slightly higher than the 1996 image (~15m), but the overall error remains less than the resolution of one pixel (30 m). This would be expected when having rectification errors added upon original (1996) errors.

Image	1996 (x)	1996 (y)	1997 (x)	1997 (y)
Average error	19 m	11 m	25 m	21 m
High error	36 m	37 m	55 m	40 m
Low error	5 m	0 m	0 m	0 m

Table 5.2 Check point accuracy of 1996 image and 1997 image against topographic map coordinates

(ii) Resampling

Three forms of interpolation were tested for the resampling process. These included linear, quadratic, and cubic convolution (Jensen, 1986). Once the interpolation method was chosen, in this case linear, one of three resampling methods of nearest-neighbour, bilinear and cubic had to be chosen. The resampling method chosen was nearest neighbour which preserved original reflectance values. To carry out this interpolation and resampling, the software uses the concept of a *from* image (1997) and a *to* image (1996) with control points stored in the header file.

5.2.2 Mosaic

Due to the 1997 image lacking a strip of data caused by sensor track differences in the final mosaic by DOLA, some 1996 data was also used (Figure 5.2). The two images, therefore, needed mosaicing. Figure 5.2 is enhanced with a pseudo-colour palette to highlight the strip of 1996 data appended to the 1997 image. Good software design allowed the mosaic to contain only the missing data in the 1997 image. Two methods for mosaic were attempted, the feather and the overlay.

The feather option in ER Mapper calculated an average for the pixels in both images to remove the line between the images. Output from this method was not used due to the alteration of pixel values in both images. Instead of using the feather option, image data matching on the border was performed with the overlay option and histogram matching. This software option matched the 1996 image statistics to those of the 1997 image. This did not alter the 1997 image, as did the feather option, and was deemed preferable.

Despite histogram matching, the final mosaic still had some problems matching the two image dates perfectly (Figure 5.2). The added strip of data covers mostly ocean and some areas on the northern coastline and the western half of Rottnest Island. The figure highlights the difference in the images after the histogram match operation. Differences in vegetation reflectance between the two images may influence classification.

5.2.3 Image Statistics

Histogram statistics for the 1996 and 1997 image along with the final mosaic are given by band in Table 5.3. The pixel values represent brightness detected on various bands of the spectrum from zero to 255.

Since vegetation detection methods are developed into indices, no investigation of principal components analysis or edge detection were performed during this research.

Year	B1	B2	B3	B4	B5	B7
1996	56-255	15-162	10-239	1-195	1-255	1-197
1997	62-255	18-200	10-255	1-217	1-255	1-255
Mosaic*	68-255	13-191	5-255	4-218	1-255	1-255

Table 5.3 Image pixel ranges (1996 statistics matched to 1997 for mosaic. * The mosaic is different from 1997 ranges due to initial boundary clipping)

5.2.4 Masking of Non Vegetation Areas

For training site and ground truth delineation, the final mosaic was masked to filter out all of the areas that did not have a vegetation response from the Normalised Difference Vegetation Index (NDVI) formula. This includes water and all non-permeable areas such as buildings, roads and parking lots, and desertified areas with no vegetation response. Masking was performed by detecting all NDVI responses less than zero and assigning the pixels a null value. This masked image was used for training site delineation to remove potential pixels with urban signatures.

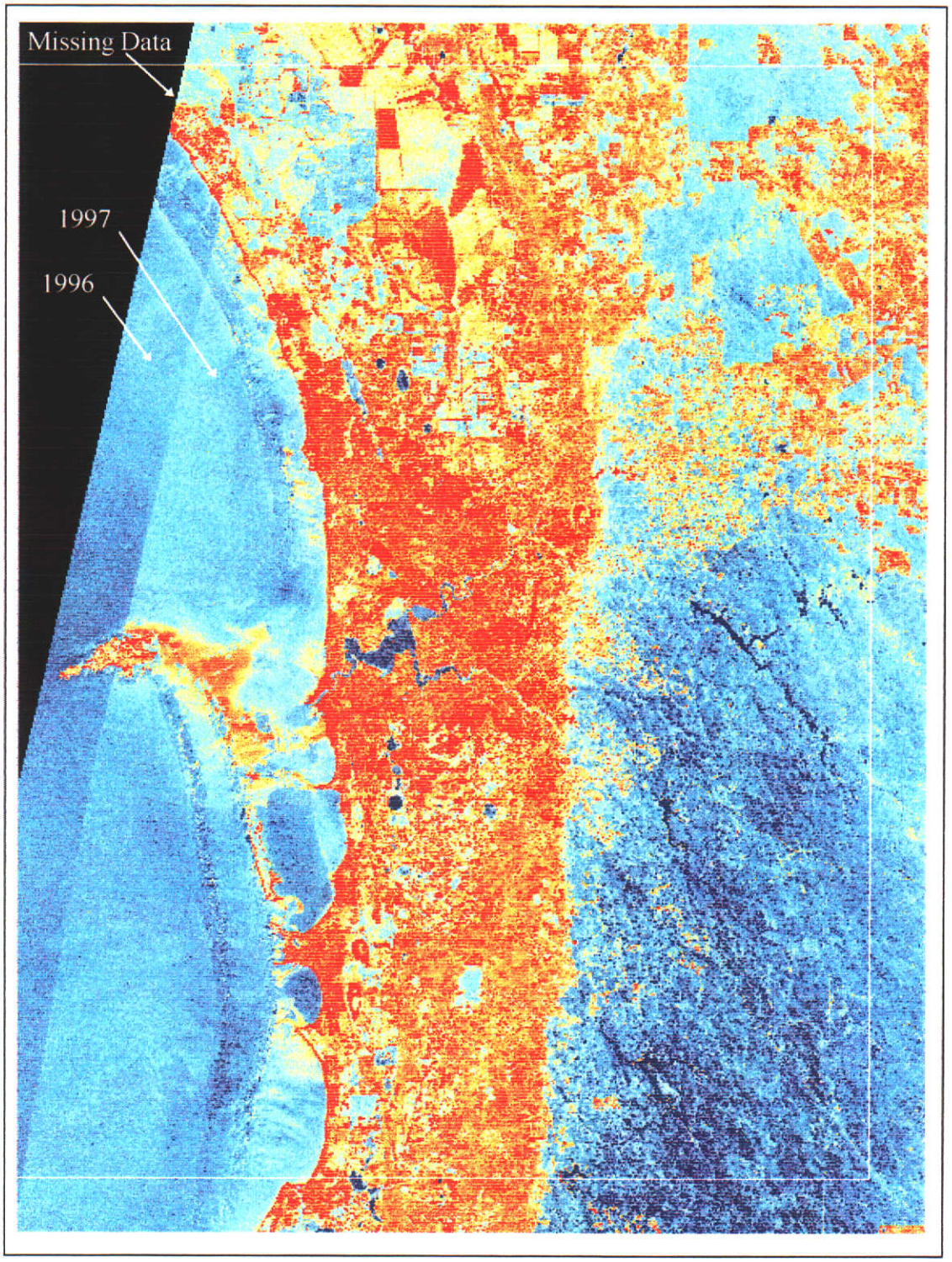

Figure 5.2 Mosaic of 1996 and 1997 images (image difference enhanced for visual purposes)

5.2.5 Boundary Clipping

Initial data reduction was performed by clipping the final mosaic by row and column numbers to eliminate processing of too much data outside of the study area border. A small buffer zone outside of the boundary was left until final generalisation had occurred to exclude edge effects during processing.

5.3 Species Classification and Density Mapping

Unsupervised and supervised methods of classification were tested to delineate vegetation species. Again, because species genera and assemblage are mixed together in the classes to be mapped, they will be referred to generally as *species*. Supervised methods proved superior and are covered below. Density maps were created by correlating several test vegetation indices to ground truth data.

Training sites of known vegetation properties can be delineated on an image to gather the spectral response for similar areas in the rest of the image, outside of the training sites. By gaining this *a priori* training site knowledge of an area on the image to be classified, spectral response across all bands was matched using supervised methods to produce desirable output classes

For both species and density maps, two sets of ground truth/training site information were collected. This included one set of field data to use as pre-classification data and one set of data for post-classification checking of accuracy. Field work was performed in early to mid summer to sample the vegetation in the same state as when the image was taken.

5.3.1 Species Classification

(a) Training Sites

Training sites for species mapping were polygons that contained unique vegetation classes. Approximately ten training sites of at least 100 m square were defined on the final mosaic for each class to be detected (90 sites) (Figure 5.3). Figure 5.3 also

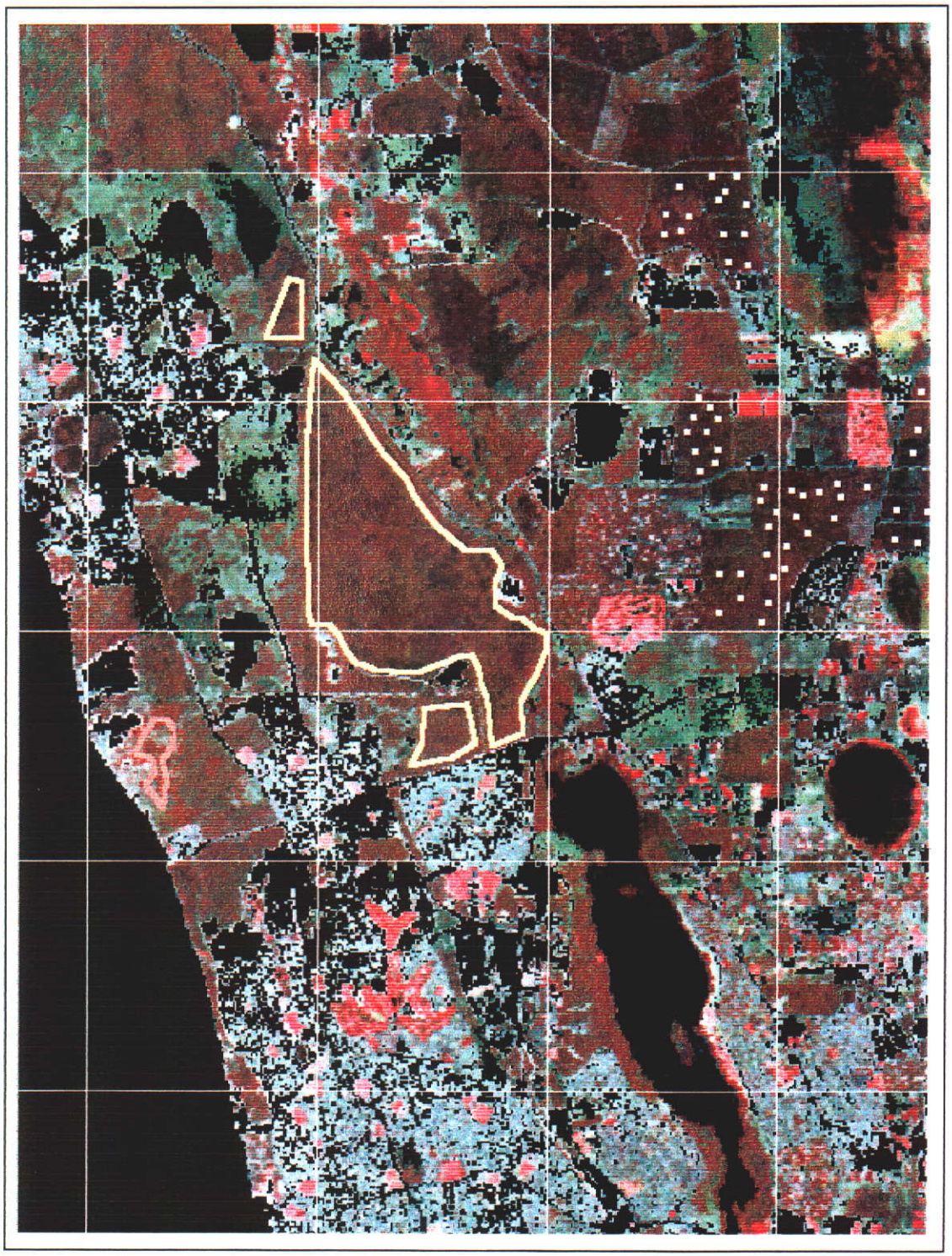

Figure 5.3 Sample training sites for species and density. Point samples are species ground truth, polygon samples are species and density training sites (over masked NDVI image for vegetation response only) Note: grid is 3 x 3 km

contains ground truth point samples. The masked NDVI image can also be seen, and this allowed only pixels with vegetation response to be used for training site delineation. Classification was performed on the entire image, regardless of NDVI value.

Field work included over 1,000 km of travel to sample various vegetation species and density by pacing distance and noting species. Field verification of the 90 training sites was also aided with the masked NDVI screen print out. All field work was noted on hardcopy maps and used in the laboratory to classify imagery.

(b) Ground Truth Sites

Ground truth sites can be selected randomly; however, access to property and potential bushfire threats made random ground truth difficult. Areas of vegetation that were likely to be a certain species were used and often found accurate. Ground truth data was obtained as point and polygon samples (Figure 5.3).

The comparison of ground truth data with the classification maps was performed for approximately ten sites per class in ER Mapper. The areas in the classified map outside of the ground truth sites were masked with a null value to correlate only the area known by ground truth (similar to training site delineation).

(c) Classification Methods

Several methods were available for supervised classification and all seven Landsat TM channels were used. The methods included maximum likelihood with several options, minimum distance to means with levels of standard deviation, parallelepiped, and mahalanobis. Parallelepiped was eliminated immediately from consideration as the software module showed overlapping signatures in spectral classes of training sites and did not classify all pixels. The remaining methods took between six and ten hours each to process.

A neighbourhood kernel was also available and could have been used to classify pixels with influence from a 3 by 3, 5 by 5, or 7 by 7 neighbour influence. These kernels would tend to make areas more homogeneous in the output image, but were

not used as already mixed vegetation classes could be further degraded with the influence of a neighbour option.

The minimum distance to means methods allowed only for the option of zero to *n* standard deviations. Several thresholds were used with zero standard deviations showing the best result. There was a drop in accuracy with one standard deviation, but accuracy increased as the number of standard deviations above zero increased. The Mahalanobis classification was also tested; however no options could be chosen. These methods were not chosen due to their approximately ten percent lesser overall accuracy as compared to maximum likelihood methods.

Maximum likelihood included a standard and enhanced mode for classification; however, all results obtained from various options gave exactly the same pixel classifications and accuracy. The remaining discussion is on the standard mode for maximum likelihood.

With the standard mode of maximum likelihood, two methods were available for classifying the image. The first method used an equal probability of each class occurring in the output image. The second used a prior known or estimated probability of each class to occur in the output image. The prior probability from existing biogenic maps for Perth was calculated and used. The results show the prior probability was the preferred method due to an estimate of total area to be found in the output image. All methods show an increase in accuracy of approximately one percent over equal probabilities.

(d) Accuracy

The method chosen for final classification was maximum likelihood with probability (and no neighbour kernel). For individual classes, high class accuracy was obtained for water (100 percent), pine plantation (95.4 percent), and open marri woodland (79.4 percent). Moderate accuracy was obtained for jarrah marri forest (69.1 percent), tuart woodland (60.9 percent), banksia low woodland (48.6 percent), and coastal heath (48.4 percent). Low accuracy was obtained in mixed species, jarrah, tuart, sheoak and banksia (38.4 percent); banksia and sheoak woodland (37.5

percent); and swampy sheoak, and melaleuca (32 percent) (Figure 5.4 and Table 5.5). Confusion matrix data are shown in Tables 5.6 and 5.7.

	Overall accuracy	Kappa
Minimum distance to means no standard deviation	52.5%	.466
Minimum distance to means one standard deviation	37.8%	.306
Minimum distance to means two standard deviations	44.4%	.381
Maximum likelihood with probability	65.8%	.617

Table 5.4 Minimum distance to means and maximum likelihood with probability classification accuracy - species

Class	Maximum likelihood with probability
Banksia low woodland	48.6%
Pine plantation	95.4%
Coastal heath	48.49%
Tuart woodland	60.9%
Open marri woodland	79.4%
Jarrah marri forest	69.1%
Banksia and sheoak woodland	37.5%
Swampy sheoak and melaleuca	32.0%
Jarrah, tuart, sheoak and banksia	38.4%
Water	100%

Table 5.5 Class accuracy for maximum likelihood with prior probability

Minimum distance to means methods are shown in Table 5.5 along with the maximum likelihood with probability method. The kappa statistic (Table 5.4) is useful in remote sensing for discriminating possible random error in the assessment and backs up the overall accuracy statistic (Jensen, 1996, p. 251; Luman and Ji, 1995).

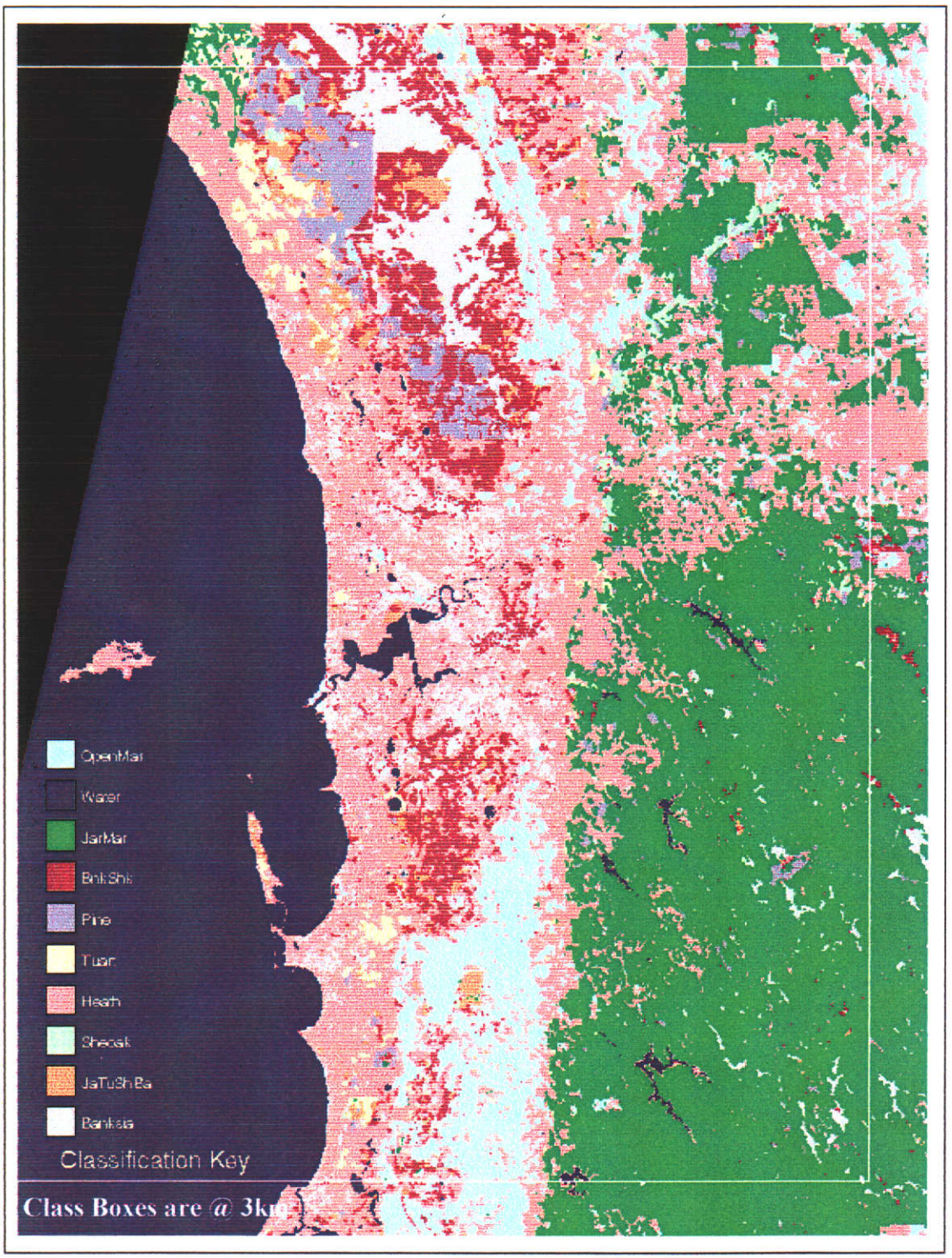

Figure 5.4 Species map before generalisation (maximum likelihood standard with prior probability)

	OM	W	JM	BS	P	T	H	S	JBSH	B
Marri	248	0	0	0	0	0	39	25	0	0
Water	0	503	0	0	0	0	0	0	0	0
JahMar	0	0	395	0	69	50	0	42	15	0
BnkShk	0	0	3	148	26	5	10	3	146	53
Pine	0	0	2	1	337	0	0	0	13	0
Tuart	0	0	1	3	3	147	0	80	7	0
Heath	129	0	0	10	1	18	242	84	15	0
Sheoak	0	0	2	2	17	1	21	26	11	1
JaTuShBa	0	0	9	33	41	59	0	17	115	25
Banksia	0	0	0	24	12	0	0	0	21	54

Table 5.6 Error matrix from image classification (maximum likelihood standard with probability)

	Omission	Errors	Commission	Errors
Class	Total	%	Total	%
Open marri	64/312	20.5	129/312	41.3
Water	0/503	0	0/503	0
JahMar	176/571	30.8	17/571	2.9
BnkShk	193/341	56.5	73/341	21.4
Pine	16/353	4.5	169/353	47.8
Tuart	94/241	39	133/241	55.1
Heath	257/499	51.5	70/499	14
Sheoak	55/81	67.9	251/81	309
JaTuShBa	184/299	61.5	228/299	76.2
Banksia	57/111	48.6	79/111	71.1

Table 5.7 Omission and commission errors for classification (maximum likelihood standard with probability)

The maximum likelihood method shows low accuracy for the swampy sheoak and melaleuca class and for coastal heath. Again, multiple species class accuracies were fairly low due to spectral mixing in woodland types and the influence of urban features (roads, houses, lawns, and exotic gardens). Pine and water were highly accurate which is reasonable due to ease of training site and ground truth data collection and contrast between other classes. The majority of pine forests in Western Australia are single species stands of the same age and are quite distinct

from native Australian vegetation species and were easily captured as compared to sheoak which was wrongly classed into several other categories.

5.3.2 Vegetation Density

The six classes of vegetation density using vegetation indices and eyeball estimates of Projected Vertical Foliage (ground truth data, 60 sites) were delineated. This map is the second input map for the biogenic aspect of the DEP's photochemical smog model.

(a) Indices

The four vegetation indices covered in Chapter 2, the NDVI, IPVI, ARVI and MSAVI2, were tested for density classification. The formulas were applied to the pixel values in the mosaic image to create new output pixel values (Figure 5.5).

(b) Regression Analysis

The resulting vegetation index maps were regressed against the 60 training and ground truth sites to determine correlation. Because ERMapper and Arc/Info could not handle regression analysis on this large dataset, it was imported into IDRISI via Erdas format.

The statistical regression model *regress* in IDRISI easily handled the large files and produced a final result with the linear equation $Y = -0.019705 + 0.373210\ X$, producing an R of 0.9678.

The vegetation index chosen for final determination of cover density was the Infra-red Percentage Vegetation Index (IPVI), with the highest correlation with field data collected (see Table 5.8). The resulting image when regression was applied is shown in Figure 5.6. The other vegetation indices were not considered due to the lower correlation with field data.

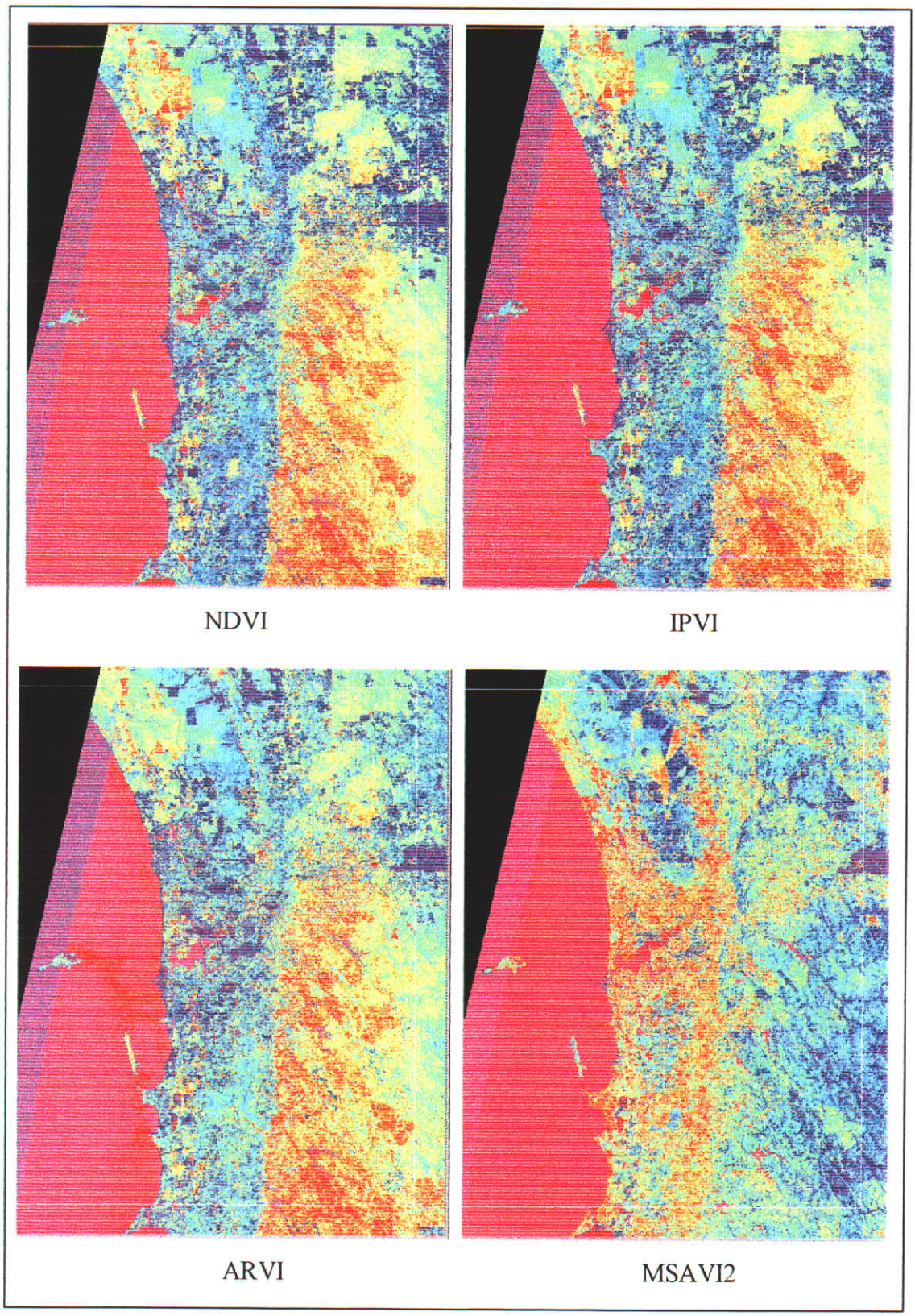

Figure 5.5 Vegetation indices for density mapping (colours used to highlight missing strip of data and relative density)

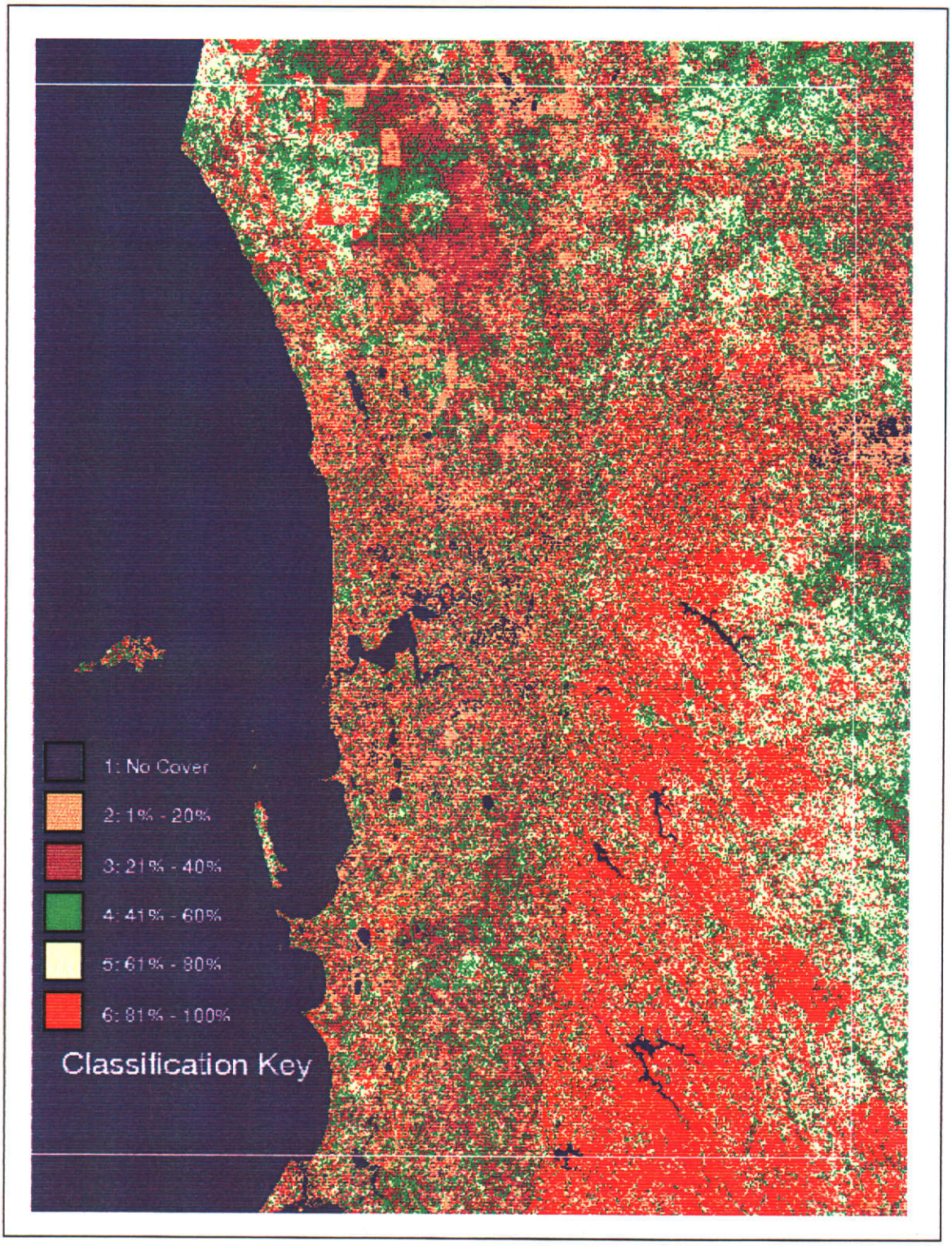

Figure 5.6 Thirty metre density map (IPVI * slope of regression between index and ground truth, then classified)

The order of processing was to run the vegetation indices on the image (ERMapper), then run a regression with the training site data (IDRISI - converted through Arc/Info), and finally to use the regression equation to produce the density map (ERMapper).

Index	Correlation (r squared)
NDVI	0.84.99
IPVI	0.93.66
ARVI	0.92.74
MSAVI2	0.73.84

Table 5.8 Vegetation index correlation with ground truth data

5.4 Final Data Preparation Species and Density

5.4.1 Generalisation

The biogenic emissions maps for Perth had to undergo a generalisation from the original 30 m resolution of Landsat TM pixels to 3 km pixels for input into the DEP photochemical smog model.

Generalisation of vegetation is limited by software functions; however, it is an important aspect of any natural resource application (Painho, 1995). Data loss and integrity issues with generalisation are discussed by Buttenfield and McMaster (1991), Muller *et al.* (1995), and Joao (1995). Most of all, when changing scales it is important to produce a result that truly reflects the phenomena being mapped.

A majority (modal) filter was computed on the two datasets with a kernel size of 101 by 101 to determine the classes with the majority of 30 m pixel responses. These 30 m images were clipped to the study area boundary and subsequently generalised to a three km pixel resolution using linear, nearest neighbour resampling method. By using a linear, nearest neighbour sampling method, output values (3 x 3 kms) were based on the very centre pixel (30 m by 30 m). That particular cell value represents the majority value of the 3 by 3 km area.

5.4.2 Final Boundary Clipping

Once generalisation was complete for both species and density maps, the data set was written to files for use by the DEP. The output file format was an ASCII text file with class numbers to be read by the DEP's Urban Airshed Model.

5.4.3. Results of Two-Dimensional Vegetation Mapping

The final generalised vegetation species and density maps are shown in Figures 5.7 and 5.8. These 3 x 3 km pixel images were given legends manually, as ERMapper did not hold predefined class names. Pixel values, however, retained correct class numbering.

Due to problems with the histogram matching option chosen when mosaicing images, ERMapper assigned null values to some of the pixel values in the output image mosaic. This did not affect density mapping, as new output pixel values were calculated. Species calculations, however, used original input values (some missing) to calculate the new values. This error showed up after generalisation as five of the 3 km pixels were blank containing no data. These missing values were reassigned manually within Microsoft Excel by giving the previous DEP vegetation class values. The image class numbers were then written to an ASCII text file for use by the DEP in Perth.

5.5 Summary

Prior to vegetation classification, the data needed to be prepared for final mapping. The 1997 image was fit to the 1996 image with acceptable accuracy. After image rectification, the two images were mosaiced to gain an input from the 1996 image in a strip of missing data from the 1997 image. Histogram matching was performed to match the data sets to remove some of the differences between the two years of data.

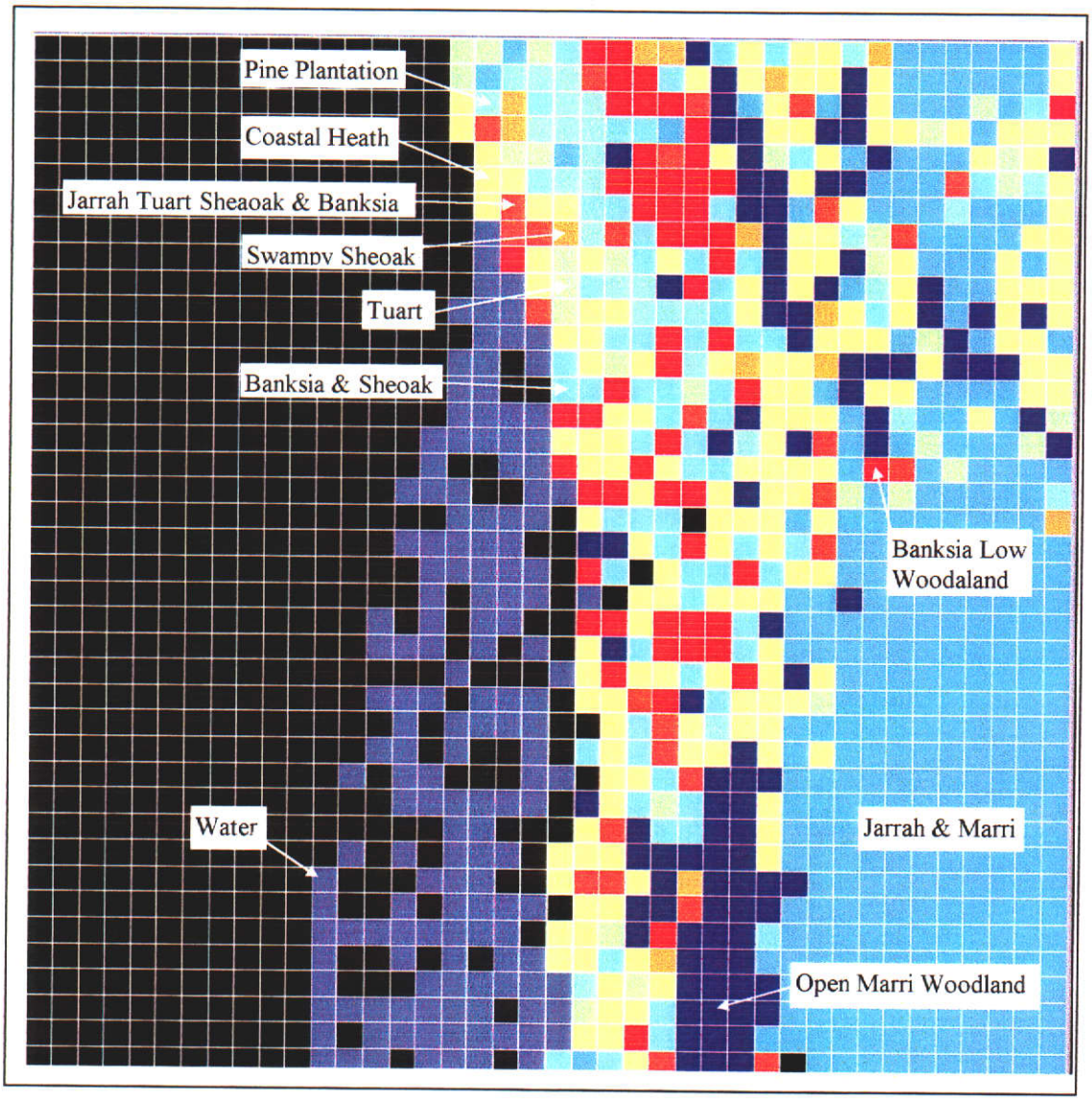

Figure 5.7 Final species map (grid is 3 x 3 km)

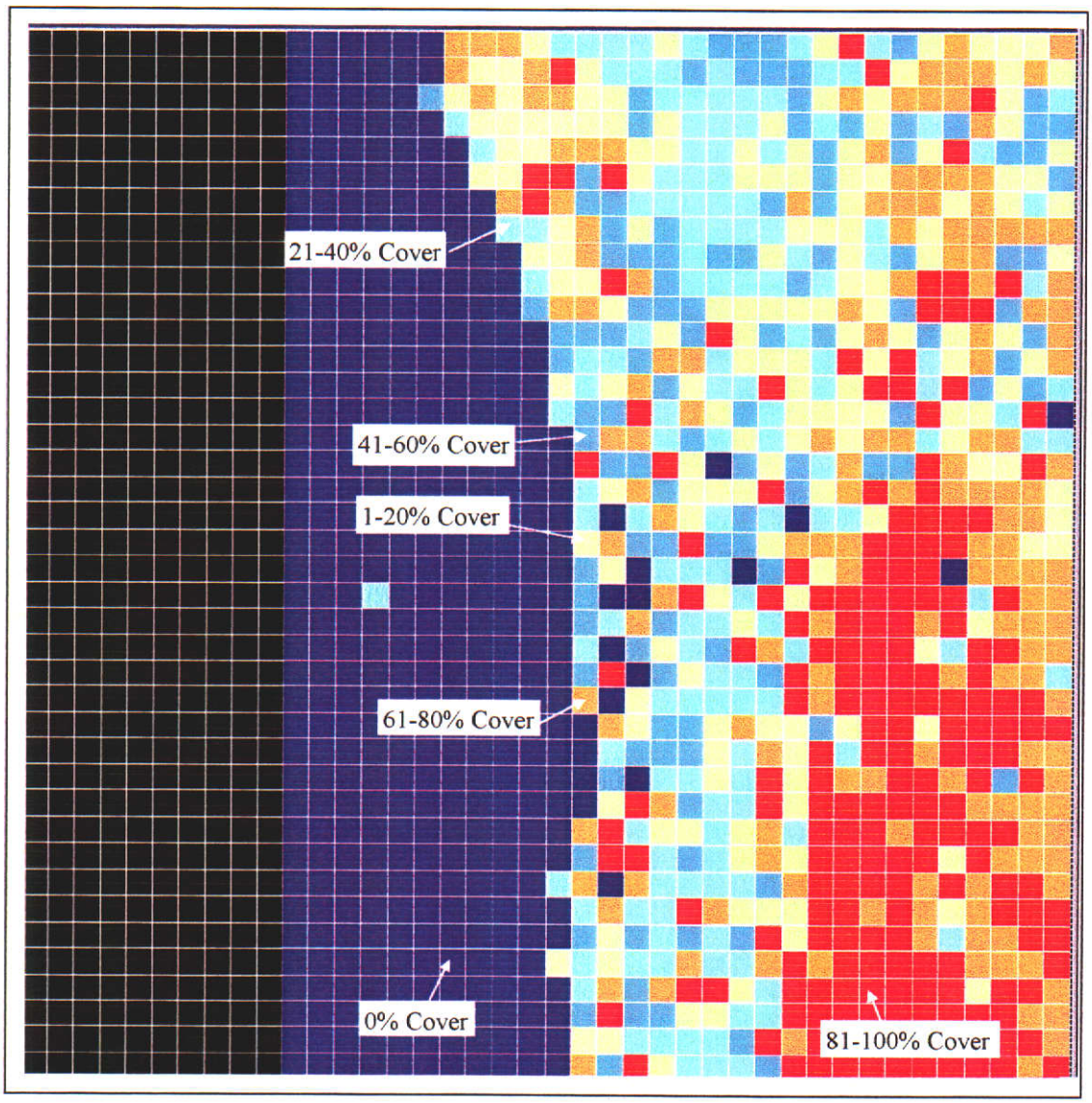

Figure 5.8 Final density map (grid is 3 x 3 km)

To define ground truth data and training sites, an enhanced NDVI image was prepared that removed all pixels with no vegetation response. Extra data was cut from the final mosaic to reduce processing requirements.

Several methods of classification were used on the whole final mosaic, and accuracy was defined by ground truth to define nine species plus water. Class accuracy was not very good for some classes, but others showed high class accuracy.

Density mapping through correlation of ground truth data and vegetation indices created six classes. Data generalisation and final boundary clipping were performed before writing the maps to files for use by the DEP's photochemical smog model.

Chapter 6

SMOG VISUALISATION RESEARCH METHODOLOGY

6.1 Introduction

Smog visualisation was performed to create animations of nitrogen oxides and ozone which highlight atmospheric environmental impacts in Perth. Further animations were created to show the best visualisation of plume movement for both chemicals. These animations show movement, interaction of the two chemicals and show, spatially, where smog occurred throughout the day of March 16, 1994.

A terrain model was used to examine the potential impact of terrain on smog movement. The terrain model was digitised into a 3D Microstation95 design file for plume overlay. Digitising was the preferred option, as digital terrain data was quoted by mapping services at DOLA at a price of over $1,000. The topographic sheets used (Appendix B) to digitise the contours were at a scale of 1:100,000 with 20 m contour intervals.

The digitised contours were generalised to reduce the number of digitised points, then converted to a TIN. The TIN was used only for a simple backdrop to visualisations to show where environmental impacts occurred. No terrain analysis was performed for the Perth region during the creation of visualisations.

For visualisation purposes, global shading and lighting parameters were used. The visualisations are comprised of up to 80 time slices, out of a possible 84, from morning until late evening. Further, the visualisation clearly shows that plume movement follows weather conditions for the day. The final visualisation products were produced in a format that is viewable on the Internet or through a media player.

6.2 Digital Terrain Model

The digital terrain model is useful for visualising potential effects of terrain on nitrogen oxide and ozone formation and movement. The relatively flat terrain was enhanced in visualisation by scaling z values. A vertical exaggeration of 50 was used for the final visualisations, but exaggerations of 10 and 25 were tested and shown. Resulting relief remained at a low resolution, but general features were shown well.

6.2.1 Digitising Contours into Microstation95

Digitising of contours was performed using two digitisers. A Calcomp 9000 digitiser was used for the first few topographic sheets; however, the digitiser malfunctioned and another smaller one (Calcomp Drawing Board III) was used. There was some difference between the digitisers which caused errors in the final design file (see Section 6.2.2). A program within Microstation, Edit DesiGn file (EDG), was used to fix these errors, yet software crashes due to the design file errors occurred even after the EDG error application was run.

Microstation95 was used for digitising into a 3D design file. Further, editing of contour heights, even though digitised at the correct height, needed to be performed. Though some errors remained in the file, most were fixed manually. Overall, representation remains good for the scale used (1:100,000).

The coastline and some contours on 20 m intervals were used for the Swan coastal plain; however, the scarp and fault block with high relief were digitised with the index contours only (100 m intervals). The resulting contour file covers the entire study area (Figure 6.1).

6.2.2 Building the Surface with Site Works

Site Works is an add-on package for Microstation95 that was used to create the Triangular Irregular Network (TIN) surface by interpolation of nodes and vertices on the contour lines. Though the contours were generalised to reduce the number of points to interpolate, file operations were computationaly intensive. The resulting triangulation is shown in Figure 6.2 with a z exaggeration of 25.

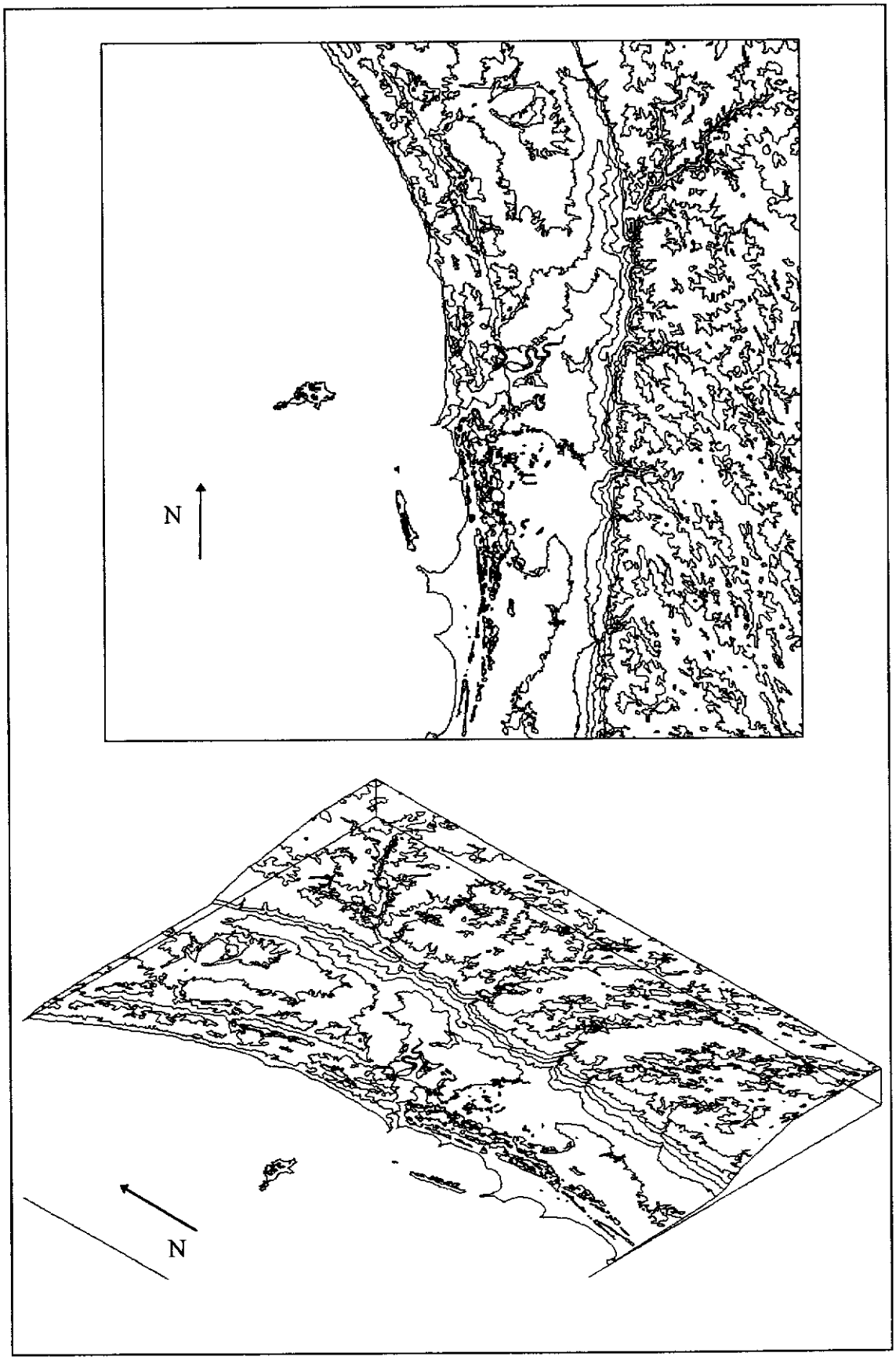

Figure 6.1 Digitised contours 2D and 2.5D (z scale 25)

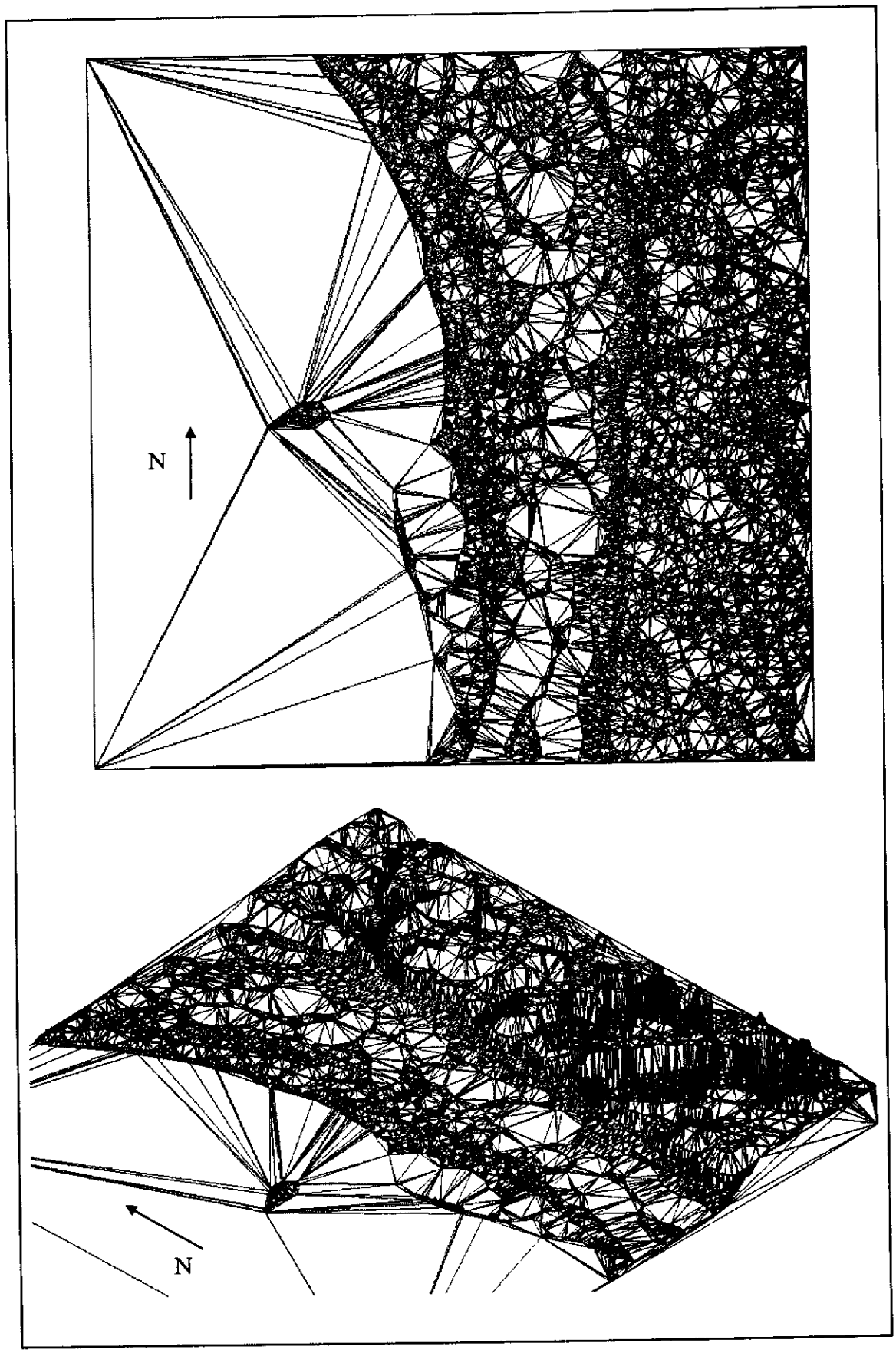

Figure 6.2 Triangulated contours 2D and 2.5D (z scale 25)

The triangulation placed some contours and points 100 to 300 m higher than they were on the digitised file. As these points were clearly visible as interpolation errors resulting from using two digitisers (see section 6.2.1), they were manually edited back to their true heights.

The terrain model was used as a backdrop for the volumetric plumes. Three-dimensional data was overlayed with the terrain model and visualised over time. The terrain model, exaggerated by a factor of ten in the z coordinate, is shown in Figure 6.3. Shading is added to aid relief interpretation.

The triangulated surface was imported directly into Voxel Analyst for overlay with the plume data. The surface was shaded with a constant option in Voxel Analyst the default setting. Other lighting sources were tested; however, the default lighting remained the best, as large shadows and dark regions appeared with other selected light sources.

6.3 Three-Dimensional Volume Generation

6.3.1 Excel to Break DEP Files into Time Slices

The files obtained from the DEP were used to extract 3D data for March 16, 1994. The times used during volume generation were strict time-slices sampled every six to 15 minutes for the whole day. The DEP typically uses hourly averaged data, but this research concentrated on time slices to visualise movement. Only two to three hours of data were collected at 15 minute intervals. The rest were collected at six minute intervals for a total of 80, out of a possible 84, time slices.

The data was manually extracted from the DEP files using Microsoft Excel. The Office97 version of Microsoft Excel was needed due to limitations on the size of files in Excel95. Once broken into smaller time-slice files, the Office95 version was used to extract the time slices for both chemicals (nitrogen oxides and ozone).

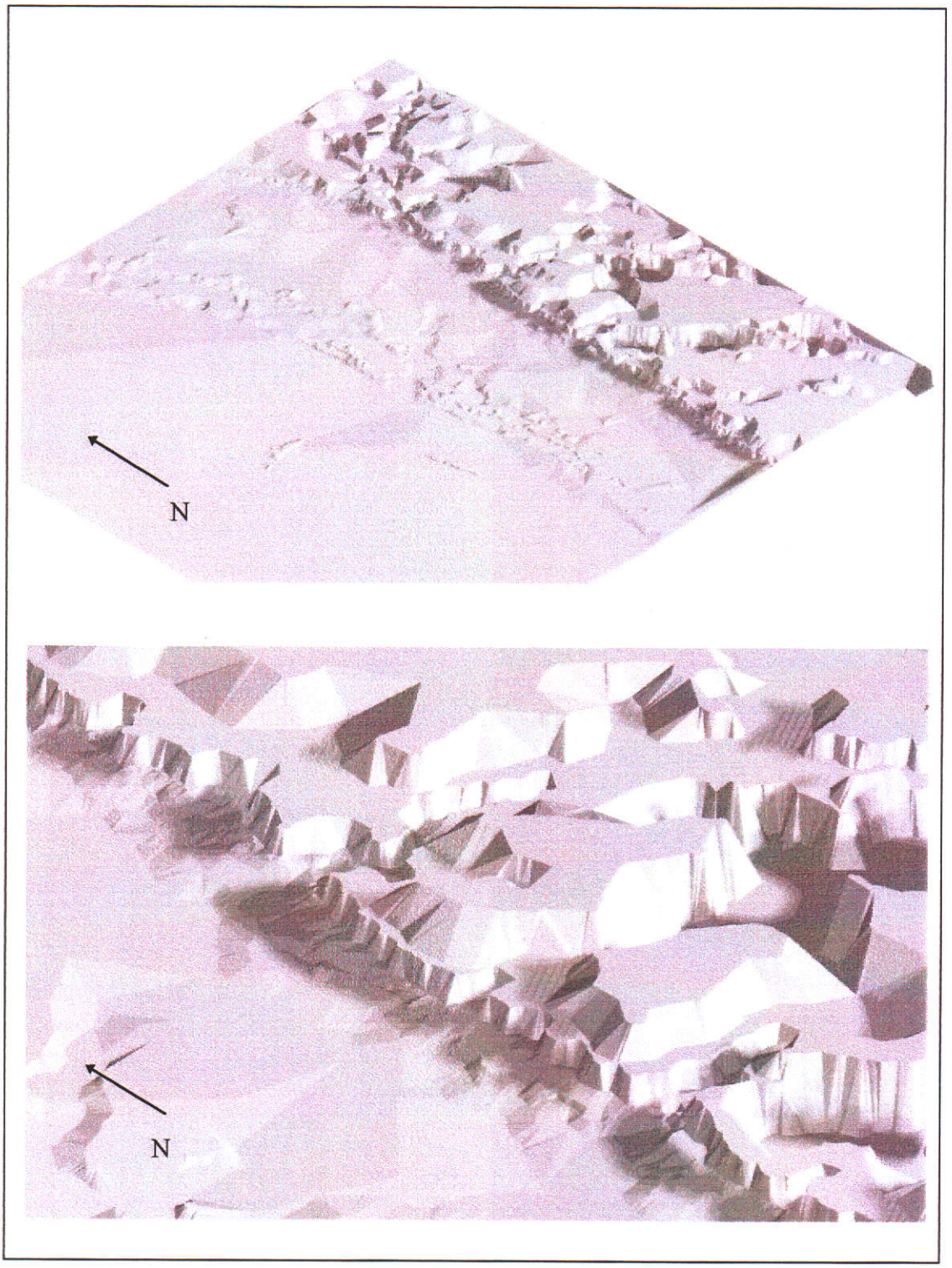

Figure 6.3 Terrain surface, exaggerated by 10 in z.

6.3.2 Using Qbasic to Reformat DEP Data for Voxel Analyst

Once the data from the DEP was extracted into time slices, a method was needed to reformat the data for input into Voxel Analyst. A program mentioned in Chapter 4, was written in Qbasic to perform the data preparation (Appendix A). This program read each hourly text file and arranged the data in Voxel Analyst format. This was performed by using vertical spacing as constants in the program and reading the DEP file into variables for x, y, and attribute. The z value was obtained from the position of points within the file. The resulting output was a space-delimited file with x, y, z, and attribute values on a separate row for each point.

6.3.3. Importing into Voxel Analyst

During 3D volume generation, data spacing was important to generate a true representation of the phenomena being mapped. Data obtained from the DEP was regular and smooth in x and y dimensions which allows for good interpolation and volume generation. In the z dimension, however, data is increasingly sparse, yet somewhat regular, as distance from the earth's surface increased making interpolation less accurate as z height increased.

(a) Sparse to Volume Interpolation

Once the point data had been converted into Voxel Analyst sample point format, volumetric data was needed. This was accomplished through the Voxel Analyst *sparse2volume* module. The resulting interpolated data sets were used to *threshold* the volumes for 4D visualisation

The x, y, z, and attribute values were read into Voxel Analyst by the module for image generation. The Voxel Analyst module converted the 12,800 points for each time slice into voxels. Several interpolation methods were available, each with custom options available. The choice of methods was dependent on the data set to interpolate.

The interpolation methods range from first-order to third-order volumetric generation. The first-order methods, shepard, and metric, are good for sampling

sparse and irregular data. A second-order and a two-and-one-half-order method, multi-quadratic and thin plate spline, along with a third-order method, volume splice are good for relatively regular and smooth data.

Since the DEP file was an interpolated data set, it was felt that these points should remain dominant in visualisation to reduce data loss in re-interpolation, so first-order interpolation methods were preferred. These first-order methods would reduce the error propagation that was likely to occur with DEP point samples and the resulting interpolation. This was done by preserving the original DEP values. Second and third-order fits interpolated to values that were not in the original file.

The Shepard method is an inverse distance weighted method. The metric method is an extension of the inverse distance weighting that uses the power of that (inverse) distance for an output weighting factor. The metric method was chosen due to flexibility in specifying the power of sampling.

Background and influence range variables were tested on the Metric method. These variables are for sparsely sampled areas to give areas a minimum interpolant value upon interpolation. Setting the power, background and influence range to five, one and one, respectively, gave a good result. The power of five gave moderate influence on output of neighbouring cells, as the power of two (the default) had vertical layering present from the sparse data.

With background and influence range set to one, sparse areas were slightly influenced by distance from sample points. These parameters allowed for good interpolation, especially with the somewhat sparse z scale.

(b) Generating Chemical Thresholds

Two sets of values were used for generating thresholds. The first values of 4 ppb (nitrogen oxides) and 50 ppb (ozone) were used to highlight plume movement. Further, environmentally significant values of 20 ppb (nitrogen oxides) and 80 ppb (ozone) were used to show potential impact to humans and vegetation. A further ozone threshold was set at 60 ppb, as little plume extent was found at 80 ppb. These

environmental impact values were requested by the DEP. The values needed to highlight plume movement were defined by this research.

To generate the desired attribute value for the 3D air body, colour tables were used. All values that equalled, or were above, the threshold were assigned the colour blue-grey (ozone) and tan (nitrogen oxides). Values below the threshold were not shown to improve visualisation of high concentrations of chemicals.

Several other thresholds were tested (for highlighting plume movement) with either too much volumetric data in the scene or too little plume movement and extent. This occurred when nitrogen oxide levels used were below four and above 20 ppb. For ozone, this occurred when levels used were below 50 and above 60 ppb.

(i) Nitrogen Oxides

Each time slice of nitrogen oxides was generated using the same colour table with a light tan colour to represent potential pollutants from cars and industry (Figure 6.4). This sample figure is for 8:00 pm on March 16, 1994 with a threshold of 4 ppb and vertical exaggeration of 50. Terrain is automatically exaggerated with the volumetric scale factor of 50 for visualisation of the plumes over the terrain surface.

It can be seen that the plume would appear to extend outside the study area to the north east and vertically. Chemical levels over the ocean are still relatively high, yet the plume remains very close to sea level.

(ii) Ozone

Each sample for hourly ozone readings was generated with the blue-grey colour to represent the clear to whitish body of ozone (Figure 6.4). This sample figure is from four pm on March 16, 1994 with the threshold set to 50 ppb. Terrain height is again exaggerated, along with volumetric plumes, by a factor of 50.

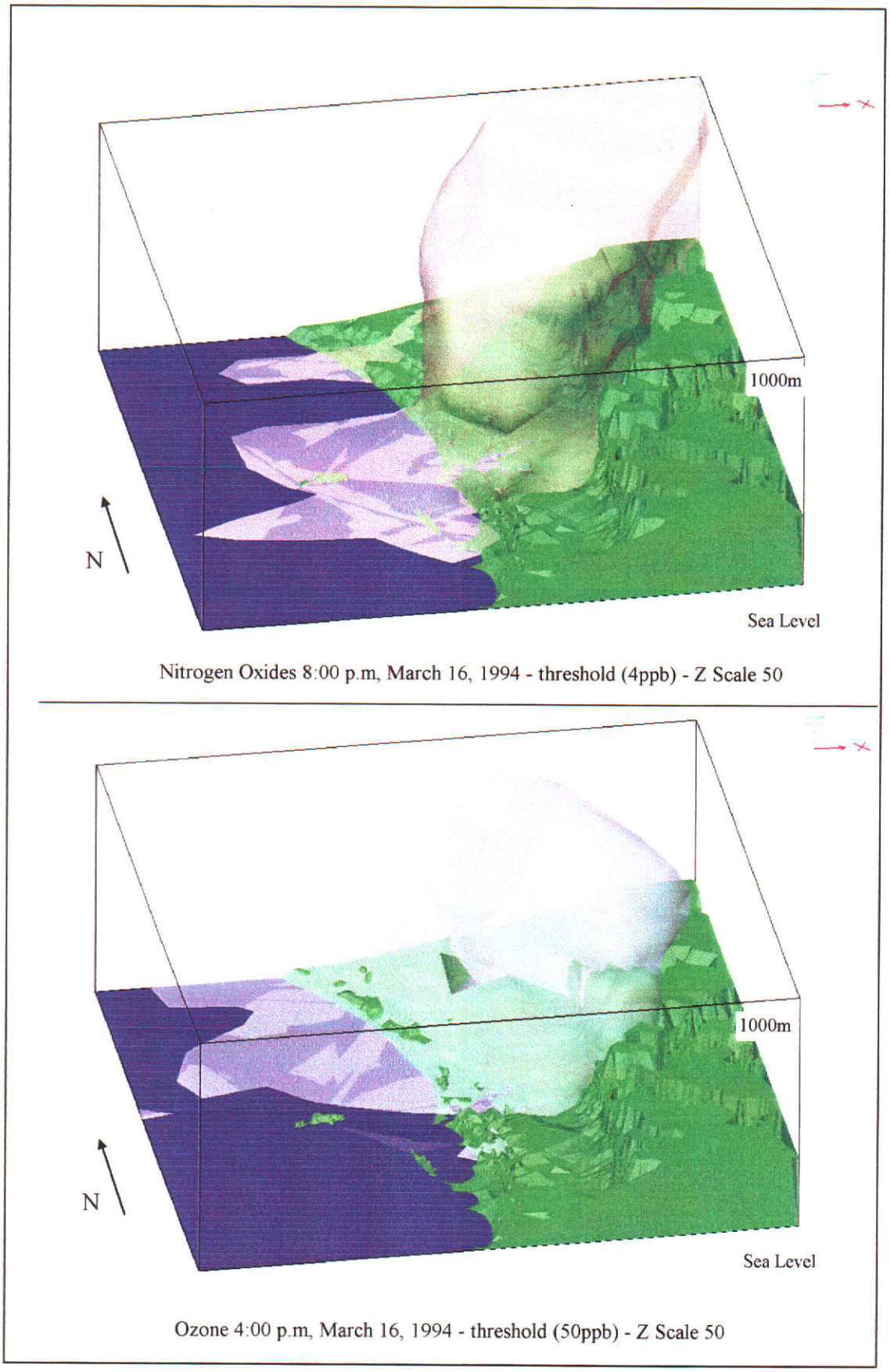

Figure 6.4 Sample Nitrogen Oxides and Ozone plumes

This ozone plume extends over the northern part of the study area. Similar to nitrogen oxides, low plume extent over the ocean is present. Over the land, a distinct wall of ozone is near the north east corner of the study area.

6.3.4 Exporting from Voxel Analyst

Export options from Voxel Analyst were limited to 3D Microstation design files and x, y, z, ASCII format. Microstation95 could only perform visualisation on objects by physically moving the individual points that comprised the object. With 12,800 points per plume and 80 time slices, this was physically impossible. Due to problems with visualising temporal and environmental data in the CAD or GIS based environments, another export format was needed to import into Macromedia Director for visualisation.

Due to the lack of import capabilities for x, y, z data into Director, the ability to capture the scene as a Windows bitmap file and import into Director remained the only suitable option.

6.3.5 Importing to Macromedia Director

Due to the memory requirements of handling up to 80 time slices, only sets of 20 images were imported into Director at a time. The software imported these images as characters to use upon a movie set. This software concept allowed each character (image) to be on the stage for just one scene in a movie.

6.4 Four-Dimensional Temporal Animation

6.4.1 Animation Development within Macromedia Director

The volumetric bodies for each time sample were used to develop time-slices in the 4D visualisation. This required placing the imported characters into different scenes or frames of the movie. Once these images were placed upon the differing frames, the movie could be edited to increase or decrease frame speed. The speed chosen for all visualisations was two frames per second.

(a) Nitrogen Oxides

Almost the maximum number of time slices, 80 out of a possible 84, were used for the visualisation to highlight plume movement. The remaining four time samples were not taken by the DEP stations due to low wind conditions in the early morning. The visualisation to highlight environmental impact contained less than ten time slices throughout the day. A sample number of time slices to highlight movement are shown in Figure 6.5.

Nitrogen oxides at four ppb are present from 7:00 am in the middle of the study area in a vertical column. This urban emission plume stays relatively stable throughout the day, with minor increases during peak traffic hours. Plume movement is somewhat easterly in the morning with a sharp change just after 10:00 am that moves it back over the city centre. The plume remains generally over the city until late in the day. Finally, after 7:00 pm, the top of the plume can be seen to move to the north-east corner of the study area. The central column may be the result of constant city traffic throughout the day plus other chemical reactions occurring near the city.

(b) Ozone

Due to ozone developing later in the day, only time slices after 12:00 pm were used. For the visualisation to highlight plume movement, the first ozone was present just past noon. For the visualisation to highlight environmental impact, the first scene of ozone from 1:36 pm was used. Sample time slices are shown in Figure 6.6 to highlight plume movement.

(i) Visualisation to Highlight Plume Movement

These time slices of ozone show a strong east-north-easterly movement as the day progresses. This matches conditions of the coastal sea breeze reported in the meteorology of the day (Rye, 1996).

(ii) Visualisation to Highlight Environmental Impact

These time slices to highlight environmental impact follow the pattern defined to highlight plume movement, yet spatially, the plume is slightly smaller and begins later in the day.

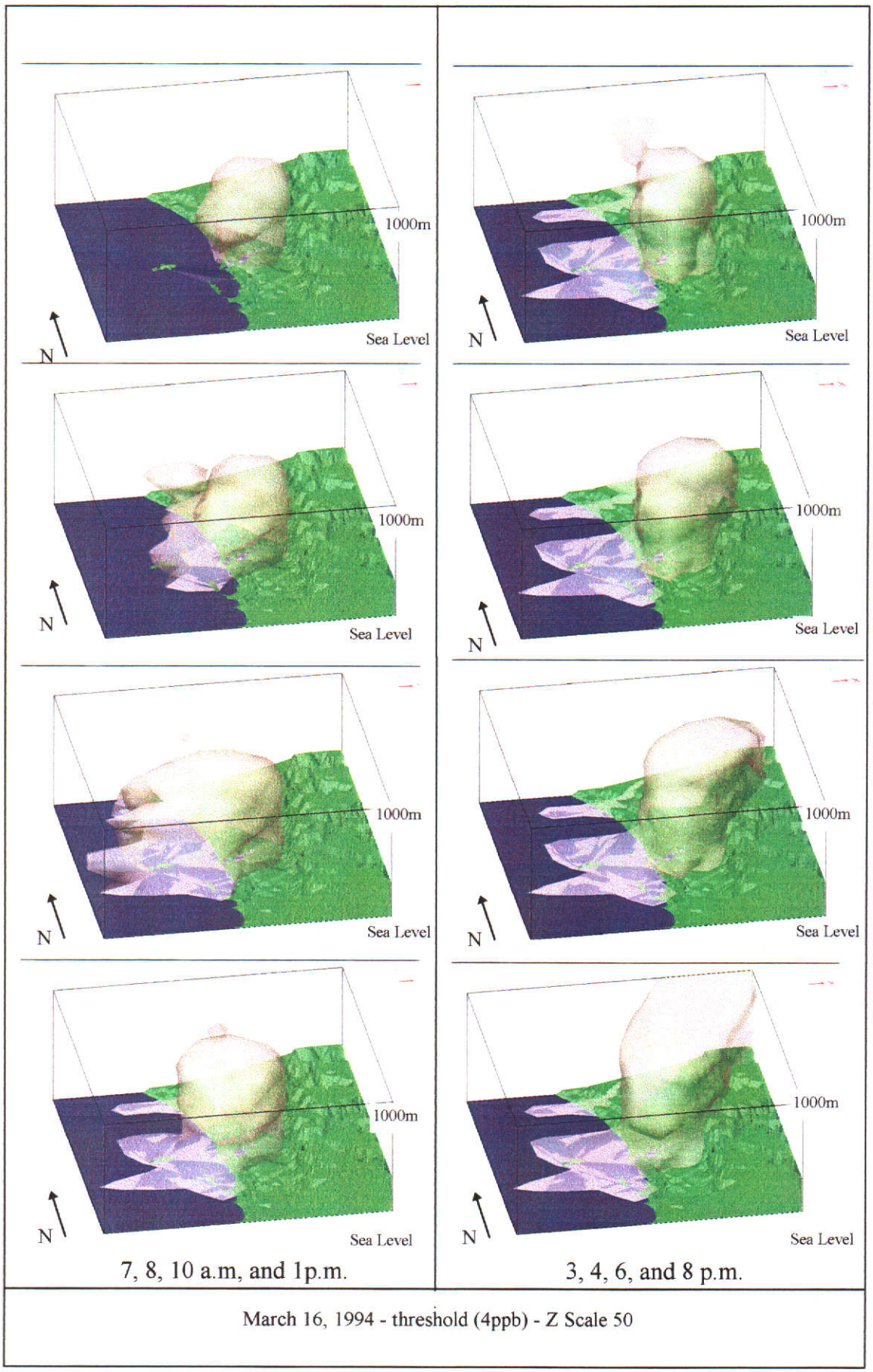

Figure 6.5 Hourly s*lices* of Nitrogen Oxides movement 7:00 am - 8:00 pm

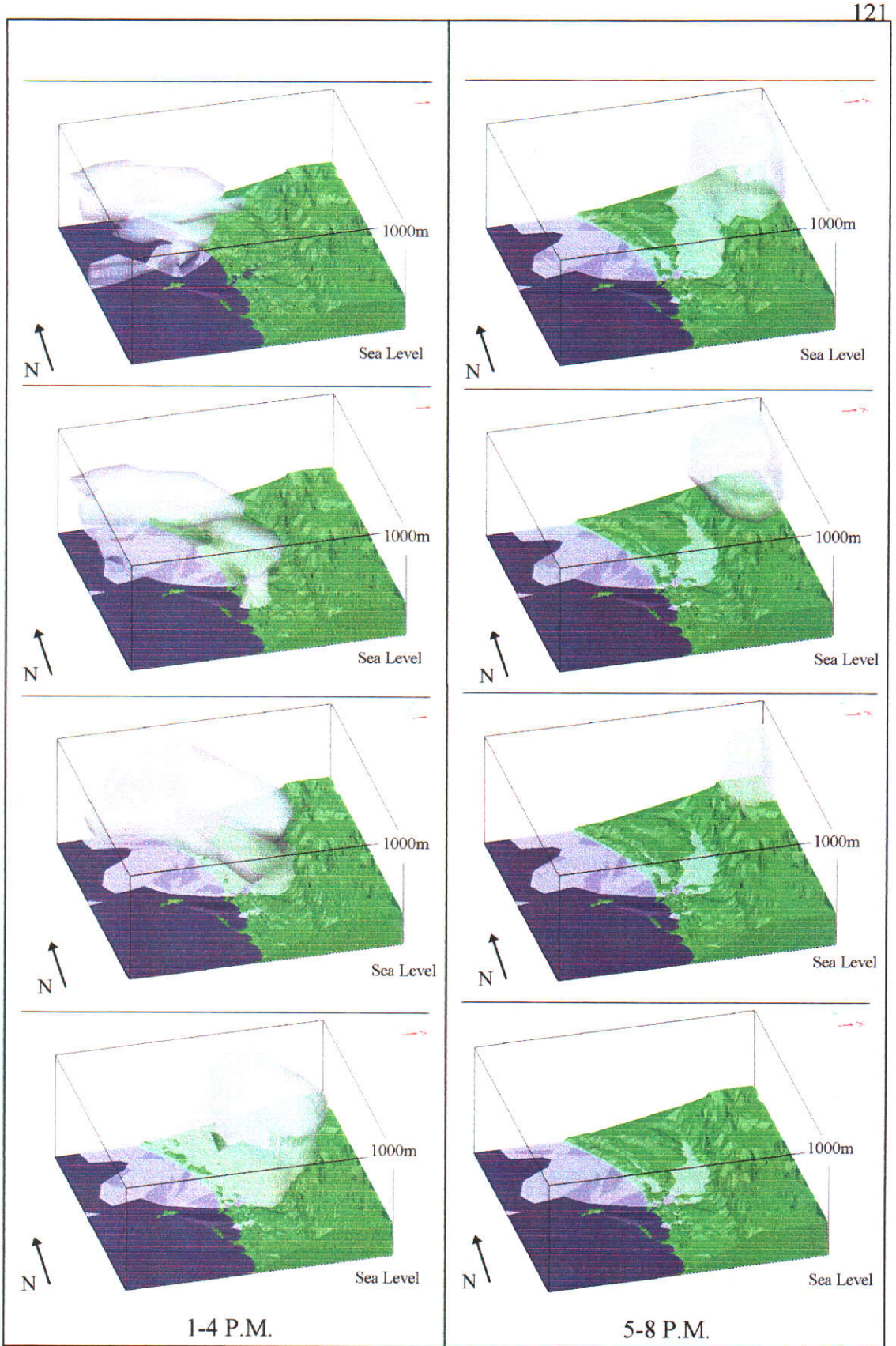

Figure 6.6 Hourly *slices* of Ozone movement 1:00 - 8:00 pm

(c) Interaction of Nitrogen Oxides and Ozone

It is difficult to understand all of the complex processes involved in photochemical smog, but nitrogen oxides can play a significant role in ozone formation. Visualising the interactions of the two plumes throughout the day can show some potential conversion from nitrogen oxides to ozone. The generally low levels of nitrogen oxides throughout the day may have hampered visualisation of the interactions. Time slices for chemical interaction are shown in Figure 6.7.

(i) Visualisation to Highlight Plume Movement

The time slices highlighting ozone and nitrogen oxide plume movement show that the ozone plume builds (due to the conversion of nitrogen oxides) near the coastline at 12:12 pm, and moves steadily east-north-east before reverting back to nitrogen oxides and passing out of the study area at around 8:00 pm. This also matches the forecasted patterns in Rye (1996). Ozone can be seen to divert towards the high levels of nitrogen oxides over the city centre. This may be due to nitrogen oxides converting into ozone under high temperatures.

Through visualisation, it appears as though nitrogen oxide is indeed a precursor to ozone on this day. It appears as if the ozone plume is pulled towards the nitrogen oxides column over the city, but this is actually a result of the sea breeze. The ozone plume steadily moves out of the study area and away from the oxides plume. The oxides plume does seem to follow in the tracks of the ozone plume and starts to exit the study area to the north-east corner during late-evening sampling. Again, different thresholds may reveal other complex interactions and processes throughout the day.

It also appears as if much of the nitrogen oxides are converted to ozone when temperatures are high. When cooler temperatures exist, however, the nitrogen oxide plume appears to expand because the conversion to ozone is not occurring.

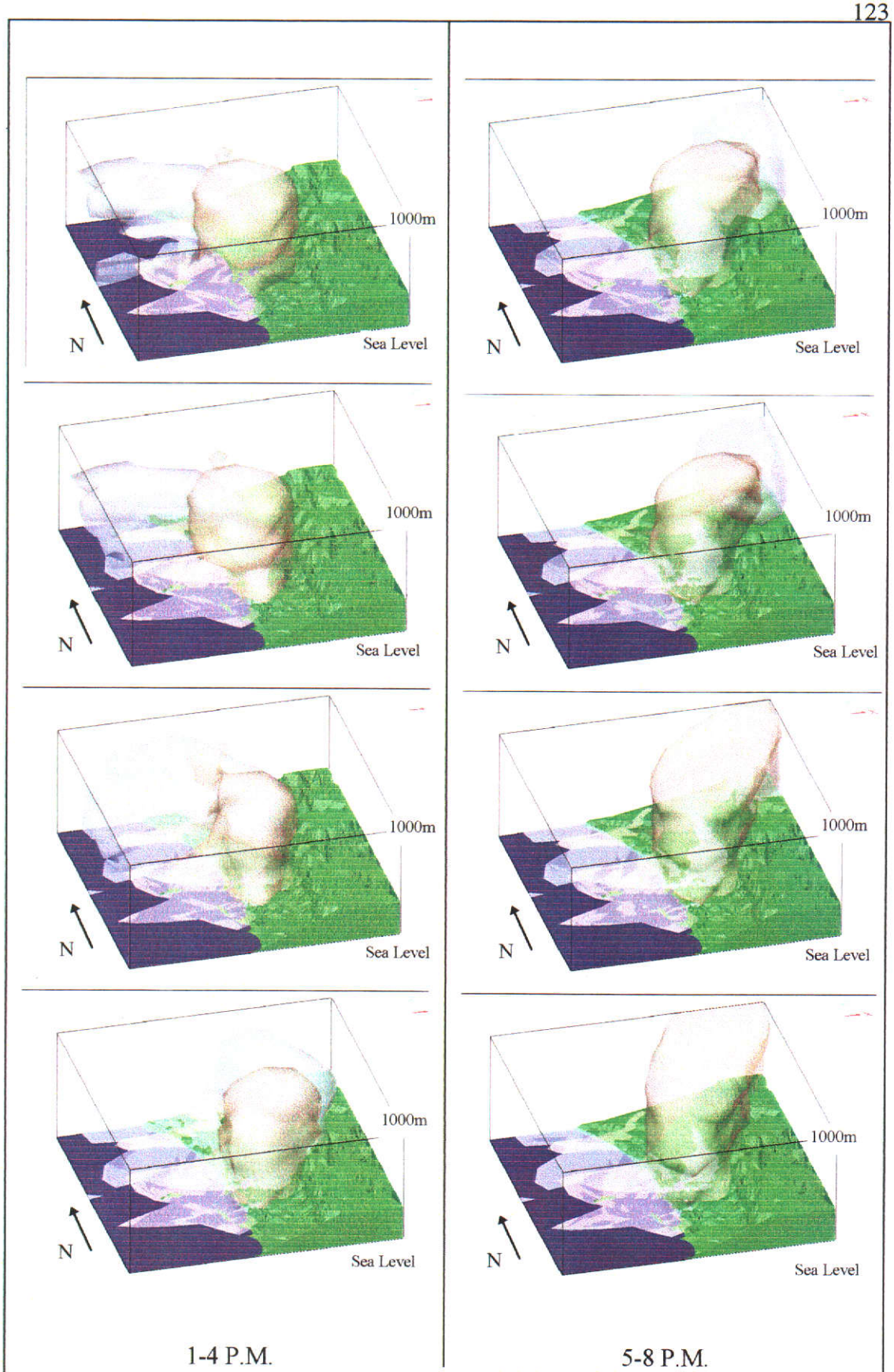

March 16, 1994 - threshold (Nitrogen Oxides: tan - 4ppb Ozone light blue - 50ppb) Z Scale 50

Figure 6.7 Hourly *slices* of Ozone and Nitrogen Oxides movement 1:00 - 8:00 pm

(ii) Visualisation to Highlight Environmental Impact

At levels of 20 ppb (nitrogen oxides) and 80 ppb (ozone), almost no plume extent was noted. No animations were created for these levels, as they were plotted as cumulative totals (all time slices shown on top of one another). Plume extent for the cumulative totals is summarised in Figure 6.8. A final test of ozone alone at 60 ppb was generated, as plume extent was large enough to warrant an animation. Forty time slices were used to create the ozone visualisation.

(d) Interaction of DTM and Plumes

The interpolated DEP data was not corrected for terrain, so examination of the interaction of plume data and the terrain model was performed in Voxel Analyst. When plumes extended above the elevation of the terrain surface (plume and surface exaggerated by 50), plumes were visible. Where the volumetric data is below the elevation of the terrain model, however, it was masked out of the image. This effect looks like fog in a valley (Figure 6.9). In future analysis, true levels should be corrected for elevation to show terrain interactions.

6.4.2 Export as AVI Format

The animated movies created in Director were exported in the Windows video format called Audio Video Interleave (AVI). This format can be viewed on most personal computers with multimedia capabilities (i.e. Netscape or Internet Explorer or a media player within Windows 95). Further, this file can be placed in a web page to allow access to the visualisation via the web. The visualisation can be downloaded from the web page to a remote computer. Once the visualisation is downloaded, it can be run relatively efficiently on the remote computer depending on the computer's speed in relation to the web connection.

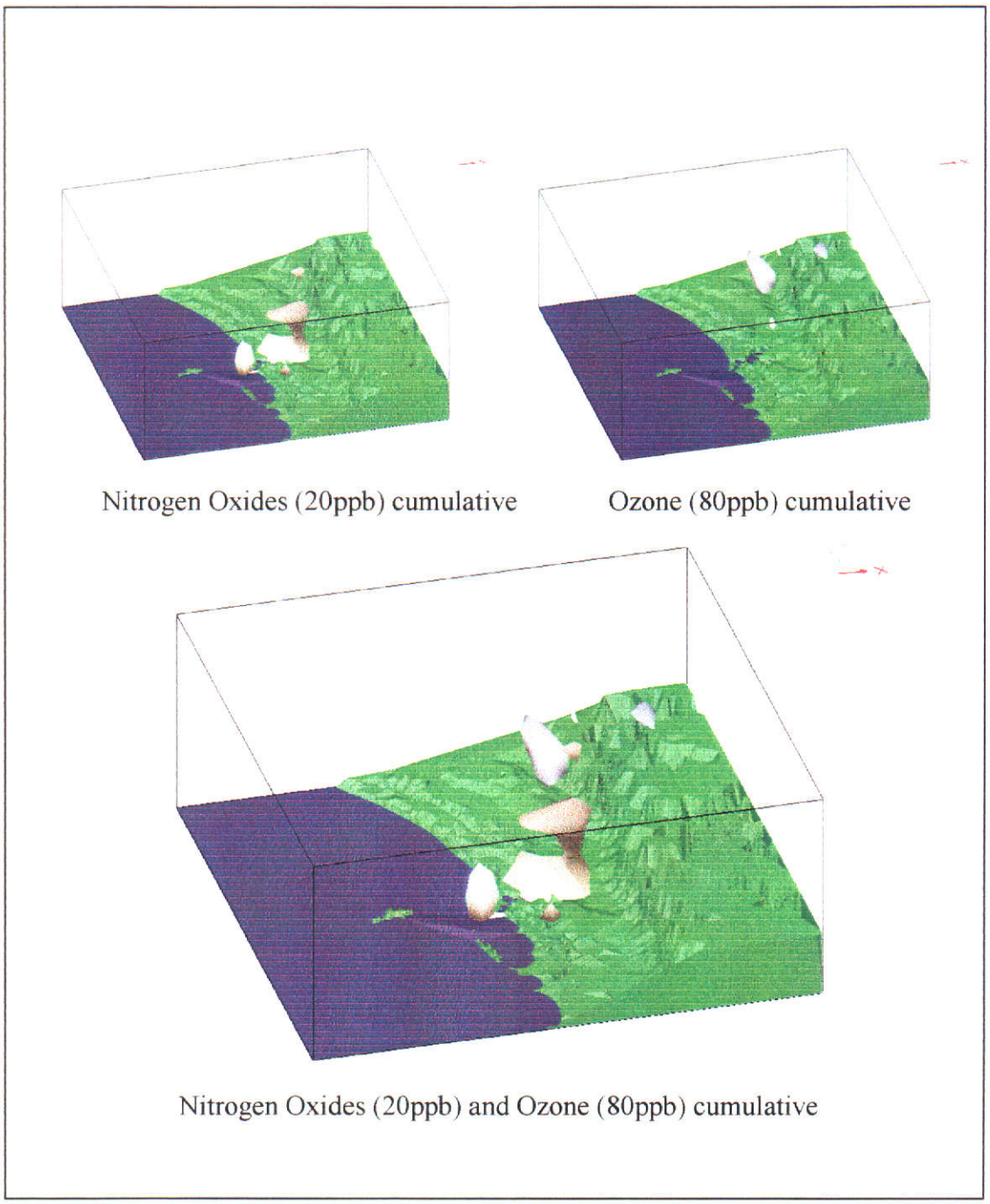

Figure 6.8 Total cumulative exposure to Nitrogen Oxides (20ppb) and Ozone (80ppb)

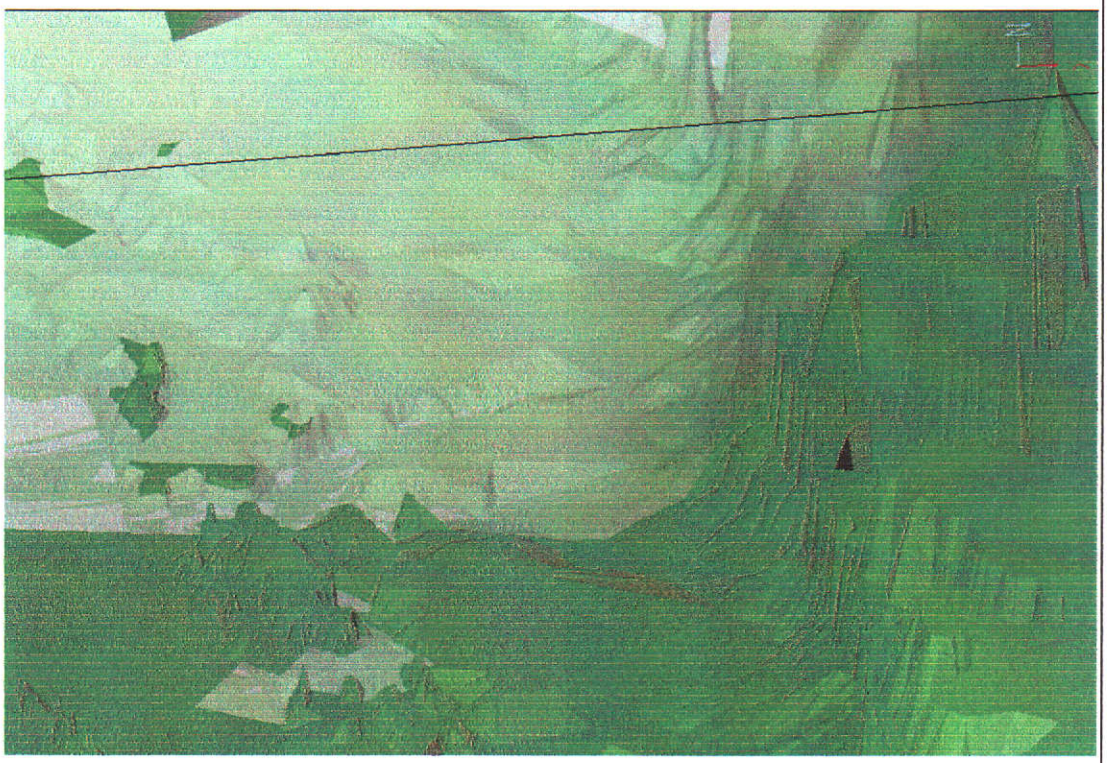

Ozone plume data above terrain (4:00 pm)

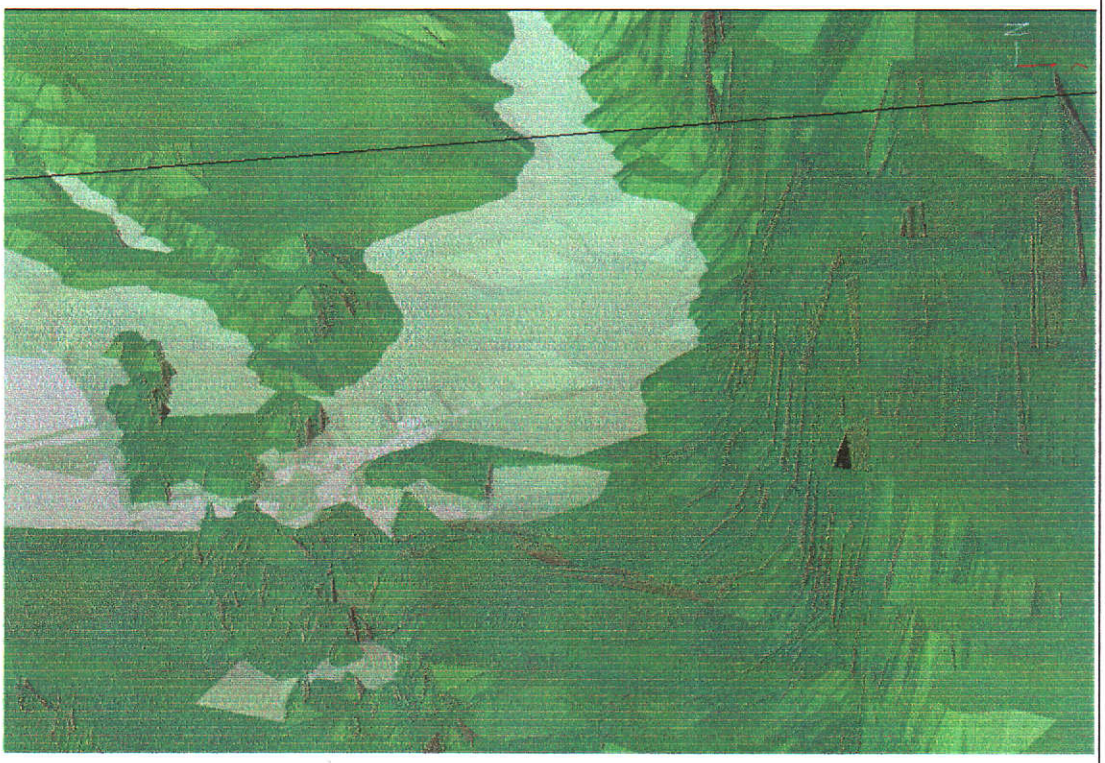

Ozone plume data below terrain (8:00 pm)

Figure 6.9 Interpolated plumes not corrected for terrain

The full visualisations (uncompressed) are over 100 MB in size per file and would be unsuitable for WWW access. Therefore, final web visualisations were compressed. Within Macromedia Director, a compression value of 25 brought file sizes down to less than 2 MB. There was little degradation of image quality, yet some blurriness occurred around plumes and text items.

Final visualisations were written to CD ROM (Appendix C) and are available at http://www.cage.curtin.edu.au/~sandisd/visuals.html. The visualisations were saved at an 800 x 600 pixel resolution and can be viewed through a media player or a web browser. The visualisation files are described in Table 6.1.

Visualisation purpose	CD ROM file name	File size
To highlight environmental impact (ozone at 60 ppb)	Ozone_impact_60.avi	38 MB
Same as above (compressed)	Ozone_60.avi	1 MB
To highlight plume movement (nitrogen oxides at 4 ppb)	Nox_move_4.avi	75 MB
Same as above (compressed)	Nox_4.avi	2 MB
To highlight plume movement (ozone at 50 ppb)	Ozone_move_50.avi	44 MB
Same as above (compressed)	Ozone_50.avi	1 MB
To highlight plume movement and interaction (nitrogen oxides at 4 ppb and ozone at 50 ppb)	Both_move_interact.avi	75 MB
Same as above (compressed)	Both.avi	2 MB

Table 6.1 Eight animation files included on CD ROM (Appendix C), compressed and full versions

6.4.3 Results of Multi-Dimensional Smog Visualisation: Nitrogen Oxides and Ozone

The nitrogen oxide plume can be seen to extend in a column over the city centre, with some easterly expansion during the morning. The plume then moves back over the city centre during midday. The plume stays relatively stable until late in the day when the plume can be shown to head north east and extend past the study area boundary. This is consistent with the day's wind conditions.

During the higher sun angle and temperature periods of the day (9:00 am to 3:00 pm), the nitrogen oxides appear to convert to ozone that can be seen to expand rapidly as the afternoon progresses. At the low chemical thresholds used to visualise this conversion, the true interactions may not be visible. A series of tests are needed to model the conversion of nitrogen oxides to ozone more accurately than visual methods.

Ozone at various chemical concentrations can be seen to dominate the northern half of the study area in the afternoon. The plumes build over the ocean just after noon, and can be seen to sweep in a north-easterly direction over the study area. The plume can be also be seen to expand slightly towards the higher concentrations over the city centre. This may be a direct result of the higher nitrogen oxides converting to ozone in the high sunlight and temperatures of just after midday. See Table 6.1 and Appendix C for final visualisations.

6.5 Summary

Contours of the Perth study area were digitised to show plume extent over land features. The resulting Microstation95 product contained some elevation spikes; however, these were edited and overall terrain representation was captured. These data were then used to build a TIN and surface shading.

Volumetric data were reformatted into an importable format through a custom software program. The resulting point file was interpolated to generate cells with attributes. Thresholding of levels was done using the level that showed the most plume movement and extent without covering too little or too much of the study area.

Screen captures were used to generate the digital video from each time slice that contained the minimum chemical threshold. Two final visualisations were performed on separate view angles. The first visualisation highlighted plume movement, and the second highlighted environmental impact.

The time slices for each hour gave a general indication of plume movement throughout the day. These separate files were imported into visualisation software

for final 4D plume movement and interaction. To distribute research results, the resulting animations can be viewed over the Internet.

Chapter 7

CONCLUSIONS AND RECOMMENDATIONS

7.1 Introduction

The vegetation mapping resulted in two new maps for the DEP in Perth for use in estimating biogenic emissions as a precursor to smog. These digitally extracted vegetation species and density maps were produced using remotely sensed image interpretation methods. Some species classes contained high accuracy results with some mixed species classes showing lower accuracy. Final species text maps had some missing values that were filled in manually with Microsoft Excel.

The distribution of smog in Perth was mapped successfully in 4D. Levels of nitrogen oxides and ozone for March 16, 1994 remained quite low throughout the day with little human or vegetation impact. Total ozone exposure for humans and vegetation due to plume movement across the scene remained fairly low. The final animations proved successful with results made easily available through the Internet in AVI format.

For future vegetation mapping, improvements could be made by obtaining software that is more stable, better field work, and better post-classification generalisation. Further, mixed class species and even some new classes for grass and parks may improve biogenic emission estimates. For future visualisations, improvements could include software that can handle multiple files from interpolation through to visualisation.

Overall, the methods used during this research should be useful for further DEP air quality studies. This may include a wider audience of those interested in urban smog problems throughout the world. Both remote sensing and 4D GIS techniques have been developed which that enable similar studies to overcome barriers that this research faced.

7.2 Limitations

7.2.1 Vegetation Mapping

(a) Numerous Bushfires

Since the date of the image acquisition, there have been hundreds of bushfires within the study area. It is common knowledge to Australians that bush fire smoke can be seen every day or two, with numerous reports of fires on television during the summer period. In Mundaring alone, some 150 bushfires have occurred in 1997 (Mundaring Shire, 1997).

During winter, CALM burn offs would also play a role in changes since the image was acquired. These burn offs may potentially be larger than summer fires; however, their severity is reduced due to generally wet or moist conditions. These fires render the density data and some species coverage somewhat dated. At this point, it is unrealistic to map vegetation in real time. An update schedule must be followed to compile an accurate biogenic emission estimate.

(b) Complexity of Vegetation

Vegetation complexity remains an important issue at either 30 m or 3 km. Various classes of mixed species were useful for mapping complexity, yet some detail is lost in the 30 m image. Further loss of complexity occurred in the final generalisation as well.

The complexity of urban vegetation is substantial and affects the mapping accuracy. Taking any bus from the city to the suburbs reveals numerous vegetation species. Much of the urban vegetation is exotic, except in parks and reserves. The mix of exotic species in vegetation classification remains difficult. Further, the human-made structures and vegetation mapped at 30 m cannot be discriminated fully and can lead to significant urban influence on the vegetation map.

(c) Scale

Obviously, the scale of mapping played an important role in this research. Data was available with 30 m pixel resolution and mapping output was at a 3 km pixel

resolution. The change of scales removed a significant portion of the accuracy obtained at 30 m.

(d) Software Problems

Numerous software crashes occurred during vegetation mapping. Image processing software caused many system conflicts and crashes requiring re-booting of the computer. In some instances, software exited with no corrupted files. In others, program set-up and configuration files were lost and required re-installation of the software. No data loss occurred; yet conflicts often set back the research progress.

Algorithms for processing a correlation between the vegetation indices and ground truth data were lacking in the software, and exporting through four software formats was needed to obtain a working regression equation.

7.2.2. Smog Visualisation

(a) Factors that Affected Accuracy

The accuracy of 3D and 4D visualisation is dependent upon the interpolation method used. The interpolation method chosen highlighted visual changes near the ground. Data errors may have been increased, however, by enhancing the weighting factor of the points used in the interpolation. After interpolation, to create the most effective visualisation product, lighting methods, viewing angle and rotation, z scale, and data set zoom are important.

(b) Software Problems

Multi-dimensional processing of terrain and volumes was difficult due to software conflicts and data corruption. Unknown data errors appeared that could not be fixed by usual routines nor by the software support staff. These bugs remain in the digital terrain model and data stability is questionable. Volume data had few processing problems, yet system stability remains a stumbling block.

Future visualisation should ideally be performed in one software package for volume generation and animation. Difficulty was encountered in creating 80 separate

volumetric figures for each visualisation generated. A 4D GIS with multiple file import and generation would be helpful as well.

(i) Microstation95 for Digital Terrain Modelling

Digitising on two different boards caused minor file inconsistencies. The resulting files had some problems, especially with elevation matching of topographic map sheets. These files were edited to remove errors, yet processing of errors occurred during triangulation and the resulting representation of the terrain.

The digital terrain modelling software Microstation95 with Site Works caused the majority of data loss and corruption problems. Some error correction available with the EDG command cleaned up files; however, further errors occurred on these files upon import into Voxel Analyst.

In the best instance of processing, some errors occurred with point geometry which were edited back to the true height. In the worst instance, system failures caused re-booting of the computer and loss of system files. Overall, the terrain model is relatively accurate as a backdrop, especially considering the large study area and quite flat terrain.

Microstation95 was unable to visualise data from different time periods. To actually perform the required 4D visualisation, each of the 12,800 points would have to be moved within one file by hand. Obviously, this CAD based model is not suited for further use in environmental studies.

(ii) Voxel Analyst for Volume Generation

Voxel Analyst was used for volume generation and creation of screen captures. Several system crashes occurred without data loss, particularly when the terrain file from Microstation95 was imported. There may have been a conflict between ERMapper and Voxel Analyst, but a link could not be proven.

7.3 Conclusions

7.3.1 Two-Dimensional Vegetation Mapping

Mapping of vegetation was performed successfully at the final 3 x 3 km grid. Software problems were encountered; however, no data loss occurred and final outputs remain stable. System performance was limited at times, yet a new version of the image processing software was used during final research stages that implemented some import/export routines that were not working in the older version.

Rectification was performed efficiently, and the mosaic used was normalised through histogram matching. Some differences remained in the mosaic, yet most of the study area was well within the 1997 image.

(a) Species

Species mapping was difficult due to the mixture of vegetation within any three km cell size in Perth. Some areas remain quite homogenous, yet most are heterogenous with up to a dozen or more species present. This problem was noted, and field work was used to find the most homogenous training sites.

(b) Density

Density mapping was performed using two platforms, as statistical extraction of an image to image correlation was not possible in ER Mapper. Export to IDRISI was performed and the Infra-red Percentage Vegetation Index (IPVI) showed the highest correlation with ground truth identified in this research.

7.3.2 Multi-Dimensional Smog Visualisation

(a) Three-Dimensional Volume Generation

Once the DEP data had been reformatted with the Qbasic program (Appendix B), volume generation and display was efficient. There were several problems getting the terrain model to import without system crashes, yet the final terrain model was used as a backdrop to volumetric plume movement.

(b) Four-Dimensional Visualisation

Final visualisation of the environmental impact of smog in Perth was quite good as the visual impact is easy to comprehend. Visual representation of the plume movement of the day in question is present in the data from the DEP, and plume movement can be seen to impact a large portion of the study area with the thresholds used.

These thresholds are somewhat low to be indicators of poor air-quality, yet some relatively high levels of chemicals, especially ozone, exist. All levels above the thresholds used were visualised to give an overall picture of chemical movement and extent.

7.3.3 Environmental Impact of Smog in Perth

Environmentally significant levels of nitrogen oxides and ozone were used to show potential impact in the Perth area. Nitrogen oxide levels throughout the day remained quite low, and little potential human and vegetation impact would have occurred under these conditions. Ozone levels were noted as moderate to high in some areas.

At 80 ppb, ozone covers almost no spatial extent and can only be seen in a small plume for a few hours of the day. At 50 and 60 ppb, ozone can be seen to cover parts of the study area for more than three to four hours. Higher chemical thresholds over shorter periods may cause similar impacts to lower thresholds over longer time. Cumulative exposure, even at moderate levels, may have some impact.

7.4 Recommendations

7.4.1 Future Two-Dimensional Vegetation Mapping

The large amount of high resolution imagery available makes future vegetation mapping possible with high accuracy. The improved scale of capture can be significant in mapping, yet data loss during generalisation remains a problem.

To overcome this limitation, a better generalisation method needs to be developed to keep vegetation classes with little spatial extent in the final map. This might be a system to measure the percentage of each class cover in the pre-generalised image and keep the percentage upon output at lower resolution.

A less viable option may be to increase the resolution of the DEP model and, thus, grid cell resolution of inputs such as biogenic emissions; however, this would require all other input data sets to be captured at a higher resolution. Further, the present model resolution appears to be efficient at highlighting Perth's smog problem.

(a) Species

Species mapping was hampered by several factors. Detecting mixed vegetation species within classes could be improved in the future by improved ground truth and knowledge of conditions suitable for mixed vegetation species.

Eliminating urban response from pixels may be desirable. It is proposed that a class for *other* or non-vegetation and non-water be added to species mapping. This would allow for the use of the masked NDVI image to remove pixels with minimal vegetation response. Final classification could simply classify this as urban or barren through ground truth and training sites. The results of this method would have to be tested to find out if generalisation of data may cause too much vegetation loss. Final mapping should take into account these human made features with no vegetation. Calculating the emission rate would be straight forward, as no vegetation would have no biogenic emissions.

Grass and grassed parkland areas can be distinguished quite easily on the imagery, and it is proposed that another class for grass and parks be used. Training sites would be easy to define, as grassed areas are quite clear on images. Biogenic emission rates of grass may be important to show in future mapping. Anderson (1998) highlights research showing that mowing of grass areas can lead to chemical emission increases of 180 times over un-mowed grass areas. So this may be a worthwhile class to investigate in the future.

Many urban species of vegetation are exotic and would not fit easily into existing classes. It is proposed that a class for *urban vegetation* or *exotic* be used to estimate the urban vegetation patterns. This could be implemented with high resolution imagery and could be important for biogenic emissions in Perth.

To improve classification methods, the use of texture, fractals, fuzzy classification and spectral mixing should be tested to find if vegetation in the metropolitan region has spatial or self-similar properties at different scales (Ryeherd and Woodcock, 1996; Jong and Burrough, 1995; Goodchild and Mark, 1987; Jensen, 1996).

Other remote sensing platforms should be investigated for vegetation discrimination. For example, Chroudhury *et al.* (1995) show that passive microwave sensors can provide useful information for vegetation and land atmosphere interactions.

Ground truth data should be collected using the Global Positioning System (GPS) to locate points easily. This would eliminate making notes on screen prints and maps. Data could be collected with attributes and downloaded into a point file for import and use in image processing software.

(b) Density

A lack of statistical features in the software used makes the calculation of density inefficient. Future studies should undertake the mapping using software that can calculate a correlation between ground truth and vegetation indices.

7.4.2 Future Multi-Dimensional Visualisation

Visualisation showed that the data sets (nitrogen oxides and ozone) extended beyond the study area boundary. A larger study area may be the answer, but sampling regimes may make cost a barrier. This expansion, if found suitable, could be done through increasing the study area in cardinal directions as well as cell resolution. It should be noted that the majority of smog in Perth is well covered by the present study area and resolution.

(a) Digital Terrain Modelling

Future terrain representation should be performed strictly on a GIS; the CAD-based platform used was inefficient and unstable.

(b) Volume Generation

Volume generation in the future should be performed on a system that can handle multiple volumetric files for generation, thresholding, and visualisation. The software platform was capable of generating efficient images, yet real GIS operations and data handling were lacking.

(c) Visualisation and Animation

This work required too many manual steps due to limited export options and capabilities within one single software platform. Future visualisation and animation within one system would be desirable. The use of multiple platforms and lack of export formats are a limitation of current volumetric GIS at the moment, but 3D software is appearing steadily on the market with improved functionality.

7.4.3 Future Visualisation of Environmental Impacts of Smog in Perth

To improve the estimation of the potential impacts upon humans, significant levels must be shown to be occurring at ground level for an extended period of time. To highlight this human impact, a 2D map would suffice. To fully grasp the movement and conditions, 4D methods remain superior.

Terrain and plume interaction could be improved over existing volumetric interpolation methods. The terrain covers some plume data (where plume elevations are lower than terrain elevation) in this model, as interpolated data are not corrected for terrain. The final visualisation scale makes the interaction difficult to see, yet future work could concentrate on methods to improve current data overlay problems by moving z values to correct for terrain.

7.5 Importance of Results

Research methods used in this study are important for all future processing of imagery for biogenic emission mapping in Perth. The vegetation maps will be important for bringing two of the DEP's photochemical smog model inputs up to date. These two inputs will enable the DEP to model biogenic emissions based on maps highlighting recent vegetation characteristics.

Visualisation of environmental phenomena is extremely important. Even with the current limitations in software, a greater understanding of the temporal and spatial (volumetric) plumes is gained with animation. A truly dynamic picture can be gained by the user in just a few seconds. The resulting output, in a format viewable over the Internet, makes dissemination of results quick and easy.

REFERENCES

Albertin, U., Shrout, J., Stankovic, G., Troutner, J., Wiggins, W. and Beasley, C.J. (1995) Computer Representation of Complex 3-D Velocity Models, *Exploration Geophysics*, Vol. 26, No. 2/3, pp. 456-460.

Anderson, I. (1998) Keep off the Grass, *New Scientist*, May 9, 1998, pp. 11.

Badhwar, G.D., MacDonald, R.B. and Mehta, N.C. (1986) Satellite-Derived Leaf-Area-Index and Vegetation Maps as Input to Global Carbon Models - A Historical Approach, *International Journal of Remote Sensing*, Vol. 2, No. 2, pp. 265-281.

Bailey, T.C. and Gatrell, A.C. (1995) *Interactive Spatial Data Analysis*, Longman Scientific and Technical, Essex, England, 413 pp.

Bak, P.R.G. and Mill, A.J.B. (1989) Three-Dimensional Representation in a Geoscientific Resource Management System for the Minerals Industry, in: *Three-Dimensional Applications in Geographical Information Systems*, Raper, J. F. (ed.), Taylor and Francis, London, England, pp. 155-182.

Baret, F. and Guyot, G. (1991) Potentials and Limits of Vegetation Indicies for LAI and APAR Assessment, *Remote Sensing of Enviroment*, Vol. 35, pp. 161-173.

Baret, F., Guyot, G. and Major, D.J. (1989) TSAVI: A Vegetation Index which Minimizes Soil Brightness Effects on LAI and APAR Estimation, in *Proceedings of the 12th Canadian Symposium on Remote Sensing*, IGARRS'90, Vancouver BC, Canada, 10-14 July, Vol. 3, pp. 1355-1358.

Batten, L. (1989) National Capital Urban Planning Project: Development of a Three-Dimensional GIS Model, *Proceedings of Auto Carto 9, Ninth International Symposium on Computer Assisted Cartography*, Baltimore, MD, April, pp. 336-340.

Beard, J.S. (1979a) The Vegetation of the Perth Area, *Vegetation Survey of Western Australia 1:250,000 series*, Vegmap Publications, Perth, WA, 47 pp.

Beard, J.S. (1979b) The Vegetation of the Pinjarra Area, *Vegetation Survey of Western Australia 1:250,000 series*, Vegmap Publications, Perth, WA, 42 pp.

Beard, J.S. (1981) The Vegetation of the Swan Area, *Vegetation Survey of Western Australia 1:1,000,000 series*, University of Western Australia Press, Perth, WA, 220 pp.

Bebb, G. (1997) *Personal Communication*, President, Surpac Corporation, Perth, WA.

Belcher R.C. and Hoffman K.S. (1992) Geologic Structural Models: Improvements to 3-D Modelling, *Geobyte*, Vol. 7, No. 4, pp. 50-54.

Bell, S.B.M., Chadwick, R.A., Cooper, A.P.R., Mason, D.C., O'Connaill, M.A. and Young, A.V. (1990) Handling Four-Dimensional Geo-Coded Data, *Proceedings of the 4th International Symposium on Spatial Data Handling*, Vol. 2, Zurich, Switzerland, July, pp. 918-927.

Bishop, I.D., Spring, J.W. and Potter, R. (1995) Extending the Geographic Information Base into the Third Dimension for Use in the Urban Environment, *URISA*, Vol. 7, No. 1, pp. 20-25.

Broome, J. (1992) An IBM-Compatible Program For Interactive Three-Dimensional Gravity Modelling, *Computers and Geosciences*, Vol. 18, No. 2/3, pp. 337-348.

Burrough, P.A. (1986) *Principles of Geographical Information System for Land Resources Assessment*, Clarendon Press, Oxford, England, 194 pp.

Buschmann, C. and Nagel, E. (1991) Reflection Spectra of Terrestrial Vegetation as Influenced by Pigment-Protein Complexes and the Internal Optics of the Leaf Tissue, *International Geoscience and Remote Sensing Symposium 1991*, Espoo, Finland, June 3-6, Vol. 4., pp. 1909-1912.

Buttenfield, B.P. and McMaster, R.B. (1991) *Map Generalisation*, Longman Scientific and Technical, Essex, England, 245 pp.

Cacetta, P. (1996) The West Australian Landsat TM Regional Mosaic, *Product Description*, Remote Sensing Services Department of Land Administration, Perth, WA, 3 pp.

Calkins, H.W. and Fuxiang, F.X. (1994) 3-D Segmentation for Water Quality Modelling with Arc/Info, *Proceedings of 14th Annual ESRI User Conference*, Redlands, CA, May, pp.1244-1255.

Cambray, B. (1993) Three-Dimensional (3D) Objects in Geographical Databases, *Proceedings of 4th European Conference and Exhibition on Geographical Information Systems*, Vol. 1, Genoa, Italy, March-April, pp. 217-226.

Carnovale, F., Alviano, P., Carvalho, C., Deitch, G., Jiang, S., Macaulay, D. and Summers, M. (1991) Air Emissions Inventory Port Phillip Control Region: Planning for the Future, *Report SRS 91/001*, Environmental Protection Authority of Victoria, Melbourne, VIC, 181 pp.

Chameides, W.L., Lindsay, R.W., Richardson, J. and Kiang, C.S. (1988) The Role of Biogenic Hydrocarbons in Urban Photochemical Smog: Atlanta as a Case Study, *Science*, Vol. 241, pp. 1473-1475.

Choudhury, B.J., Kerr, Y.H, Njoku, E.G. and Pampaloni, P. (1995) *Passive Microwave Remote Sensing of Land-Atmosphere Interactions*, Koninklijke Wohrmann, Zutphen, Netherlands, pp. 685.

Clarke, K.C. (1990) Terrain Analysis, in: *Analytical and Computer Cartography*, Clarke, K.C. (ed.), Prentice Hall, Englewood Falls, NJ, pp. 204-237.

Cleavers, J.G.P.W. (1988) The Derivation of a Simplified Reflectance Model for the Estimation of Leaf Area Index, *Remote Sensing of Environment*, Vol. 25, pp. 53-69.

Coleman, T.L. (1991) Three-Dimensional Modelling of an Image Based Geographical Information System for Land Use Planning, *Proceedings of Urban and Regional Information Systems Association Annual Conference*, Vol. 2, San Francisco, CA, August, pp. 159-168.

Cope, M.E., Carnovale, F., Galbally, I.E., Cook, B.J. and Hearn, D.R. (1988) Modelling Photochemical Smog in the Latrobe Valley, *Clean Air*, Vol. 22, No. 4, pp. 185-191.

Cope, M.E. and Ischtwan, J. (1995) Perth Photochemical Smog Study: Airshed Modelling Component, *Final Report*, Environmental Protection Authority of Victoria, Melbourne, VIC, 320 p.

Coppin, P.R. and Bauer, M.E. (1992) Optimization of the Information Content of Multitemporal Landsat TM Data Sets for Monitoring Forest Cover Disturbance, *International Geoscience and Remote Sensing Symposium 1992*, Houston, TX, May 26-29, Vol. 2, pp. 983-985.

Crapo J., Miller, F.J., Mossman, B., Pryor, W.A. and Kiley, J.P. (1992) Relationship Between Acute Inflammatory Responses to Air Pollutants and Chronic Lung Disease, *American Review of Respiratory Diseases*, Vol. 145, pp. 1506-1512.

Crippen, R.E. (1990) Calculating the Vegetation Index Faster, *Remote Sensing of Environment*, Vol. 34, pp. 71-73.

Cronin, L. (1988) *Key Guide to Australian Trees*, Reed Books Pty. Ltd., Frenchs Forest, NSW, 191 pp.

Davis, B.E. and Williams, R. (1989) The Five Dimensions of GIS, *Proceedings of GIS/LIS 89*, Vol. 1, Orlando, FL, November, pp. 50-58.

De Blis, H.J. and Muller, P.O. (1996) *Physical Geography of the Global Environment*, John Wiley and Sons, New York, NY, 597 pp.

Dobkin, D.P. and Laszlo, M.J. (1987) Primitives for the Manipulation of Three-Dimensional Subdivisions, *Proceedings of 3rd Annual Symposium on Computational Geometry*, Ontario, Canada, June, pp. 86-98.

Dreschler-Parks, D.M. (1987) Effect of Nitrogen Dioxide, Ozone, and Peroxyacetyl Nitrate on Metabolic and Pulmonary Function, *Cambridge MA Health Effects Institute*, Research Report No. 6.

Eddy, C.A. and Looney, B. (1993) Three-Dimensional Digital Imaging of Environmental Data: Selection of Gridding Parameters, *International Journal of Geographical Information Systems*, Vol. 7, No. 2, pp. 165-172.

Edwards, R. (1995) Ozone Alert Follows Cancer Warning, *New Scientist*, No. 27, May 4, p. 27.

Ellis, R.G. (1995) Airborne Electromagnetic 3D Modelling and Inversion, *Proceedings of ASEG 11th Geophysical Conference and Exhibition*, Adelaide, SA, September, pp. 138-143.

Elsom, D.M. (1992) *Atmospheric Pollution, A Global Problem*, Blackwell Publishers, Oxford, England, 319 pp.

Elvidge, C.D. and Chen, Z. (1995) Comparison of Broad-Band and Narrow-Band Red and Near-Infrared Vegetation Indicies, *Remote Sensing of Environment*, Vol. 54, pp. 38-48.

Elvidge, C.D. and Lyon, R.J.P. (1985) Influence of Rock-Soil Spectral Variation on the Assessment of Green Biomass, *Remote Sensing of Environment*, Vol. 17, pp. 265-279.

Evans, L.F., Weeks, I.A., Eccleston, A.J. and Packham, D.R. (1977) Photochemical Ozone in Smoke from Prescribed Burning of Forests, *Environmental Science and Techniques*, Vol. 11, pp. 896-900.

Ferguson, A., Bayer, E., Flinn, J. and Mullin, L. (1996) Hazardous Waste Characterisation Using 3D GIS, *Proceedings of Mapping Sciences 1996*, Canberra, ACT, Sep 22-26, pp. 166-170.

Finlayson-Pitts, B. and Pitts, J.N. Jr. (1986) *Atmospheric Chemistry Fundamentals and Experimental Techniques*, John Wiley and Sons, New York, NY, pp. 1098.

Fischer, M., Scholten, H.J. and Unwin, D. (1996) *Spatial Analytical Perspectives on GIS*, GISDATA IV, Taylor and Francis, Bristol, PA, 256 pp.

Fowles, J. (1995) Rust Saves Customer $10 Million, *Global Link - Integraph's International GIS Newsletter*, Vol. 1, No. 2, pp. 1-2.

Friedl, M.A., Davis, F.W., Michaelsen, J. and Moritz, M.A. (1995) Scaling and Uncertainty in the Relationship Between the NDVI and Land Surface Biophysical Variables: An Analysis Using a Scene Simulation Model and Data from FIFE, *Remote Sensing of Environment*, Vol. 54, pp. 233-246.

Fritsch, D. (1990) Towards Three-Dimensional Data Structures in Geographic Information Systems, *Proceedings of First European Conference of Geographical Information Systems*, Vol. 1, Amsterdam, Netherlands, April, pp. 335-345.

Gaston, G.G., Bradley, P.M., Vinson, T.S. and Kolchugina, T.P. (1997) Forest Ecosystem Modelling in the Russian Far East Using Vegetation and Land-Cover Regions Identified by Classification of GVI, *Photogrammetric Engineering and Remote Sensing*, Vol. 63, No. 1, pp. 51-58.

Geron, C.D., Guenther, A.B. and Pierce, T.E. (1994) An Improved Model for Estimating Emissions of Volatile Organic Compounds from Forests in the Eastern United States, *Journal of Geophysical Research*, Vol. 99, No. D6, pp. 12,773-12,791.

Gholz, H.L. (1982) Environmental Limits on Above Ground Net Primary Production, Leaf Area, and Biomass in Vegetation Zones of the Pacific Northwest, *Ecology*, Vol. 63, No. 2, pp. 469-481.

Gholz, H.L., Nakane, K. and Shimoda, H. (1997) *The Use of Remote Sensing in the Modeling of Forest Productivity*, Forestry Sciences Vol. 50, Kluwer Academic Publishers, Boston, MA, 323 pp.

Gitelson, A.A., Merzlyak, M.N. and Grits, Y. (1996) Novel Algorithms for Remote Sensing of Chlorophyll Content in Higher Plant Leaves, *International Geoscience and Remote Sensing Symposium 1996*, Lincoln, NE, Vol. 4, pp. 2355-2357.

Gjertsen, A.K. (1993) Testing TM and SPOT Data as Input to a Canopy Reflectance Model for Mapping Density and Size of Trees in Forest Stands, *International Geoscience and Remote Sensing Symposium 1993*, Tokyo, Japan, Aug 18-21, Vol. 4, pp. 750-752.

Goel, N.S. and Qin, W. (1996) From Leaf to Scene: Scaling Problems in Remote Sensing of Vegetation, *International Geoscience and Remote Sensing Symposium 1996*, Lincoln, NE, Vol. 1, pp. 526-528.

Gold, C.M. (1989) Surface Interpolation, Spatial Adjacency and GIS, in: *Three-Dimensional Applications in Geographical Information Systems*, Raper, J. F. (ed.), Taylor and Francis, London, England, pp. 21-35.

Goodchild, M.F. and Mark, D.M. (1987) The Fractal Nature of Geographic Phenomena, *Annals of the Association of American Geographers*, Vol. 77, No. 2, pp. 265-278.

Goward, S.N., Tucker, C.J. and Dye, D.G. (1985) North American Vegetation Patterns Observed with the NOAA-7 Advanced Very High Resolution Radiometer, *Vegetatio*, Vol. 64, pp. 3-14.

Graedel, T.E. and Crutzen, P.J. (1995) *Atmosphere, Climate, and Change*, Scientific American Library, New York, 196 pp.

Grant, R. (1992) State of the Environment Report, *Environmental Protection Authority Report*, Government of Western Australia, Perth, WA, December, 208 pp.

Guenther, A.B., Monson, R.K. and Fall, R. (1991) Isoprene and Monoterpine Emission Rate Variability: Observations with Eucalyptus and Emission Rate Algorithm Development, *Journal of Geophysical Research*, Vol. 96, No. D6, pp. 799-808.

Guenther, A.B., Zimmerman, P.R., Harley, P.C., Monson, R.K. and Fall, R. (1993) Isoprene and Monoterpene Emission Rate Variability: Model Evaluations and Sensitivity Analyses, *Journal of Geophysical Research*, Vol. 98, No. D7, pp. 12,609-12,617.

Guenther, A.B., Zimmerman, P.R. and Wildermuth, M. (1994) Natural Volatile Organic Compound Emission Rate Estimates for U.S. Woodland Landscapes, *Atmospheric Environment*, Vol. 28, No. 6, pp. 1197-1210.

Gugan, D.J. and Downman, I.J. (1988) Topographic Mapping from SPOT Imagery, *Photogrammetric Engineering and Remote Sensing*, Vol. 54, No. 10, pp. 1404-1409.

Hack, R. and Sides, E. (1994) Three-Dimensional GIS: Recent Developments, *ITC Journal*, Vol. 1994-1, pp. 64-72.

Henderson-Sellers, A. and McGuffie, K. (1987) *A Climate Modelling Primer*, John Wiley and Sons, New York, NY, 217 pp.

Hickey, R. J. and Jankowski, P. (1997) GIS and Environmental Decision Making to Aid Smelter Reclamation Planning, *Environment and Planning*, Vol. 29, No. A, pp. 5-19.

Hickey, R. J., Smith, A. and Jankowski, P. (1994) Slope Length Calculations from a DEM within Arc/Info Grid, *Computers, Environment and Urban Systems*, Vol. 18, pp. 365-380.

Hingston, F.J., Dimmock, G.M. and Turton, A.G. (1980/1981) Nutrient Distribution in a Jarrah (Eucalyptus Marginata Donn Ex Sm.) Ecosystem in the South-West of Western Australia, *Forest Ecology and Management*, Vol. 3, pp. 183-207.

Hoinkes, R. and Lange, E. (1995) Toolkit Expands Visual Dimensions in GIS, *GIS World*, Vol. 8, No. 7, pp. 54-56.

Holliday, I. and Watton, G. (1989) *A Field Guide to Australian Native Shrubs*, Hamlyn Australia, Port Melbourne, VIC, 240 pp.

Hood, L. and Summerson, R. (1997) Seeing in Four-Dimensions, *GIS User*, No. 22, pp. 18-22.

Hoop, S., Meij, L. and Molenaar, M. (1993) Topological Relationships in 3D Vector Maps, *Proceedings of 4th European Conference and Exhibition on Geographical Information Systems*, Vol. 1, Genoa, Italy, March-April, pp. 448-455.

Houlding, S.W. (1994) *3D Geoscience Modelling*, Houlding. S. (ed.), Springer Verlag, New York, NY, 309 pp.

Huemmrich, K.F. (1996) Effects of Shadows on Vegetation Indices, *International Geoscience and Remote Sensing Symposium 1996*, Lincoln, NE, Vol. 4, pp. 2372-2374.

Huemmrich, K.F. and Goward, S.N. (1992) Spectral Vegetation Indexes and the Remote Sensing of Biophysical Parametres, *International Geoscience and Remote Sensing Symposium 1992*, Houston, TX, May 26-29, Vol. 2, pp. 1017-1019.

Huete, A.R. (1988) A Soil-Adjusted Vegetation Index (SAVI), *Remote Sensing of Environment*, Vol. 25, pp. 295-309.

Huete, A.R., Jackson, R.D. and Post, D.F. (1985) Spectral Response of a Plant Canopy with Different Soil Backgrounds, *Remote Sensing of Environment*, Vol. 17, pp. 37-53.

Huete, A.R., Liu, H., de Lira, G.R., Batchilly, K. and Escadafal, R. (1994) A Soil Color Index to Adjust for Soil and Litter Noise in Vegetation Index Imagery of Arid Regions, *International Geoscience and Remote Sensing Symposium 1994*, Pasadena, CA, Aug 8-12, Vol. 2, pp. 1042-1043.

Hurst, D.F., Griffith, D.W.T. and Cook, G.D. (1994) Trace Gas Emissions from Biomass Burning in Tropical Australian Savannas, *Journal of Geophysical Research*, Vol. 99, pp. 16441-16456.

Jackson, R.D. (1983) Spectral Indices in *n*-Space, *Remote Sensing of Environment*, Vol. 13, pp. 409-421.

Jacquemond, S., Verdebout, J., Schmuck, G., Andreoli, G., Hosgood, B. and Hornig, S.E. (1994) Investigation of Leaf Biochemistry by Statistics, *International Geoscience and Remote Sensing Symposium 1994*, Pasadena, CA, Aug 8-12, Vol. 2, pp. 1239-1241.

Jensen, J.R. (1986) *Introductory Digital Image Processing*, Prentice-Hall, Englewood Cliffs, NJ, 379 pp.

Jensen, J.R. (1996) *Introductory Digital Image Processing*, Second Edition, Prentice-

Hall, Englewood Cliffs, NJ, 316 pp.

Joao, E.M. (1995) The Importance of Quantifying the Effects of Generalisation in: *GIS and Generalisation*, Muller, J.C., Lagrange, J.P. and Weibel, R. (ed.), Taylor and Frances, New York, NY, pp. 183-193.

Jones, C.B. (1989) Data Structures for Three-Dimensional Spatial Information Systems in Geology, *International Journal of Geographical Information Systems*, Vol. 3, No. 1, pp. 15-31.

Jong, S.M. and Burrough, P.A. (1995) A Fractal Approach to the Classification of Mediterranean Vegetation Types in Remotely Sensed Images, *Photogrammetric Engineering and Remote Sensing*, Vol. 61, No. 8, pp. 1041-1053.

Jordan, C.F. (1969) Derivation of Leaf Area Index from Quality of Light on the Forest Floor, *Ecology*, Vol. 50, pp. 663-666.

Justice, C.O., Townshend, J.R.G., Holben, B.N. and Tucker, C.J. (1985) Analysis of the Phenology of Global Vegetation Using Meteorological Satellite Data, *International Journal of Remote Sensing*, Vol. 6, No. 8, pp. 1271-1318.

Kaufman, Y.J., Tanre, D., Holben, B.N., Markham, B. and Gitelson, A. (1992) Atmospheric Effects on the NDVI - Strategies for its Removal, *International Geoscience and Remote Sensing Symposium 1992*, Houston, TX, May 26-29, Vol. 2, pp. 1238-1241.

Kauth, R.J. and Thomas, G.S. (1976) The Tasseled Cap - A Graphical Description of Spectral-Temporal Development of Agricultural Crops as seen by Landsat, *Proceedings of the Symposium on Machine Processing of Remotely Sensed Data*, LARS, Perdue, IA, pp. 41-51.

Kharuk, V.I., Theisen, A.F., Rock, B.N. and Williams, D.L. (1994) Some Aspects of Chlorophyll Fluorescence Application in Remote Sensing, *International Geoscience and Remote Sensing Symposium 1994*, Pasadena, CA, Aug 8-12, Vol. 2, pp. 973-975.

Kim, M.S., Chappelle, E.W., Corp, L. and McMurtrey, E. III. (1993) The Contribution of Chlorophyll Fluorescence to the Reflectance Spectra of Green Vegetation, *International Geoscience and Remote Sensing Symposium 1993*, Tokyo, Japan, Aug 18-21, Vol. 3, pp. 1321-1324.

Kimes, D.S. (1991) Inferring Vegetation Characteristics Using a Knowledge-Based System, *International Geoscience and Remote Sensing Symposium 1991*, Espoo, Finland, June 3-6, Vol. 4, pp 2299-2302.

Kluijtmans, P. and Collin, C. (1991) 3D Computer Technology for Environmental

Impact Studies, *Proceedings of Second European Conference on Geographical Information Systems*, Brussels, Belgium, April, pp. 547-550.

Knapp, L. (1991) Volumetric GIS: Generic or Domain Specific, *Proceedings of GIS/LIS 91*, Vol. 2, Atlanta, GA, October-November, pp. 776-785.

Kogan, F. (1991) A Method for Real-Time Monitoring of Vegetation from Satellite, *International Geoscience and Remote Sensing Symposium 1991*, Espoo, Finland, June 3-6, Vol. 4, pp. 2295-2298.

Koussoulakou, A. (1994) Spatial-Temporal Analysis of Urban Air Pollution in: *Visualisation in Modern Cartography*, Maceachren, A.M. and Taylor, F. (ed.), Galliard Printers, Great Yearmouth, England, pp. 243-267.

Kraak, M.J. (1989) Computer-Assisted Cartographical 3D Imaging Techniques, in: *Three-Dimensional Applications in Geographical Information Systems*, Raper, J. F. (ed.), Taylor and Francis, London, England, pp. 99-113.

Kraak, M.J. (1994) Interactive Modelling Environment for Three-Dimensional Maps: Functionality and Interface Issues in: *Visualisation in Modern Cartography*, Maceachren, E.A.M. and Taylor, F. (ed.), Galliard Printers, Great Yearmouth, England, pp. 269-285.

Kraak, M.J. and Verbree, E. (1992) Tetrahedrons and Animated Maps in 2D and 3D Space, *Proceedings of 5th International Symposium on Spatial Data Handling*, Vol. 1, Charleston, SC, August, pp. 63-71.

Kummler, M.P. (1994) An Intensive Comparison of Triangular Irregular Networks (TINs) and Digital Elevation Models (DEMs), *Cartographica*, Vol. 31, No. 2, Summer 1994, 99 pp.

Lamb, B., Gay, D., Westberg, H. and Pierce, T. (1993) A Biogenic Hydrocarbon Emission Inventory for the U.S.A. Using a Simple Forest Canopy Model, *Atmospheric Environment*, Vol. 27A, No. 11, pp. 1673-1690.

Lamb, B., Guenther, A.B., Gay, D. and Westberg, H. (1987) A National Inventory of Biogenic Hydrocarbon Emissions, *Atmospheric Environment*, Vol 21, No. 8, pp. 1695-1705.

Langran, G. (1992a) Time in a Geographical Information System in: *Time in Geographic Information Systems*, Langran, G (ed.), Taylor and Frances, London, England, pp.27-44.

Langran, G. (1992b) *Time in Geographic Information Systems*, Taylor and Frances, London, England, 189 pp.

Lee, G., Lifeson, A. and Peart, N. (1974-1999) *Personal Communication*, RUSH, Toronto, Canada.

Leenaers, H., Burrough, P.A. and Okx, J.P. (1989) Efficient Mapping of Heavy Metal Pollution on Floodplains by Co-kriging from Elevation Data, in: *Three-Dimensional Applications in Geographical Information Systems*, Raper, J. F. (ed.), Taylor and Francis, London, England, pp. 37-50.

Lillesand, T.M. and Kiefer, R.W. (1994) *Remote Sensing and Image Interpretation*, John Wiley and Sons, New York, NY, 750 pp.

Lin, H. (1997) STIN Operation: A Study on Searching for Spatiotemporal Measures, *Cartography*, Vol. 26, No. 1, pp. 27-36.

Lin, H. and Choi, S.K. (1994) 3-D Visualisation of Spatiotemporal Intersection (STIN) Operation: An Approach to Test Spatiotemporal Correlation, *Cartography*, Vol. 23, No. 2, pp. 13-20.

Lukatela, H. (1989) GIS Future: Automated Cartography or Geo-Relational Solid Modelling?, *Proceedings of Auto Carto 9, Ninth International Symposium on Computer Assisted Cartography*, Baltimore, MD, April, pp. 341-347.

Luman, D.E and Ji, M. (1995) The Lake Michigan Ozone Study: An Application of Satellite-Based Land-Use and Land-Cover Mapping to Large-Area Emissions Inventory Analysis, *Photogrammetric Engineering and Remote Sensing*, Vol. 61, No. 8, pp. 1021-1032.

Major, D.J., Baret, F. and Guyot, G. (1990) A Ratio Vegetation Index Adjusted for Soil Brightness, *International Journal of Remote Sensing*, Vol. 11, No. 2, pp. 720-727.

Manson, D. (1997) GIS Moves Into the Third-Dimension, *Earth Observation Magazine*, Vol. 6, No. 1, pp. 24-26.

Mantyla, M. (1988) *An Introduction to Solid Modelling*, Computer Science Press Inc., Rockville, MD, 401 pp.

Maracci, G., Schmuck, G., Hosgood, B. and Andreoli, G. (1991) Interpretation of Reflectance Spectra by Plant Physiological Parameters, *International Geoscience and Remote Sensing Symposium 1991*, Espoo, Finland, June 3-6, Vol. 4, pp. 2303-2306.

Marceau, J. D., Gratton, D.J, Fournier, R.A. and Fortin, J.P. (1994b) Remote Sensing and the Measurement of Geographical Entities in a Forested Environment. 2. The Optimal Spatial Resolution, *Remote Sensing of Environment*, Vol. 49, pp. 105-117.

Marceau, J. D., Howarth, P.J. and Gratton, D.J. (1994a) Remote Sensing and the Measurement of Geographical Entities in a Forested Environment. 1. The Scale and Spatial Aggregation Problem, *Remote Sensing of Environment*, Vol. 49, pp. 93-104.

Marschallinger, R. (1991) Interface Programs To Enable Full 3-D Geological Modelling with a Combination of AutoCAD and Surfer, *Computers & Geosciences*, Vol. 17, No. 10, pp. 1383-1394.

Mason, D.C. (1997) Two-Dimensional GIS Software is Customized to Fit a Three-Dimensional Environment for a Mining Project in New Mexico, *Earth Observation Magazine*, Vol. 6, No. 1, pp. 24-26.

Mason, D.C., O'Conaill, M.A. and Bell, S.B.M. (1994) Handling Four-Dimensional Geo-Referenced Data in Environmental GIS, *International Journal of Geographical Information Systems*, Vol. 8, No. 2, pp. 191-215.

Matheson, W. and Ringrose, S. (1994) The Development of Image Processing Techniques to Assess Changes in Green Vegetation Cover Along a Climatic Gradient Through Northern Territory Australia, *International Journal of Remote Sensing*, Vol. 15, No. 1, pp. 17-47.

Matthews, E. (1983) Global Vegetation and Land Use: New High Resolution Data Bases for Climate Studies, *Journal of Climate and Applied Meteorology*, Vol. 22, March, pp 475-487.

Mazzinghi, P., Agati, G. and Fusi, F. (1994) Interpretation and Physiological Significance of Blue-Green and Red Vegetation Fluorescence, *International Geoscience and Remote Sensing Symposium 1994*, Pasadena, CA, Aug 8-12, Vol. 1, pp. 640-642.

McConomy, K. (1993) The Advantages of Three-Dimensional Mapping in a Municipality, *Proceedings of ACTES Canadian Conference on Geographical Information Systems*, Vol. 1, Ottawa, Canada, March, pp. 511-523.

McGonigal, D., Borthwick, J., Jarratt, P., Jameson, N., McGregor, C. and Perkins, C. (1993) *Insight Guides Australia Special*, APA Houghton Mifflin, Singapore, 382 pp.

McLaren, R.A. and Kennie, T.J.M. (1989) Visualisation of Digital Terrain Models: Techniques and Applications, in: *Three-Dimensional Applications in Geographical Information Systems*, Raper, J. F. (ed.), Taylor and Francis, London, England, pp. 70-98.

Molenaar, M. (1990) A Formal Data Structure for Three Dimensional Vector Maps, *Proceedings of First European Conference on Geographical Information System*, Vol. 2, Amsterdam, Netherlands, April, pp. 770-781.

Molenaar, M. (1992) A Topology for 3D Vector Maps, *ITC Journal*, Vol. 1992-1, pp. 25-33.

Monk, R. (1994) Effects of Urban Ozone on Australian Native Vegetation, *Proceedings of the 12th International Clean Air Conference*, Perth, WA, October, pp. 141-149.

Montieth, J.L. (1976) *Vegetation and the Atmosphere*, Vol. 2: Case Studies, Academic Press, New York, NY, 439 pp.

Moody, A., Walsh, S.J., Allen, T.R. and Brown, D.G. (1995) Scaling Properties of NDVI and Their Relationship to Land-Cover Spatial Variability, *International Geoscience and Remote Sensing Symposium 1995*, Firenze, Italy, July 10-14, Vol. 3, pp. 1962-1964.

Muller, J.C. (1992) Geographical Distribution and Seasonal Variation of Surface Emissions and Deposition Velocities of Atmospheric Trace Gases, *Journal of Geophysical Research*, Vol. 97, No. D4, pp. 3787-3804.

Muller, J.C., Weibel, R., Lagrange, J.P. and Salge, F. (1995) Generalisation: State of the Art and Issues in: *GIS and Generalisation*, Muller, J.C., Lagrange, J.P. and Weibel, R. (ed.), Taylor and Frances, New York, NY, pp. 3-17.

Newbey, K. (1968) *West Australian Wildflowers for Horticulture*, Surrey Beatty and Sons, Chipping Norton, NSW, 128 pp.

Nogi, A., Sun, W. and Takagi, M. (1993) An Alternative Correction of Atmospheric Effects for NDVI Estimation, *International Geoscience and Remote Sensing Symposium 1993*, Tokyo, Japan, Aug 18-21, Vol. 3, pp. 1137-1139.

O'Conaill, M. A., Bell, S.B.M. and Mason, D.C. (1992) Developing a Prototype 4D GIS on a Transputer, *ITC Journal*, Vol. 1992-1, pp. 47-54.

O'Connor, J.A., Parbery, D.G. and Strauss, W. (1975) The Effects of Phytotoxic Gases on Native Australian Plant Species: Part 2, Acute Injury Due to Ozone, *Environmental Pollution*, No. 82, pp. 197-200.

Painho, M. (1995) The Effects of Generalization on Attribute Accuracy in Natural Resource Maps in: *GIS and Generalisation*, Muller, J.C., Lagrange, J.P. and Weibel, R. (ed.), Taylor and Frances, New York, NY, pp. 194-206.

Peterson, D.L., Spanner, M.A., Running, S.W. and Teuber, K.B. (1987) Relationship of Thematic Mapper Simulator Data to Leaf Area Index of Temperate Coniferous Forests, *Remote Sensing of Environment*, Vol. 22, pp. 323-341.

Petrie, G. and Kennie, T.J.M. (1990) *Terrain Modelling in Surveying and Civil Engineering*, Whittles Publishing, London, England, pp. 351.

Peuquet, D.J. and Marble, D.F. (1990) *Introductory Reading in Geographical Information Systems*, Taylor and Francis, New York, NY, 372 pp.

Pierce, L.L. and Running, S.W. (1988) Rapid Estimation of Coniferous Forest Leaf Area Index using a Portable Radiometer, *Ecology*, Vol. 66, No. 6, pp. 1762-1767.

Pigot, S. (1992) A Topological Model for a 3D Spatial Information System, *Proceedings of 5th International Symposium on Spatial Data Handling*, Vol. 1, Charleston, SC, August, pp. 344-360.

Pigot, S. and Hazelton, B. (1992) The Fundamentals of a Topological Model for a Four-Dimensional GIS, *Proceedings of 5th International Symposium on Spatial Data Handling*, Vol. 2, Charleston, SC, August, pp. 580-591.

Pinter, Jr., P.J. and Moran, M.S. (1994) Remote Sensing of Soils and Vegetation, *Remote Sensing of Environment*, Vol. 49, pp. 167-168.

Price, J.C. and Bausch, W.C. (1995) Leaf Area Index Estimation from Visible and Near-Infrared Reflectance Data, *Remote Sensing of Environment*, Vol. 52, pp. 55-65.

Price, S. (1989) Modelling the Temporal Element in Land Information Systems, *International Journal of Geographical Information Systems*, Vol. 3, No. 3, pp. 233-243.

Qi, J., Chehbouni, A., Huete, A.R., Kerr, Y.H. and Sorooshian, S. (1994) A Modified Soil Adjusted Vegetation Index, *Remote Sensing of Environment*, Vol. 48, pp. 119-126.

Qi, J., Moran, M.S., Cabot, F. and Dedieu, G. (1995) Normalization of Sun/View Angle Effects Using Spectral Albedo-Based Vegetation Indicies, *Remote Sensing of Environment*, Vol. 52, pp. 207-217.

Raper, J. F. (1989a) *Three-Dimensional Applications in Geographical Information Systems*, Taylor and Frances, London, England, 189 pp.

Raper, J.F. (1989b) The 3-Dimensional Geoscientific Mapping and Modelling System: A Conceptual Design, in: *Three-Dimensional Applications in Geographical Information Systems*, Raper, J. F. (ed.), Taylor and Francis, London, England, pp. 11-19.

Renard, P. and Courrioux, G. (1994) Three-Dimensional Geometric Modelling of a Faulted Domain: The Soultz Horst Example (Alsace, France), *Computers and Geosciences*, Vol. 20, No. 9, pp. 1379-1390.

Richardson, A.J. and Wiegand, C.L. (1977) Distinguishing Vegetation from Soil Background Information, *Photogrammetric Engineering and Remote Sensing*, Vol. 43, No. 12, pp. 1541-1552.

Rikkers, R., Molenaar, M. and Stuvier, J. (1994) A Query Oriented Implementation of a Topologic Data Structure for 3-Dimensional Vector Maps, *International Journal of Geographical Information Systems*, Vol. 8, No. 3, pp. 243-260.

Rouse, J.W., Haas, R.H., Schell, J.A. and Deering, D.W. (1973) Monitoring Vegetation Systems in the Great Plains with ETRS, in *Third ETRS Symposium*, NASA SP353, Washington D.C., Vol. 1, pp. 309-317.

Running, S.W., Nemani, P.R., Peterson, D.L., Band, L.E., Potts, D.F., Pierce, L.L. and Spanner, M.A. (1989) Mapping Regional Forest Evapotranspiration and Photosysnthesis by Coupling Satellite Data with Ecosystem Simulation, *Ecology*, Vol. 70, No. 4, pp. 1090-1101.

Rychkun, E. (1995) 3D Geostatistical Modelling Applied to Radioactive Waste Site, *Earth Observation Magazine*, Vol. 4, No. 10, pp 42-44.

Rychkun, E. (1997) 3D Geoscience Modelling Cleans Up, *Earth Observation Magazine*, Vol. 6, No. 1, pp. 32-35.

Rye, P.J. (1989) Evaluation of a Simple Numerical Model as a Mesoscale Forecasting Tool, *Applications in Meterology*, Vol. 28, pp. 1257-1270.

Rye, P.J. (1996) Meteorological and Source Analysis of Smog Events During the Perth Photochemical Smog Study, *Technical Series Report 83*, Department of Environmental Protection, Perth, WA, 58 pp.

Rye, P.J. (1997) *Personal Communication*, Department of Environmental Protection, Perth, WA.

Rye, P.J. (1998) *Personal Communication*, Department of Environmental Protection, Perth, WA.

Rye, P.J. (1999) *Personal Communication*, Department of Environmental Protection, Perth, WA.

Rye, P.J., Rayner, K. and Weir, P. (1996) The Perth Photochemical Smog Study, *Western Power Report CS20/96, Department of Environmental Protection Report 16*, Perth, Australia, 94pp.

Ryeherd, S. and Woodcock, C. (1996) Combining Spectral and Texture Data in the Segmentation of Remotely Sensed Images, *Photogrammetric Engineering and Remote Sensing*, Vol. 62, No. 2, pp. 181-194.

Sabins, F.F. (1997) *Remote Sensing Principles and Interpretation*, Third Edition, W.H. Freeman and Co., New York, NY, pp. 494.

Samet, H. (1990a) Introduction, in: *Applications of Spatial Data Structures*, Samet H. (ed.), Addison-Wesley, Boston, MA, pp. 1-27.

Samet, H. (1990b) Volume Data, in: *Applications of Spatial Data Structures*, Samet H. (ed.), Addison-Wesley, Boston, MA, pp. 315-376.

Scheffe, R.D. and Morris, R.E. (1993) A Review of the Development and Application of the Urban Airshed Model, *Atmospheric Environment*, Vol. 27B, No. 1, pp. 23-29.

Schetselaar, E.M. (1995) Computerized Field-Data Capture and GIS Analysis for Generation of Cross Sections in 3-D Perspective Views, *Computers and Geosciences*, Vol. 21, No. 5, pp. 687-701.

Sides, E. and Hack, R. (1995) Three-Dimensional GIS: Future Developments, *ITC Journal*, Vol. 1995-2, pp. 151-164.

Smith, D.R. and Paradis, A.R. (1989) Three-Dimensional GIS for the Earth Sciences, *Proceedings of Auto Carto 9, Ninth International Symposium on Computer Assisted Cartography*, Baltimore, MD, April, pp. 324-335.

Soares, A. (1993) *Geostatistics Troia '92*, Volume 2, Kluwer Academic Publishers, Boston, MA, 1088 pp.

Solberg, R., Solberg, A.H.S., Koren, H. and Kjersti, A. (1996) The Suitability of Future High Resolution Satellite Imagery for Forest Inventory, *Proceeding of IEEE International Geoscience and Remote Sensing Symposium*, NJ, April, pp. 2307-2309.

Spencer, R.D., Green, M.A. and Biggs, P.H. (1997) Integrating Eucalypt Forest Inventory and GIS in Western Australia, *Photogrammetric Engineering and Remote Sensing*, Vol. 63, No. 2, pp. 179-181.

Strahler, Alan and Strahler, Arthur (1997) *Physical Geography Science and Systems of the Human Environment*, John Wiley and Sons, New York, NY, 637 pp.

Street, G. (1995) *Personal Communication*, World Geoscience Corporation, Perth, WA.

Sun, D., Hnatiuk, R.J. and Neldner, V.J. (1996) Vegetation Classification and Mapping Systems for Australian Forest Management, Bureau of Resource Sciences, Kingston, ACT, Australia, 51 pp.

Tanner, R.L. and Zielinska, B. (1994) Determination of the Biogenic Emission Rates of Species Contributing to VOC in the San Joaquin Valley of California, *Atmospheric Environment*, Vol. 18, No. 6, pp. 1113-1120.

Townshend, J.R.G. and Justice, C.O. (1990) The Spatial Variation of Vegetation Changes at Very Coarse Scales, *International Journal of Remote Sensing*, Vol. 11, No. 1, pp. 149-157.

Tucker, C.J. (1979) Red and Photographic Infrared Linear Combinations for Monitoring Vegetation, *Remote Sensing of Environment*, Vol. 8, pp 127-150.

Tucker, C.J., Townshend, J.G.R. and Goff, T.E. (1985) African Land-Cover Classification Using Satellite Data, *Science*, Vol. 227, No. 4685, pp. 369-375.

Turner, K.A. (1989) The Role of Three-Dimensional Geographic Information Systems in Subsurface Characterization for Hydrogeological Applications, in: *Three-Dimensional Applications in Geographical Information Systems*, Raper, J. F. (ed.), Taylor and Francis, London, England, pp. 115-127.

Turner, K.A. (1997a) What's the Difference Among 2-D, 3D and 4D?, *GIS World*, Vol. 10, No. 4, 54 pp.

Turner, K.A. (1997b) Separate Truth from Fiction in Geological Characterisation, *GIS World*, Vol. 10, No. 4, pp 56-57.

Unger, J.D, Liberty, L.M., Phillips, J.D. and Wright, B.E. (1989) Creating a 3-Dimensional Transect of the Earth's Crust from Craton to Ocean Basin Across the North Appalachian Orogen, in: *Three-Dimensional Applications in Geographical Information Systems*, Raper, J. (ed.), Taylor and Francis, London, England, pp. 137-148.

Van Driel, J.N. (1989) Three Dimensional Display of Geologic Data, in: *Three-Dimensional Applications in Geographical Information Systems*, Raper, J. (ed.), Taylor and Francis, London, England, pp. 1-9.

Wakamatsu, S., Uno, I. and Schere, K.L. (1988) Application of a Three-Dimensional Photochemcial Smog Formation Model to the Tokyo Metropolitan Area, *Air Pollution Modelling and its Applications*, Han Van Dop (ed.), Royal Netherlands Meteorological Institute, Debilt, Netherlands, pp. 259-270.

Wallace, J.F. (1999) *Personal Communication*, CSIRO Mathematical and Information Sciences, Floreat Park, WA.

White, R., Rappaport, S., Lieber, K., Gorman, A., DuMelle, F., Maple, D., Bhawnani, M. and Edelman, N. (1995) Children at Risk from Ozone Air Pollution: United States 1991-1993, *Morbidity and Mortality Weekly Report*, Air Pollution and Respiratory Health Branch, Center for Disease Control, No. 44, pp. 309-312.

Williams, J. and Jones, B. (1994) Computer-Aided Cleanup, *Civil Engineering*, Vol. 64, No. 10, pp. 46-49.

Woodcock, C.E. and Strahler, A.H. (1987) The Factor of Scale in Remote Sensing, *Remote Sensing of Environment*, Vol. 21, pp. 311-332.

Woodward, A., Guest, C., Steer, K. Harman, R., Scicchitano, R., Pisanello, P. and McMichael, I. (1995) Respiratory Effects of Troposhperic Ozone: Implications for Australian Air Quality Goals, *Journal of Epidemiology and Community Health*, Vol. 49, pp. 401-407.

Worboys, M.F. (1995) *GIS A Computing Perspective*, Taylor and Frances, Bristol, PA, 376 pp.

World Health Organisation (1992) Accute Effects on Health of Smog Episodes, European Series No. 43, Geneva, World Health Organisation.

Youngmann, C. (1989) Spatial Data Structures for Modeling Subsurface Features, in: *Three-Dimensional Applications in Geographical Information Systems*, Raper, J. (ed.), Taylor and Francis, London, England, pp. 129-136.

APPENDIX A

QBASIC PROGRAM 'CONVERT.BAS'

Convert.bas (version 4)

```
'-----------------------------------------------------------------

'PROGRAM FOR READING DEP ATTRIBUTE FILES & REFORMATTING FOR
VOXEL INPUT
'This program reads files in a format from the Dept. of Environmental
'Protection.  These files contain air_quality data, and will be reformatted
'into a format that can be input into the 4D visualisation package VOXEL.
'(note: user must delete the first four lines of the original DEP files)

'-----------------------------------------------------------------

'created by:   Dan Sandison
'filename:     E:\air_quality\depdata\working\convert.bas (QBASIC)
'last updated: February 10, 1998

'-----------------------------------------------------------------

'Constants:

CONST llx& = 322000   '(lower left x coord)
CONST lly& = 6400000  '(lower left y coord)
CONST inc% = 3000     '(for 3km intervals)
CONST count% = 41     '(loop counter)
CONST count2% = 9     '(loop counter)
CONST zed1! = 4.14    '(1/2 of 8.3)
CONST zed2! = 16.65   '(1/2 of 16.7 + 8.3)
CONST zed3! = 45.85   '(1/2 of 41.7 + 16.7 + 8.3)
CONST zed4! = 91.7    '(1/2 of 50 + 41.7 + 16.7 + 8.3)
CONST zed5! = 141.7   '(1/2 of 50 + 50 + 41.7 + 16.7 + 8.3)
CONST zed6! = 200.05  '(1/2 of 66.7 + 50 + 50 + 41.7 + 16.7 + 8.3)
CONST zed7! = 350.05  '(1/2 of 266.7 + 66.7 + 50 + 50 + 41.7 + 8.3)
CONST zed8! = 618.4   '(1/2 of 500 + 266.7 + 66.7 + 50 + 50 + 41.7 + 8.3)

'-----------------------------------------------------------------

'Variables:

'att!       (attribute value from input file)
'xout&      (x value of sample point)
'yout&      (y value of sample point)
'zout!      (z value of sample point)
'counter1%  (loop counter)
'counter2%  (loop counter)
'counter3%  (loop counter)

'-----------------------------------------------------------------
```

```
CLS
OPEN "e:\air_q\dep\m_16_94\work\nox\filein.dat" FOR INPUT AS #1
OPEN "e:\air_q\dep\m_16_94\work\nox\fileout.smp" FOR OUTPUT AS #2
LET counter1% = 1
DO UNTIL counter1% = count2%                    'loop for 8 zed points
  IF counter1% = 1 THEN
      zout! = zed1!
  ELSE
  END IF
  IF counter1% = 2 THEN
      zout! = zed2!
  ELSE
  END IF
  IF counter1% = 3 THEN
      zout! = zed3!
  ELSE
  END IF
  IF counter1% = 4 THEN
      zout! = zed4!
  ELSE
  END IF
  IF counter1% = 5 THEN
      zout! = zed5!
  ELSE
  END IF
  IF counter1% = 6 THEN
      zout! = zed6!
  ELSE
  END IF
  IF counter1% = 7 THEN
      zout! = zed7!
  ELSE
  END IF
  IF counter1% = 8 THEN
      zout! = zed8!
  ELSE
  END IF
  LET counter2% = 1
  yout& = lly&
  DO UNTIL counter2% = count%                   'loop for 40 y points
      LET counter3% = 1
      xout& = llx&
      DO UNTIL counter3% = count%               'loop for 40 x points
        INPUT #1, att!                  'write x,y,z,val to file
        WRITE #2, xout&, yout&, zout!, att!
        xout& = xout& + inc%
        counter3% = counter3% + 1
      LOOP
      yout& = yout& + inc%
```

```
        counter2% = counter2% + 1
    LOOP
    counter1% = counter1% + 1
LOOP
CLOSE #1
CLOSE #2
```

APPENDIX B

BIBLIOGRAPHY

Bibliography

AURISA 95 Conference Proceedings (1995), 23rd Annual , *Providing Community Befefits in the '90s and Beyond*, Melbourne, VIC, November, 570 pp.

Bradley, C.R. (1994) Evaluating the Antrim Shale Formation Using a Geographic Information System, *AAPG Bulletin*, Vol. 78, No. 8, p. 1328.

Bushfires Report, Bush Fire Advisory Committee Minutes, February, 1998, Appendix One - Fire Reports, Mundaring Shire, WA.

Buttner, P.J.R. (1995) CAD, DTM and GS Tools for Mapping, Modelling, and Analysis of Geologic Data; Coastal Erosion and Satellite Tracking of El Nino, *AAPG Bulletin*, Vol. 79, No. 7, p. 1411.

Bykerk-Kauffman, A. (1994) Developing Student Skills in 3-D Analysis of Geologic Maps, *Geological Society of America*, Vol. 26, No. 7, p. 420.

Congalton, R.G. (1991) A Review of Assessing the Accuracy of Classifications of Remotely Sensed Data, *Remote Sensing of Environment*, Vol. 37, pp. 35-46.

Heymans, M.J., Steed, D.A., Hamilton, D.E. and Pavlov, B.A. (1992) Testing Hydrocarbon Saturation Models for Use in Original Oil-In-Place Estimation; South Dome of Oregon Basin Field, Park County, Wyoming, *AAPG Computer Applications In Geology*, Vol. 1, pp. 105-121.

Hiura, H., Sassa, K. and Fukuoka, H. (1992) Monitoring System of a Crystalline Landslide; Three Dimensional Displacement Meters and Underground Erosion, *Proceedings of 6th International Symposium on Landslides*, Vol. 6, Christchurch, New Zealand, February, pp. 1141-1146.

Li, R., Chen, Y., Xu, C. and Hughes, J.D. (1995) Modelling 3D Geological Subsurface Information in GIS, *Proceedings of ACSM/ASPRS Annual Convention and Exposition*, Charlotte, NC, February, pp. 392-400.

McEachran, D.B. (1992) Mathematical and Logical Manipulation of Grid Models, *Geobyte*, Vol. 7, No. 5, pp. 31-35.

Miller, B.M. (1992) Guide to the Development and Application of Geographical Information Systems for Sedimentary Basin Analysis; Case Study for the San Juan Basin, New Mexico and Colorado, *Report No. B 2025*, US Geological Survey, Washington D.C., p. 37.

Oloufa, A.A. and Ikeda, M. (1994) The Fujita Integrated Environment for Automation, *Proceedings of 11th International Symposium on Automation and Robotics in Construction*, Brighton, England, May, pp 539-546.

OZRI 10 ESA 5 Conference Proceedings (1996), 10th Annual Australia, 5th Annual South Asia, *ESRI and ERDAS User Conference*, Perth, WA, September, 100 pp.

Raffy, M. (1992) Change of Scale in Models of Remote Sensing: A General Method for Spatialization of Models, *Remote Sensing of Environment*, Vol. 40, pp. 101-112.

Sakamoto, M., Shiono, K., Masumoto, S. and Wadatsumi, K. (1993) A Computerized Geologic Mapping System Based on Logical Models of Geologic Structures, *Nonrenewable Resources*, Vol. 2, No. 2, pp. 140-147

Slatt, R., Thompson, R., Graves, R., Davis, T., Benson, R., Van Kirk, C., Edington, D., Huffman, C., Araujo, H., Prestridge, A., Bergstrom, J., Banahene, A., Schenk, T., Jalaludin, J. and Muhamed, K. (1995) Multi-disciplinary Team Modelling of a Complex Sandstone Reservoir, Colorado, *AAPG Bulletin*, Vol. 79, No. 8, p. 1248.

WALIS Forum 96 Proceedings (1996), Perth, WA, April, 104 pp.

WALIS Forum 97 Proceedings (1997), Perth, WA, March, 121 pp.

WALIS Forum 98 Proceedings (1998), Perth, WA, March, 118 pp.

UBD Perth Street Directory (1995), 37th Edition, Universal Press, Perth, WA, 582 pp.

DOLA topographic quadrangle No. 2033 (1978) Fremantle, 1:100,000 series.

DOLA topographic quadrangle No. 2034 (1976) Perth, 1:100,000 series.

DOLA topographic quadrangle No. 2134 (1979) Wooroloo, 1:100,000 series.

DOLA topographic quadrangle No. 2133 (1979) Jarrahdale, 1:100,000 series.

DOLA topographic quadrangle No. 2032 (1979) Pinjarra, 1:100,000 series.

DOLA topographic quadrangle No. 2132 (1979) Dwellingup, 1:100,000 series.

DOLA topographic quadrangle No. 2035 (1978) Gingin, 1:100,000 series.

DOLA topographic quadrangle No. 2135 (1982) Chittering 1:100,000 series.

International Journal of Geographical Information Systems

Cartography

Transactions in Geographical Information Systems

GIS World Magazine

GIS User Magazine

The World Wide Web

Idrisi for Windows Manual

Er Mapper 5.2 Manual

Arc/Info Online Help

Arc/View Manual

Voxel Analyst Manual

APPENDIX C

CD ROM OF VISUALISATIONS

Note: The CDRom of Visualisations is not able to be converted for the purposes of the Australian Digital Theses Project. Refer to the print copy of the thesis, or refer to the author directly.

(Co-ordinator, ADT Project (Retrospective), Curtin University of Technology, 17.2.03)